March 1976 WRRI Report No. 065

STUDIES ON RAINFALL-RUNOFF MODELING

Partial Technical Completion Report

Project No. 3109-206

2. A Distributed Kinematic Wave Model of Watershed Surface Runoff

STUDIES ON RAINFALL-RUNOFF MODELING

2. A Distributed Kinematic Wave Model of Watershed Surface Runoff

Vijay P. Singh, Assistant Professor of Hydrology

Partial Technical Completion Report

Project No. 3109-206

New Mexico Water Resources Research Institute
in cooperation with
New Mexico Institute of Mining and Technology
Socorro, New Mexico 87801

March 1976

The work upon which this report is based was supported in part by funds provided through the New Mexico Water Resources Research Institute by the Department of the Interior, Office of Water Research and Technology, as authorized under the Water Resources Research Act of 1964, Public Law 88-379 as amended, under project number 3109-206.

LIST OF CONTENTS

LIST OF FIGURES

LIST OF TABLES

ABSTRACT

The traditional formulation of kinematic wave theory assumes the kinematic wave friction relationship parameter to be constant. The present study waives this assumption of parameter constancy, allows continuous spatial variability in the parameter and develops a more general formulation of the kinematic wave theory. This concept of parameter variability leads to a completely distributed model, and might eliminate the necessity of utilizing a complex network model to represent the watershed system. Furthermore, this more general formulation will reduce the complexity of modeling watershed surface runoff, and will greatly save computational time and effort.

A systematic treatment to the problem of surface runoff is developed. It is shown when and where explicit analytical solutions are feasible. To develop mathematical solutions two cases are distinguished: one leading to the equilibrium hydrograph and the other leading to the partial equilibrium hydrograph.

The overland flow on an infiltrating plane is formulated as a free boundary problem. Mathematical solutions are developed to study the effect of infiltration on nonlinear overland flow dynamics. To develop explicit mathematical solutions infiltration and rainfall are represented by simple space-and-time invariant functions.

The proposed distributed kinematic wave model is utilized to predict surface runoff from three natural agricultural watersheds. For determination of the kinematic wave friction relationship parameter a simple relationship between the parameter and topographic slope is hypothesized. The simple relation contains two constants which are optimized for each watershed by the Rosenbrock-Palmer optimization

algorithm. The model results are in good agreement with runoff observations from these watersheds. It is shown that if model structure is sound it will suffice to optimize parameters on hydrograph peak only, even for prediction of the entire hydrograph.

Current kinematic wave models of watershed runoff incorporate either numerical or analytical solutions, depending upon the type of input (rainfall pattern) and representation of watershed geometry. Numerical solutions are time-consuming; analytical solutions are not always feasible. This study formulates these models in terms of an approach called hybrid approach which is part numerical and part analytical. By applying it to a set of nine rainfall-runoff events on a natural watershed it is demonstrated that this approach is computationally far more efficient than a totally numerical one, and is applicable where analytical solutions are not feasible.

ACKNOWLEDGEMENTS

The author learned much of the kinematic wave theory and its hydrologic applications from Dr. D. A. Woolhiser, Supervisory Research Hydraulic Engineer, USDA-ARS, Engineering Research Center, Colorado State University, Fort Collins, Colorado. Dr. Bernard Sherman, Professor of Mathematics, New Mexico Institute of Mining and Technology, Socorro, New Mexico, helped in some of the mathematics utilized in this investigation.

CHAPTER 1

INTRODUCTION

1.1 GENERAL REMARKS

The development of a methodology for watershed runoff is vital for the solution of many water resource problems. It is useful in the design of surface water control facilities, economic appraisal of flood prevention programs, study of the effects of existing and proposed watershed projects, evaluation of the effects of changes in land management, and design of experimental watersheds.

The phenomenon of runoff generation is characterized by the response function describing watershed behavior. This response function is a result of numerous processes-complex and interdependent- that participate in the transformation of rainfall into runoff. The transformation process encompasses virtually the entire domain of the hydrologic cycle, and in it are reflected the scope, the magnitude, and the complexity of the problem of modeling the runoff phenomenon. The complexity of runoff phenomenon is enhanced further by spatial variations in geologic formations, soil conditions and vegetation, and by spatial and temporal variations in hydrometeorological conditions.

During the past half a century there have been numerous approaches to modeling the runoff phenomenon. These approaches can be grouped into two categories:

1. Hydrodynamic Approach
2. Operational Approach

The former approach requires the assumption that certain laws of physics hold and further requires a geometrical abstraction of the real-

world phenomenon. The latter approach develops input-output relationships by data fitting without making any explicit assumptions regarding the internal structure of the system.

This dichotomy over the modes of approaches emanates from the extreme positions taken by the representatives of these two groups of investigators. Quoting Amorocho and Hart (1964):

> The first group espouses the pursuit of scientific research into the basic operation of each component of the hydrologic cycle in order to gain full understanding of their mechanisms and interactions. Although the immediate motivation of an individual researcher may not transcend the narrow confines of a set of special phenomena, it is implicit that a full synthesis of the hydrologic cycle may eventually be sought. The concept of a full synthesis is held to be the only rational approach to hydrology.
>
> The second group is motivated by the need to establish workable relationships between measurable parameters in the hydrologic cycle to be used in solving pressing practical technological problems. These people generally hold that the vast complexity of the systems involved in these studies and the inadequacy of the knowledge now available and the knowledge likely to exist in the foreseeable future, make the possibility of a full synthesis so remote in most cases that it must be discarded for practical purposes.

The seeming dichotomy in the extreme positions of the research workers is more fictitious than real. In the quantification of watershed response function or the derivation of rainfall-runoff relationship two basic questions must be addressed:

1. What principles and mechanisms govern surface runoff, and how can they be integrated to accurately simulate it?
2. What physiographic characteristics of a watershed in conjunction with spatial and temporal distributions of rainfall affect the runoff phenomenon, and how much detail is required in their representation?

The key to a systematic study of watershed runoff lies in answering these questions. A hydrodynamic approach is perhaps the best way to answer them, and to develop insight into the runoff phenomenon.

There are many plausible hydrodynamic approaches. In the present study we will consider the one that is based on the kinematic wave theory.. The traditional formulation of kinematic wave theory assumes the kinematic wave friction relationship parameter to be constant. The present study waives this assumption of parameter constancy, allows continuous spatial variability in the parameter and develops a more general formulation of the kinematic wave theory. This concept of parameter variability leads to a completely distributed model and eliminates the necessity of utilizing a complex network model to represent the watershed system. Furthermore, more general formulation reduces the complexity of modeling watershed surface runoff, and will greatly save computational time and effort.

Previous studies have treated surface runoff and infiltration as separate components of hydrologic cycle. A combined study of these phases is required for modeling surface runoff. The conventional approach to combine these phases has been through the familiar notion of so-called rainfall-excess. In this approach infiltration is independently determined and subtracted from rainfall; the residual is termed as rainfall-excess, which forms input to the surface runoff model. It seems that this concept of rainfall-excess is more of an artifice than a reality. The processes of infiltration and runoff occur simultaneously in nature during and after the occurrence of rainfall and, therefore, require a combined study.

Studies in the past have postulated one model, and have proceeded to show that it results in "sufficiently good" fit for a very limited amount

of data (often a few events). It is recognized in the present study that there may be many plausible alternative models, and that any meaningful study must consider model performance for several rainfall-runoff events on different watersheds. Only then a systematic statistical interpretation of model results can be made.

1.2 OBJECTIVES

Objectives of the study are:

1. To develop a distributed nonlinear kinematic wave model for watershed surface runoff.
2. To develop a combined treatment of infiltration and overland flow.
3. To apply the proposed model to predict surface runoff from natural agricultural watersheds.

CHAPTER 2

A SURVEY OF KINEMATIC WAVE MODELS OF WATERSHED RUNOFF

2.1 ROLE OF MODELS IN HYDROLOGY

The need for modeling is well expressed in a quote by Rosenblueth and Wiener (1945):

> No substantial part of the unvierse is so simple that it can be grasped and controlled without abstraction. Abstraction consists in replacing the part of the universe under consideration by a model of similar but simpler structure. Models, formal or intellectual on one hand, or material on the other, are thus a central necessity of scientific procedure.

To this quote it may well be added that models are also a central necessity of engineering design and of watershed engineering in particular. A watershed is an extremely complex system. To understand it in all detail is beyond human expectation. Therefore, modeling is inevitable to control or understand some aspects of its behavior.

2.2 KINEMATIC WAVE MODELS

The evolution of surface runoff models based on the kinematic wave theory can be traced along the following lines:

1. Development of kinematic wave theory
2. Validity and verification of kinematic wave theory
3. Application of kinematic wave theory to hydrograph prediction
4. Dynamics of flood frequency
5. Laboratory investigation of kinematic wave theory
6. Solution techniques

7. Parameter estimation and optimization

8. Determination of watershed characteristic parameters

We will present a comprehensive review of the kinematic wave models along these lines.

2.2.1 Development of Kinematic Wave Theory

Lighthill and Whitham (1955) introduced the kinematic wave theory, and utilized it in describing flood movement in long rivers. They also developed kinematic wave equations for overland flow. In their general treatment of the theory it was suggested that the solution could be found by numerical integration along the characteristics when the inflow was a function of time and distance, and explicit solution could be found for the lateral inflow being constant or a function of distance only. While clarifying the role of dynamic waves it was shown that at the "Froude Numbers" appropriate to the flood waves, dynamic waves were rapidly attenuated and the main disturbance was carried downstream by the kinematic waves. Some account was given of the behavior of flow at high Froude numbers. A variety of factors influencing the stage-discharge relation were considered. A criterion for kinematic shock waves was delineated. General properties of shock waves along with kinematic waves were discussed. Full equations of motion were employed to investigate the structure of the kinematic shock.

About the same time Iwagaki (1955) developed an approximate method of characteristics for steady flow in open channels of any cross-sectional shape, and proposed that the method would be applicable to hydraulic analysis of runoff estimation in actual rivers. The kinematic

assumption was implicitly utilized in the analysis. The lateral inflow was taken nearly uniform. The agreement between the results of the method and the experiments was reported to be good.

These investigators laid down the foundation, developed the mathematical base, and demonstrated the applicability of the kinematic wave theory.

2.2.2 Validity and Verification of Kinematic Wave Theory

Some questions remained unresolved regarding the applicability of the kinematic wave theory to watershed hydrology. They were, for example: what is the criterion for the choice between the complete dynamic equations and the kinematic equations? What degree of approximation is introduced in the solution by the kinematic approximation? How good is the kinematic approximation in hydrologic problems as opposed to full dynamic equations?

Woolhiser and Ligget (1967) solved equations for overland flow, in three one-dimensional forms, for the rising hydrograph by finite difference techniques. A single dimensionless parameter was found to delineate a criterion for choice between the complete equations and the kinematic approximation. It was shown that for most hydrologically significant cases the kinematic wave solution would give accurate results. This parameter is now known as kinematic wave number. It was concluded that there was no unique dimensionless hydrograph for overland flow, contradicting the unit hydrograph theory.

A similar conclusion was reached by Overton (1972) when he analyzed more than 200 overland flow hydrographs generated by simulated rainfall on long impermeable planes. It was shown that kinematic waves prevailed

over dynamic waves. It was observed that most flows appeared to be either in the transition from laminar to turbulent state or in a fully developed turbulent state. The transition was found to be significantly affected by rainfall intensity. However, error involved in treating all flows as turbulent would be small with the resulting analysis made considerably less complex.

Some earlier studies by Ishihara (1964), Yu and McNown (1964) and Harbaugh (1966) subscribed implicitly to that same contention on the applicability of kinematic wave theory to problems of hydrologic significance.

2.2.3 Application of Kinematic Wave Theory to Hydrograph Prediction

No attempt was made to utilize the kinematic wave theory in watershed hydrology until Henderson and Wooding (1964). They used it in describing the hydrograph from a steady rain of finite duration for laminar or turbulent flow over a sloping plane, neglecting the slope of water surface relative to the slope of plane. The relationships developed by them showed certain distinct differences from those postulated in the unit hydrograph theory (Sherman, 1932; Nash, 1957; Dooge, 1959). The results of calculations based on the theory were found to be in close agreement with the experimental measurements. The kinematic wave solution was also compared with the solution to the problem embodying groundwater flow through a porous medium overlying a sloping impermeable stratum; significant differences were noted between the two.

Later, Wooding (1965a, 1965b, 1966) employed the kinematic wave theory in the development of a 2-component, 4-parameter runoff model for a V-shaped watershed geometry (two planes contributing runoff to a channel between

them). Analytical and numerical solutions were presented, and numerical solutions were compared with runoff measurements from three natural watersheds. All watersheds, regardless of their complexity, were represented as a single V-shaped watershed with overland flow planes contributing lateral inflow to a channel in the apex of V. In spite of good agreement reported between observed and computed runoff hydrographs he concluded that a better geometrical description of stream network would be desirable. One feature of the hydrograph that his model was unable to reproduce was the steeply rising portion of the hydrograph caused by concentration of runoff.

In his model, Wooding considered two parameters as constants which were the indices in the power law equations of motion for catchment and stream. No objective way was specified for arriving at these constants, and for determination of other parameters. The model did not account for temporal and spatial variability in rainfall and watershed characteristics. No attempt was made to relate model parameters to watershed geometry, or rainfall characteristics or both. He did not offer any explanation for choosing rectangular geometry and ignored the sensitivity of model parameters.

The work of these investigators provided a real impetus to further research on applications of the kinematic wave theory (Eagleson, 1967, 1968, 1971, 1972; Overton and Brakensiek, 1970; Li, 1974; Singh, 1974). In these attempts a V-shaped geometry, proposed by Wooding (1965a), was taken to represent the natural watershed. Some dissatisfaction was expressed by Wooding himself with regard to the inadequacy of the proposed geometrical representation of a natural watershed. Investigators continued to use it until Brakensiek (1967a) came up with the concept of kinematic cascade.

He utilized this notion in the transformation of an upland watershed into a cascade of planes discharging into a single channel. The transformation technique was based on the preservation of the hypsometric curve and the contour-length-elevation curve of the watershed.

The kinematic cascade concept has since been incorporated in several investigations. Woolhiser, et al (1970) utilized this concept to describe overland flow and channel flow for small rangeland watersheds. The friction relation was assumed to be of the Darcy-Weisbach form, with initially lamilar flow becoming turbulent flow at a transitional Reynolds number of 300. Optimum values of the friction parameter were obtained by a univariate optimization procedure for four heavily gaged watersheds and four lightly gaged watersheds for a single storm. Although these watersheds showed substantial differences in vegetal composition and cover and in weight of vegetation per unit area, the roughness parameters were not significantly different. The average of the eight optimized parameters was used in the kinematic cascade to predict runoff hydrographs.

Kibler and Woolhiser (1970, 1972) developed dimensionless equations for the kinematic cascade, and derived general equations for a single element in the cascade. Properties of the solution for a kinematic cascade with pulsed lateral inputs were examined. They developed a criterion by which to delineate the development of kinematic shock waves.

Rovey (1974), Singh (1974) and Lane (1975) applied the kinematic cascade to predict surface runoff from experimental, agricultural and urban watersheds. Brakensiek (1967b) gave a formal definition of kinematic flood routing and its application. Harley, et al (1967) developed a general purpose river basin distributed simulation model. The problems

of network decomposition and lumped parameter recognition were discussed, and a scheme suitable for any specific tree-like network was proposed. Flood routing within the individual elements was performed using a non-linear kinematic wave model. The properties and behavior of the model under various conditions were examined, and recommendations were made regarding their suitability in various flow regimes.

Besides V-shaped geometry and cascade of planes and channels, alternate geometric representations were proposed and applied. Woolhiser (1969) suggested that a watershed consisting of a V-shaped section plus a portion of the surface of a cone at the upstream end might result in a better description than the simple V-shaped catchment because of the concentration of flow in the cone; such a model could be taken to represent a watershed of any complexity or it could be used as a basic element in a network model. The kinematic wave equations for an experimental converging surface were solved numerically for a number of values of the convergence parameter. An analytic solution was given for recession from equilibrium. He found for pulse inputs of lateral inflow that the shape of the hydrograph might be changed appreciably by varying the convergence parameter.

In order to test the utility of such a model, Woolhiser, et al (1971) presented experimental data for two types of surfaces from a converging overland flow section, and compared the properties of the experimental hydrographs with those predicted by kinematic wave theory. Chezy's friction law, and both laminar and turbulent regimes were incorporated. The shape of the recession hydrographs predicted by kinematic wave theory showed that there was no general basis for the commonly accepted negative exponential.

Following the work of Woolhiser, Singh (1974, 1975a) utilized the converging section geometry in developing a nonlinear kinematic wave model

for watershed runoff. For steady input he developed analytical solutions. The model was utilized to predict runoff hydrographs from an experimental rainfall-runoff facility and a large number of experimental agricultural watersheds. The behavior of kinematic wave parameters was examined, and an experimental justification was advanced to reduce the number of model parameters. An objective methodology was given to estimate and optimize model parameters. The performance of the model was compared with that of kinematic wave models based on other geometric configurations and Nash's linear model. The model results supported the contention expressed by Woolhiser (1969).

Some attempts were made to use the kinematic wave theory to establish the relation between watershed geomorphology and runoff response. Golany and Larson (1971) developed a model for a watershed of 4th order stream. It included overland flow planes, an elementary channel and a channel system. Morphological relationships and physical characteristics of small watersheds were used in the model. Excess rainfall was routed by a numerical solution of the kinematic wave equations through the overland flow plane and the elementary channel. The outflow hydrographs of the elementary channel were used as input to the channel system where the flow was routed by successive numerical solutions of the dynamic wave equations of the unsteady flow to obtain the runoff hydrographs of the watershed. Backwater effect was considered above the major junctions in the main channels of all orders except one. The model was used to study the effects of watershed characteristics, length, slope and roughness of the main channel and watershed area on the time to virtual equilibrium. The effect of each factor was determined by varying it independently while keeping others constant. The roughness and slope were also varied. They inferred that

the relationships developed by them would be applicable only to the model watershed.

Wei and Larson (1971) attempted to incorporate the effects of time distribution and areal distribution of rainfall storm movement, and watershed shape on the runoff hydrograph. The attempts were directed to find a relationship between an appropriate input parameter and a modification (peak flow) coefficient to be used in adjusting the peak discharge estimated by the methods based on constant intensity uniformly distributed over the watershed.

Rastogi and Jones (1969, 1971) applied the kinematic wave model to a third order stream representing conditions on the catchment under study. The model drainage basin was considered as a distributed hydrologic system with stream network, channel characteristics and overland flow lengths as distributed hydrologic variables. Different order channel lengths, channel cross-sections and channel-slopes were treated as spatially distributed. The results of the model indicated that various time parameters were affected by change in rainfall-excess intensity. The peak flow rates for a given rainfall-excess duration showed a nonlinear response with rainfall-excess intensity. No verification of the mathematical model was made.

In these investigations little attention was focused on the problem of estimating water entering the soil mass, and coupling it with the kinematic wave models of surface runoff. In most investigations rainfall-excess was determined in a rather empirical fashion. To resolve this complex problem Foster, Huggins and Meyer (1968) coupled an infiltration model with a kinematic wave model to predict overland flow on very rough, short slopes. The model incorporated retention storage, provision for a variable point infiltration rate, a variable coefficient

of friction, the drying up of the upstream end of the slope during recession and a variable area infiltration rate - a function of water surface area during recession. Field hydrographs from fallow erosion study plots were analyzed for retention storage, and values of the Darcy-Weisbach coefficient of friction were estimated. These results were used in a model to simulate hydrographs that were compared with field hydrographs to test the concept used in the model.

Smith and Woolhiser (1971a, 1971b) combined the kinematic wave approximation for unsteady overland flow on cascaded planes with a mathematical model of infiltration based on the partial differential equation for vertical, one-phase, unsaturated flow in soils. Numerical solutions were employed to obtain the solution. Model results were compared with experimental and field data. The agreement was adequate, although there were some differences in recession lengths. This same approach was later implicit in a study by Singh (1973).

In most investigations very little attention was paid to the variability in rainfall and watershed characteristics and its effect on character of runoff phenomenon. Eagleson (1967) used the kinematic wave model by Wooding (1965a) for the determination of the peak discharge from an impulse of rainfall-excess located at any distance from the catchment outlet. The spatial impulse response was employed in linearization of the catchment dynamics to obtain a simple, superposition relation for estimating the effect of areal variability in rainfall distribution on peak surface runoff.

Singh (1975h) derived general solutions to kinematic wave equations using space-time variant input. Several special cases were considered by imposing conditions on input and kinematic wave parameters. The model

was applied to a natural agricultural watershed, and the agreement between model results and observations of runoff was reported to be good. In optimizing model parameters the role of the choice of an objective function was examined.

2.2.4 Dynamics of Flood Frequency

In other studies by Eagleson (1971, 1972) the kinematic wave method was generalized through the incorporation of random variations in temporal and areal distribution of storm rainfall-excess. Expressions were derived for the peak direct runoff and streamflow in terms of the statistics of rainfall rate and duration.

Probability density functions of storm duration and storm rainfall depth were assumed. The classical flood frequency curve was derived as an explicit function of parameters defining the rainfall duration and the catchment stream physiography. The flood frequency relation expressed the mean annual flood as a function of catchment area, and its comparison was made with observations from natural catchments. The curve was found to be sensitive to the particular value of direct runoff fraction and that of catchment area.

2.2.5 Laboratory Investigation of Kinematic Wave Theory

Laboratory watershed models provide opportunities to study unsteady flow in a number of geometrically different systems. They appear to be a powerful tool in testing purely mathematical models of watershed hydraulics, and also in testing the applicability of lumped system models (linear or nonlinear) over the range of prototype size that can be accomodated. Studies of surface runoff on small prototypes without spatial variation in rainfall

will unquestionably answer interesting hydraulic and hydrologic questions. When used in conjunction with mathematical models they aid in understanding and predicting watershed behavior.

Experiments on a natural watersheds are very time consuming, and there is no control over the input. The physical size is also a problem; so for practical reasons some investigators attempted to model hydrologic systems utilizing a change in scale (Chery, 1966). They found that this was not a viable approach. Grace and Eagleson (1965, 1967) demonstrated that scale models were feasible only in very special cases.

An important consideration is that laboratory model must duplicate the most important features of the complex system. If it does not, it cannot give insight into real system behavior. Realizing the significance of laboratory watersheds in hydrologic research several investigators studied the kinematic wave theory experimentally.

In his famous experimental study Izzard (1943) collected data on the hydraulics of overland flow from paved and turf plot surfaces. These data have often been used to verify analytic and numerical results (Morgali and Linsley, 1965; Mongali, 1970). From his data analysis he concluded that detention on the rising side of the hydrograph, or at any time that rain was falling, was definitely and appreciably greater than the detention required to maintain the same rate of flow on the recession side of the hydrograph after all rain had ceased.

Izzard (1944) applied the experimental data to the equations of motion (Keulegan, 1944) in order to compute the surface profile of overland flow. The attempt was limited to consideration of flow at equilibrium during rainfall at constant rate and did not involve flow on the rising or falling limb of the hydrograph, except for some data based on the

recession curve at the point where discharge was equal to the discharge during rainfall equilibrium.

Since Izzard, very few experiments were conducted pertaining to the hydraulics of overland flow. It is only recently that growing interest in watershed experimentation was renewed.

Woo and Brater (1962) made a study of spatially varied flow produced by uniform rainfall for two types of uniform surfaces for slopes varying from 0 to 0.06. A rainfall applicator was developed by means of which raindrops of desired size could be applied at a reasonably high velocity and a uniform intensity. Rainfall was applied to a flume 29 feet 7 inches long and 6 1/4 inches wide, with intensities of 1.65, 2.95 and 5.04 inches per hour, keeping the intensity constant during each test. The flow was laminar. The study indicated that the effect of rainfall impact on overland flow profile could be included in the analysis by a change in the friction coefficient. A method for computing the water surface profile during rain was developed for practical use.

Amorocho and Hart (1965) discussed three types of laboratory catchments: model catchment, hydromechanic prototypes, and prediction analysis prototypes. The first type, used for the simulation of natural watershed behavior, involved a number of questions related to the problem of incomplete similitude. A procedure for systematic adjustment of these catchments in order to obtain experimental predictability was suggested. The second type was employed in watershed hydraulics for the investigation of individual flow mechanics. The third type was used to test the methods of nonlinear analysis of hydrologic systems (Amorocho, 1963; Amorocho and Orlob, 1961). A description of the results of experimentation with these devices indicated their usefulness in hydrologic research.

Chery (1966) discussed theoretical considerations and described design criteria, fabrication, and tests of a physical hydrologic model including a storm simulating device. Model performance during a series of preliminary tests was discussed. Based on the information obtained from the tests the author proposed further investigation into physical hydrologic models to establish rainfall-runoff relationship.

Robertson, et al (1966) discussed overland flow experiments performed at Stillwater, Oklahoma. The principle purpose was to develop and test analytic procedures for predicting the surface profile for overland flow resulting from application of rainfall simulation over steep rough surfaces.

Chow and Harbough (1965) described a technically efficient method for producing artificial raindrops. The approach was based on broad basic requirements to be adapted in the experimental investigation on watershed hydraulics. Modular construction of the raindrop producing device was adapted, allowing variable time distribution and areal coverage of intensities from 0.75 to 13 inches per hour. The rainfall producer provided fast response to on-off commands and produced in the laboratory controllable simulated storms of flexible time and areal distribution patterns.

Chow (1967) described the laboratory approach investigating the basic laws and principles controlling the mechanics of runoff from the watershed. It employed a watershed experimentation system based on integrated hydraulic, electronic and structural design. A discussion was given of the system, the rationale behind its construction and some of the research tactics that had been used or proposed. The system was a laboratory device to study unsteady, free surface hydraulic problems. It could produce an artifical rainfall of variable time and space distribution to move over a laboratory

area 40 square feet or less, thus capable of simulating a storm moving in any direction over a testing drainage basin constructed within the area. The study considered the time factor in runoff process, the conceptual watershed runoff and the effect of storm movement on peak discharges.

Harbaugh and Chow (1967) utilized the laboratory experimentation system in studying the roughness of a conceptual river system or watershed for various slopes and shapes. The sensitivity of the conceptual roughness to depth of flow and raindrop impact on the laboratory watershed was investigated.

Yen and Chow (1969) studied the importance of movement of rainstorm on the time distribution of surface runoff from watershed through the use of a laboratory watershed experimentation system. Experiments were performed for 2 rainfall intensities, 4 surface slopes, and 14 rainstorm velocities. Analysis of the mechanics of water flowing on watersheds was attempted to explain the influence of movement of rainfall on the characteristics of surface runoff hydrograph.

Dass and Huggins (1970) developed a kinematic wave model to study overland flow on a laboratory catchment. Their study indicated that surface roughness greatly influenced the time distribution of surface runoff and the time to equilibrium. Their depth hydrographs suggested a significant increase in depth of water and consequently in detention volume on the flow of plane with increase in surface roughness. Their recommendation was to study the effects of raindrop impact for a variety of slopes, intensities, depths of water and surface roughness conditions.

Kundu (1971), following the above recommendation, studied in the laboratory the characteristics of surface runoff on a watershed element with very rough surfaces. The relative importance of slope, roughness

and rainfall on the flow characteristics was investigated. A roughness concentration index was defined to measure the surface roughness and it was conjectured that this would be a better measure than either Chezy's coefficient or Manning's coefficient. A consistent trend of friction factor with respect to Reynolds number (200-1,000) was reported in the transition zone of flow.

Langford and Turner (1973) described an experimental test to establish the accuracy of kinematic wave theory as applied to overland flow over a rough, uneven surface. The depression storage, and the hydraulic roughness for flows without rain were measured in separate tests; the hydraulic roughness for flows under rain was calculated from the rising limbs of the runoff hydrographs from a series of simulated storms. Recession curves were calculated using the kinematic wave theory. Close agreement between experimental and calculated recessions showed accuracy of the theory in predicting behavior of flows over rough, uneven surfaces. Hysteresis was observed in the storage-discharge curves; this was explained in terms of the theory. The continuity equation was linked with a uniform flow equation (e.g. Manning's formula) relating discharge to depth of flow; the effect of momentum of both overland flow and rain was ignored. In the experimental evaluation of the theory it was found that these assumptions did not cause important errors in the ability of the theory to predict the behavior of overland flow. This implied that certain amount of averaging in time and space was permissible. The major weakness of the study was the limited nature of the experimental program; only one surface with one slope was used.

Muzik (1973, 1974a, 1974b) studied the response of a well-defined impervious surface to a specified input of rainfall, using the state

variable approach of systems analysis. The mathematical model was tested by simulating the experimental hydrographs of surface runoff from the laboratory catchment for uniform, time and space variable rainfall inputs. A mathematical relationship describing the raindrop impact effect was developed by the method of dimensional analysis and subjected to empirical evaluation. The experimental hydrographs were simulated by kinematic wave and instantaneous unit hydrograph models. The nonlinearity of the rainfall-runoff process was studied. The kinematic wave model was found to provide fairly consistent results but had a tendency to overpredict the time to peak and the peak discharge.

Woolhiser and Schulz (1973) described a large-scale experimental rainfall-runoff facility. The applicability of kinematic mathematical model to the experimental results was demonstrated. The friction resistance to flow was hypothesized by a 4-parameter relation. The facility was utilized in earlier studies by Woolhiser (1969), Smith and Woolhiser (1971), Woolhiser, et al (1971), and Kibler and Woolhiser (1972), Rovey (1974), Singh (1974, 1975a) and Lane (1975).

Singh (1974, 1975a, 1975b) studied the applicability of the kinematic wave theory on a large experimental rainfall-runoff facility. The runoff hydrographs predicted by the theory were in close agreement with the experimental hydrographs. The behavior of kinematic wave friction relationship parameter was examined. Upon comparing the model with Nash's linear model, it was found that the former was consistently better than the latter.

Lane (1975) studied experimentally the influence of simplifications of watershed geometry in simulation of surface runoff. He developed a methodology

whereby one could define the simplest kinematic cascade geometry which when used in simulation will, on the average, preserve selected hydrograph characteristics to a given degree, given rainfall, runoff and watershed topography data. Several goodness-of-fit statistics were defined. The influence of geometric distortion on impulse response was quantified.

2.2.6 Solution Techniques

The solution of kinematic wave equations depends on (a) geometric representation, and (b) rainfall pattern. There are three basic geometric elements: converging section, plane, and channel, that are utilized in different combinations to represent the watershed geometry. The rainfall pattern can also be of three types: impulse, pulse and complex. For pulse and impulse rainfall analytical solutions were developed for all three elemental sections (Wooding, 1965a, 1965b; Woolhiser, 1969; Kibler and Woolhiser, 1970, 1972; Eagleson, 1971, 1972; Singh, 1974, 1975e). For complex inputs, however, numerical solutions for these sections were developed (Singh, 1974, 1975e; Li, et al, 1975; Kibler and Woolhiser 1970, 1972; Brakensiek, 1966; Ligget and Woolhiser, 1967). Hybrid solutions-combination of analytical and numerical solutions - were also presented (Singh, 1974, 1975e).

2.2.7 Parameter Estimation and Optimization

A very few studies, indeed, considered the problem of systematic determination of kinematic wave parameters. The usual procedure has been to optimize the parameters over a set of events and utilize these optimized values for another set of events for which predictions were desired. Although this method does provide a way to get around the

problem, but it does not solve it basically. Some studies, rather more suggestive than conclusive, were conducted by Singh (1974, 1975f, 1975g, 1975h), where parameters were correlated with watershed physiography. Although the importance of geomorphology has long been recognized in hydrologic synthesis, it is surprising that only limited effort has been made in this direction.

2.2.8 Determination of Watershed Characteristic Parameters

Overton (1971) presented hydraulic solutions of lag time for idealistic surfaces using the kinematic wave equations. The surfaces included (1) uniform plane, (2) hill slope as a cascade of planes, (3) V-shaped watershed, (4) V-shaped watershed with hill slope, (5) converging surface, and (6) concave surface. Lag times were shown to be related to roughness and catchment slope, and the input rate. A lag relation was developed for a nonuniform catchment in terms of the lag of a uniform plane and a converging factor. A numerical procedure was shown whereby the converging factor could be evaluated for any nonuniform catchment from observed input and output data.

Singh (1975e) derived general expressions for Overton's lag time for a converging surface, and showed that Overton's solutions were a special case of his. A similarity factor was defined. In another study Singh (1975d) employed the kinematic wave theory to derive general expressions for the time of concentration for plane and converging sections. Several conditions were considered with regard to space-time distribution of rainfall and spatial distribution of kinematic wave friction relationship parameter. Some traditional misconceptions in the notion of time of concentration were pointed out. It was shown that the generalized

expressions would give, under very special conditions, rise to familiar time of concentration formula (Mulvany, 1855).

Ragan and Duru (1972) presented a nomograph for times of concentration employing the kinematic wave theory. They recognized the influence of rainfall intensity on the time of concentration. Using the Manning's flow formula they specialized in the equation developed by Henderson and Wooding (1964) and proceeded to develop a graphical technique to solve for the time of concentration. Using field data they showed that the time of concentration based on kinematic wave theory was accurate for most engineering design purposes.

CHAPTER 3

KINEMATIC WAVE THEORY

3.1 GENERAL REMARKS

The equations of motion (Kibler and Woolhiser, 1970; Mahmood and Yevjevich, 1975) for a wide rectangular channel or plane can be written as: the continuity equation,

$$\frac{\partial h}{\partial t} + \frac{\partial Q}{\partial x} = q(x,t) \tag{3-1}$$

and the monentum equation,

$$\frac{\partial u}{\partial t} + u\,\frac{\partial u}{\partial x} + g\,\frac{\partial h}{\partial x} = g(S_o - S_f) - \frac{q(x,t)}{h}\,u \tag{3-2}$$

where h = local depth of flow, u = local average velocity, q(x,t) = rate of space-time variable lateral inflow, Q = rate of flow per unit width, g = acceleration due to gravity, S_o = bottom slope, S_f = slope of the energy line, x = distance measured along channel axis in the direction of flow, and t = time. These equations are often referred to as de Saint Venant equations. Note that width of the section has been taken as unity in the derivation of these equations. This implies that cross-section area (A) is equal to depth of flow (h). We must also note:

$$Q = uh \tag{3-3}$$

These equations characterize gradually varied unsteady free surface flow with lateral inflow. Let us now examine implications of each term in

Eqs. (3-1) and (3-2).

The term $\frac{\partial h}{\partial t}$ accounts for the change in storage with time in the section due to water surface elevation; the term $\frac{\partial Q}{\partial x}$ accounts for the difference between outflow from and inflow to the section due to areal variation in velocity with space; the term $q(x,t)$ is lateral inflow which provides the net mass change spatially and temporally beyond the storage terms. If we substitute Eq. (3-3) into Eq. (3-1), an alternative form of the continuity equation is obtained:

$$\frac{\partial h}{\partial t} + h \frac{\partial u}{\partial x} + u \frac{\partial h}{\partial x} = q(x,t) \qquad (3\text{-}4)$$

Then the term $\frac{\partial h}{\partial t}$ is called as the rate of rise term; $u \frac{\partial h}{\partial x}$ is the wedge storage term; and $h \frac{\partial u}{\partial x}$ is the prism storage term.

In Eq. (3-2) the term $\frac{\partial u}{\partial t}$ is the acceleration term and accounts for the local acceleration of the fluid; $u \frac{\partial u}{\partial x} + g \frac{\partial h}{\partial x}$ is the convective term in which the former term relates to change in kinetic energy and the latter relates to potential energy; the term $g S_o$ accounts for the component of gravitational force in the direction of flow; the term $g S_f$ accounts for the frictional force component along the channel; and the term $\frac{u}{h} q(x,t)$ accounts for the momentum that must be imparted to the lateral inflow by the water flowing in the channel.

Equations (3-1) and (3-2) give rise to a complete dynamic wave model. By specializing in Eq. (3-2) the following models can be obtained:

3.1.1 Storage Model

In this model we ignore the momentum equation completely, and consider only the continuity equation. Thus the storage model is represented as:

$$\frac{\partial h}{\partial t} + \frac{\partial Q}{\partial x} = q(x,t)$$

If we consider a small reach (Δx) then $\frac{\partial Q}{\partial x}$ can be replaced by $\frac{\Delta Q}{\Delta x}$; for a given time interval Δt and a reach of length Δx we can write $\frac{\Delta Q}{\Delta x} = (I - 0)/\Delta x$, where I = inflow and 0 = outflow. The first term $\frac{\partial h}{\partial t}$ can be replaced for small Δt by $\frac{\Delta h}{\Delta t}$. Thus we can write:

$$I - 0 = \frac{\Delta h}{\Delta t} \cdot \Delta x \qquad (3\text{-}5)$$

The quantity $\Delta h \cdot \Delta x$ is ΔS where S = storage. Then

$$I - 0 = \frac{\Delta S}{\Delta t} \qquad (3\text{-}6)$$

If we let $\Delta t \to 0$, Eq. (3-6) becomes

$$I - 0 = \frac{ds}{dt} \qquad (3\text{-}7)$$

Equation (3-7) is the familiar form of storage model (Yevjevich, 1959), and is nothing but spatially lumped continuty of mass. One must note here that I is identical to q(t) and 0 is related to Q(t).

3.1.2 Kinematic Wave Model

The kinematic wave model retains continuity equation given by Eq. (3-1), and imposes certain restrictions to simplify Eq. (3-2). It is assumed (Eagleson, 1970) that acceleration, convective and inflow terms are negligible as compared to bottom slope and friction. This implies a balance between gravitational and frictional forces, or an equivalence

between bed slope and friction slope. Thus the kinematic wave model is represented as:

$$\frac{\partial h}{\partial t} + \frac{\partial Q}{\partial x} = q(x,t)$$

$$S_o = S_f \tag{3-8}$$

The average boundary shear stress can be written as:

$$\tau = \gamma h\ S_f \tag{3-9}$$

where γ = weight density of water. Substituting Eq. (3-8) into Eq. (3-9) we obtain:

$$\tau = \gamma h\ S_o \tag{3-10}$$

This is a well-known shear stress relation for steady, uniform flow in a wide rectangular channel. If we define

$$\tau = C_f\ \gamma\ \frac{u^2}{2g} \tag{3-11}$$

where C_f is a coefficient, a function of Reynolds number and relative roughness parameter. Combining Eqs. (3-10) and (3-11) we obtain:

$$u = \left[\frac{2ghS_o}{C_f}\right]^{0.5} \tag{3-12}$$

or

$$u = C(hS_o)^{0.5} \tag{3-13}$$

where $C = (2g/C_f)^{0.5}$, Chezy's coefficient. Assuming C to be constant (as a first approximation) Eq. (3-13) can be written as:

$$u = \alpha h^{0.5} \tag{3-14}$$

where $\alpha = C(S_o)^{0.5}$. More accurately, of course, because of the variability of C we can write:

$$u = \alpha h^{m} \tag{3-15}$$

$$Q = \alpha h^{n} \tag{3-16}$$

where $n = m + 1$ because of Eq. (3-3). Equation (3-15) or (3-16) is often referred to as kinematic approximation to momentum equation, or simply kinematic momentum equation. We defer further discussion of kinematic wave model until next section.

3.1.3 Diffusion Model

The diffusion model includes continuity equation given by Eq. (3-1), and imposes slightly less restrictions to simplify Eq. (3-2) than does the kinematic wave model. It is assumed (Henderson, 1966) that acceleration, kinetic energy and inflow terms are negligible as compared to gravitational force, frictional force and pressure force. That is, we include the potential energy term or pressure term in the kinematic wave model. Thus the diffusion model can be represented as:

$$\frac{\partial h}{\partial t} + \frac{\partial Q}{\partial x} = q(x,t)$$

$$\frac{\partial h}{\partial x} = S_o - S_f \tag{3-17}$$

For wide rectangular channel we can write Chezy's law as:

$$u = C\sqrt{h\, S_f} \tag{3-18}$$

Writing Eq. (3-17) as

$$\frac{\partial h}{\partial x} = S_o - \frac{u^2}{C^2 h} \tag{3-18}$$

Solving Eq. (3-18) for u

$$u = C \left\{ h\left(S_o - \frac{\partial h}{\partial x}\right) \right\}^{0.5} \tag{3-19}$$

Substituting Eq. (3-19) into Eq. (3-1) we obtain:

$$\frac{\partial h}{\partial t} + \frac{\partial}{\partial x} \left\{ Ch \left(h \left[S_o - \frac{\partial h}{\partial x} \right] \right)^{0.5} \right\} = q(x,t) \tag{3-20}$$

Upon simplification Eq. (3-20) becomes:

$$\frac{\partial h}{\partial t} + \frac{3}{2} C \left\{ h \left(S_o - \frac{\partial h}{\partial x} \right) \right\}^{0.5} \frac{\partial h}{\partial x} = - \frac{Ch^{1.5}}{2\left\{ S_o - \frac{\partial h}{\partial x} \right\}^{0.5}} \frac{\partial^2 h}{\partial x^2} + q(x,t) \tag{3-21}$$

For constant Chezy's C and a wide rectangular channel we know that

$$c = \frac{3}{2} u \tag{3-22}$$

where c = wave celerity. Substituting Eq. (3-19) into Eq. (3-22) and then into Eq. (3-21) we obtain:

$$\frac{\partial h}{\partial t} + c \frac{\partial h}{\partial x} = K \frac{\partial^2 h}{\partial x^2} + q(x,t) \tag{3-23}$$

where $K = \frac{ch}{3\left(S_o - \frac{\partial h}{\partial x}\right)}$. The term K is often referred to as the diffusion

coefficient. Sometimes K is simply written as:

$$K = \frac{ch}{3S_o} \tag{3-24}$$

Equation (3-23) is also a standard form of wave equation, containing an extra "diffusion" term $K \frac{\partial^2 h}{\partial x^2}$, whose effect is to make h decrease in the view of an observer moving with velocity c. In this diffusion term is summed up the effects of the pressure term, which modifies the kinematic character of the flood wave and makes it subside.

The great advantage of the diffusion model is that if K and c are assumed to be constant, Eq. (3-23) has well-known explicit solutions, and thus the movement of the entire wave profile, however irregular it may be, can be traced with confidence.

3.2 MORE ON KINEMATIC WAVE MODEL

There is indeed a wide spectrum of problems encountered in hydrology where the kinematic assumption is valid; that is, the inflow, free surface slope, and inertia terms of the momentum equation are negligibly small in comparison with those of bottom slope and friction. An order of magnitude analysis will show that these conditions are satisfied by overland flow and certain gradually varied flows (Eagleson, 1970). Then there exists, to sufficient accuracy, a functional relationship (considering a one-dimensional flow system) between (a) the flow Q (quantity passing a given point in unit time), (b) the concentration, h (quantity per unit distance), and (c) the position x. Under these conditions there exist waves that are referred to as kinematic waves. On the assumption of this functional relationship the wave property follows from the equation of continuity

alone (Lighthill and Whitham, 1955). The classical wave motions are in contrast described by dynamic waves.

One important difference between the kinematic waves and the dynamic waves is that the former possess only one wave velocity at each point, while the latter possess at least two (forwards and backwards relative to the medium). This is because the equation of continuity Eq. (3-1) is of the first order only (which states that the quantity in a small element of length changes at a rate equal to the difference between the inflow and outflow).

Consider the continuity equation without lateral inflow (i.e., $q(x,t) = 0$); that is

$$\frac{\partial h}{\partial t} + \frac{\partial Q}{\partial x} = 0 \tag{3-25}$$

If it is assumed that

$$Q = Q(h,x) \tag{3-26}$$

then, on multiplying Eq. (3-25) by

$$c = \left(\frac{\partial Q}{\partial h}\right)_{x \text{ constant}} = c(h,x) \tag{3-27}$$

we obtain:

$$\frac{\partial Q}{\partial t} + c \frac{\partial Q}{\partial x} = 0 \tag{3-28}$$

This implies that Q is constant on waves travelling past the point with velocity c given by Eq. (3-27). Mathematically, the equation has one

system of 'characteristics' given by dx = c dt, and along each of these the flow Q is constant. The wave velocity, c, given by Eq. (3-27), is the slope of the flow-concentration curve for fixed x. This is often referred to as Kleitz-Seddon Law.

We can express the wave velocity c in terms of the mean velocity u at a point. That is

$$u = \frac{Q}{h} \tag{3-29}$$

$$c = \frac{d}{dh}(uh) = u + h\frac{du}{dh}$$

Thus c > u when the mean velocity increases with concentration, as is the case in rivers and channels, while c < u when it decreases with concentration (as in traffic flow).

Kinematic waves are not dispersive, but they suffer change of form due to nonlinearity (dependence of the wave velocity c on the flow Q carried by the wave) exactly as do the travelling sound waves of finite amplitude. This might be called 'amplitude dispersion' in contrast to 'frequency dispersion'. Accordingly, continuous wave forms may develop discontinuities, due to the overtaking of slower waves by faster ones. This results in the formation of shock and the waves responsible for this phenomenon are called shock waves.

The law of motion of kinematic shock is derived from equation of continuity, as was the law governing continuous kinematic waves. If the flow and concentration take the values Q_1, h_1 on one side, and Q_2, h_2 on the other side, of the shock wave which moves with speed U, then the

quantity crossing per unit time may be written either as $Q_1 - Uh_1$ or as $Q_2 - Uh_2$. This gives the velocity of the shock wave as:

$$U = \frac{Q_2 - Q_1}{h_2 - h_1} \tag{3-30}$$

This is the slope of the chord joining the two points on the flow concentration curve (for given x) which correspond to the states ahead of and behind the shock wave when it reaches x. In the limit when the shock wave becomes a continuous wave, the slope of the chord becomes the slope of the tangent and the velocity given by Eq. (3-30) coincides with that given by Eq. (3-27). We will not dwell upon the shock phenomenon in this report. For an elaborate mathematical discussion on it see the reference by Lighthill and Whitham (1955).

3.3 ADEQUACY OF KINEMATIC WAVE THEORY

In this section we show under what conditions the kinematic wave theory is adequate for application to problems of hydrologic significance.

3.3.1 Kinematic Wave Number

Woolhiser and Ligget (1967) derived a single dimensionless parameter, later called as kinematic wave number, by which to show the goodness of kinematic wave approximation. In order to derive this parameter it is convenient to normalize Eqs. (3-1) and (3-2) by introducing the following normalizing quantities:

$Q_{max} = q_{max} L_o$, maximum steady-state flow rate at $x = L_o$; q_{max} is maximum rate of lateral inflow; and L_o = length of the plane.

H_o = normal depth at $x = L_o$ with a discharge Q_{max} and velocity $V_o = Q_{max}/H_o = C\, H_o^{0.5}\, S_o^{0.5}$ where C = Chezy's coefficient.

Utilizing these normalizing quantities the following dimensionless quantities, denoted with asterisks, are obtained.

$$x_* = \frac{x}{L_o} \; ; \; h_* = \frac{h}{H_o} \; ; \quad u_* = \frac{u}{V_o} \; ; \; t_* = \frac{tV_o}{L_o} \; ; \; R = \frac{q}{q_{max}} \tag{3-31}$$

Substituting these dimensionless quantities into Eqs. (3-1) and (3-2) we obtain:

$$\frac{\partial h_*}{\partial t_*} + \frac{\partial Q_*}{\partial x_*} = R \tag{3-32}$$

This is the dimensionless form of continuity equation given by Eq. (3-1).

$$\frac{V_o^2}{L_o} \frac{\partial u_*}{\partial t_*} + \frac{V_o^2 u_*}{L_o} \frac{\partial u_*}{\partial x_*} + g \frac{H_o}{L_o} \frac{\partial h_*}{\partial x_*} = gS_o\left(1 - \frac{S_f}{S_o}\right) - \frac{R\, q_{max}\, V_o u_*}{H_o\, h_*} \tag{3-33}$$

Recalling $F = \frac{V_o}{(gH_o)^{0.5}}$; $S_f = \frac{u^2}{Ch}$; where F is Froude number; we can write Eq. (3-33) as:

$$\frac{\partial u_*}{\partial t_*} + u_* \frac{\partial u_*}{\partial x_*} + \frac{1}{F^2} \frac{\partial h_*}{\partial x_*} = \frac{S_o L_o}{F^2 H_o} \left(1 - \frac{u_*^2}{h_*}\right) - \frac{R u_*}{h_*} \tag{3-34}$$

This is a dimensionless form of momentum equation given by Eq. (3-2).

Then the kinematic wave number, K, is defined as:

$$K = \frac{S_o L_o}{F^2 H_o} \tag{3-35}$$

This parameter reflects the effects of length and slope of the plane as well as the normal flow variables. Woolhiser and Ligget (1967) showed experimentally that for $K > 20$ the kinematic wave approximation was very good, and for $10 \leq K < 20$ the errors introduced by the kinematic wave approximation would be small and acceptable for most engineering purposes.

3.3.2 Froude Number

In a natural flood wave both kinematic and dynamic wave movements are present. The bed slope, S_o, is by far the most important slope term; the major bulk of the flood wave moves substantially as a kinematic wave, even if the other three slope terms (acceleration and convective terms) are not negligible. The presence of these less significant slope terms modifies the character of the flood wave, but its speed may be expected to approximate to that of the kinematic wave. Unless these three slope terms are absolutely negligible (which they seldom are) they will produce dynamic wave fronts moving at speeds $u \pm\sqrt{gy}$ in front of and behind the main body of the flood wave as shown in Fig. 3-1.

In contrast with single wave speed of kinematic waves, dynamic waves have two speeds, indicated by the two characteristic directions on the x-t plane. The physical implication is that a dynamic disturbance will propagate in both the upstream and downstream directions; while a kinematic disturbance will propagate only in the downstream direction.

For a wide rectangular channel with constant Chezy's C we see that

$$c = \frac{3}{2} u \tag{3-36}$$

where c = kinematic wave speed. This is less than the speed of the leading

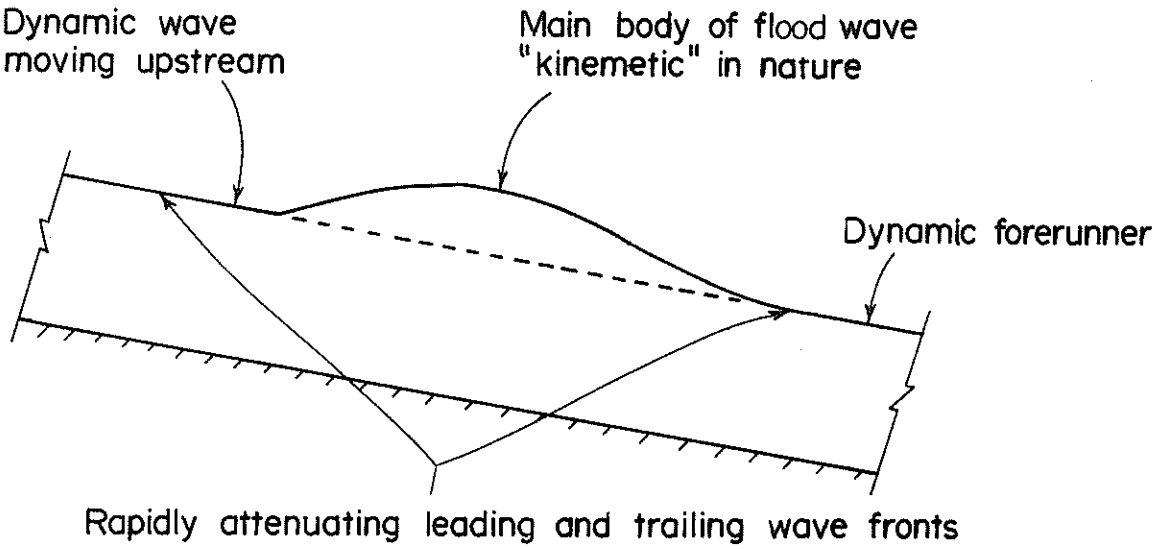

Fig. 3-1. Movement of the natural flood wave (after Lighthill and Whitham, 1955).

dynamic wave, $u + \sqrt{gh}$, provided that $\frac{1}{2} u < \sqrt{gh}$; that is, $F < 2$, a condition which is fulfilled in most natural rivers except mountain torrents. If this condition is fulfilled the leading dynamic wave will be ahead of the main (kinematic) wave; the other dynamic wave will be behind the main wave, since $(u - \sqrt{gh})$ must always be less than c.

The above explanation establishes that the leading dynamic wave acts as a forerunner of the main wave. The question arises whether it will bring about any appreciable rise of the water level before the arrival of the main wave. If $F < 2$, a positive wave of this kind will attenuate as it moves downstream in most cases. In the normal natural flood the dynamic forerunner will attenuate rapidly unless $F > 2$. When $F > 2$, the kinematic wave should overtake the dynamic forerunner; clearly, such an event would lead to the steepening of the dynamic wave front. This particular interpretation gives a deeper significance to the criterion $F \gtrless 2$, for it suggests an actual mechanism by which the wave front steepens when $F \geq 2$.

3.3.3 Escoffer's Criterion

The analysis by Escoffer shows that the general form of the criterion, $F \gtrless 2$, is

$$\frac{du_o}{dw} \gtrless 1 \qquad (3\text{-}36)$$

where u_o = uniform flow velocity appropriate to a given depth, and w = stage variable, defined by

$$dw = C_d \frac{dA}{A} \qquad (3\text{-}37)$$

where $C_d = \sqrt{gA/B}$, dynamic wave velocity relative to the water, A = cross-sectional area of flow, and B = width of the section. Then the kinematic wave speed will be greater or less than the dynamic wave speed according to

$$A \frac{du_o}{dA} \gtrless C_d \tag{3-38}$$

where u has been replaced by u_o because the existence of the kinematic wave postulates a uniform flow relationship between u and A.

CHAPTER 4

KINEMATIC WAVE MODELS OF SURFACE RUNOFF FROM IMPERVIOUS SURFACES

4.1 GENERAL REMARKS

The traditional formulation of the kinematic wave theory assumes the kinematic wave friction relationship parameter to be constant. The present study waives this assumption of parameter constancy, allows continuous spatial variability in the parameter and develops a more general formulation of the kinematic wave theory. This concept of parameter variability leads to a completely distributed model and might eliminate the necessity of utilizing a complex network model to represent the watershed system. Furthermore, more general formulation will reduce the complexity of modeling watershed surface runoff, and will greatly save computational time and effort.

The traditional formulation of the kinematic wave theory has been as follows:

The continuity equation for a plane section,

$$\frac{\partial h}{\partial t} + u \frac{\partial h}{\partial x} + h \frac{\partial u}{\partial x} = q(x,t) \tag{4-1}$$

and the kinematic approxiamtion to momentum equation,

$$Q = \alpha h^n \tag{4-2}$$

where h = local depth, u = local average velocity, $q(x,t)$ = rate of effective lateral inflow per unit area varying in time and space, Q = outflow per unit width, x = space coordinate, t = time coordinate, n = exponent, and α = kinematic wave friction relationship parameter.

Equations (4-1) and (4-2) constitute the traditional formulation of kinematic wave theory. A close examination of Eqs. (4-1) and (4-2) can easily show that the structure of a kinematic wave model of watershed surface runoff will depend on the characterization of parameter α and the geometric configuration chosen to represent the natural watershed geometry. It is apparent from

Eq. (4-2) that in the traditional formulation the kinematic wave friction relationship parameter is treated as constant. One approach that partly relaxes the assumption of parameter constancy is to employ a network model which considers the parameter to be different for different elements in the network. Although a network model may be made so complex as to provide an almost perfect representation of the watershed system, it will be too complex and too time-consuming to be of any operational value.

Four geometric configurations have been hypothesized in the literature to represent the geometry of a natural watershed. Accordingly, kinematic wave models of watershed surface runoff can be classified into four groups:

1. Converging overland flow model as shown in Fig. 4-1.
2. Wooding's model as shown in Fig. 4-2.
3. Composite section model as shown in Fig. 4-3.
4. Cascade model as shown in Fig. 4-4.

These models involve varying degrees of geometric abstractions, and are either lumped or at most quasi-distributed depending upon the characterization of parameter α . The converging flow model (Woolhiser, 1969; Singh, 1974, 1975a, 1975b) is a lumped parameter model. Of all it has the highest degree of geometric abstraction. Wooding's model (Wooding, 1965a, 1965b, 1966) has relatively lesser degree of abstraction. This is also a lumped parameter model, or at most quasi-distributed if the parameter α is allowed to vary from one element to another in the network geometry. The composite section model (Singh, 1974) - a combination of the two previous models - has even lesser degree of abstraction. This will be quasi-distributed if the parameter α is allowed to be different for different elements in the network geometry. The cascade model (Brakensiek, 1967; Kibler and Woolhiser, 1970; Singh, 1974) has the least order of abstraction and hence more close to reality.

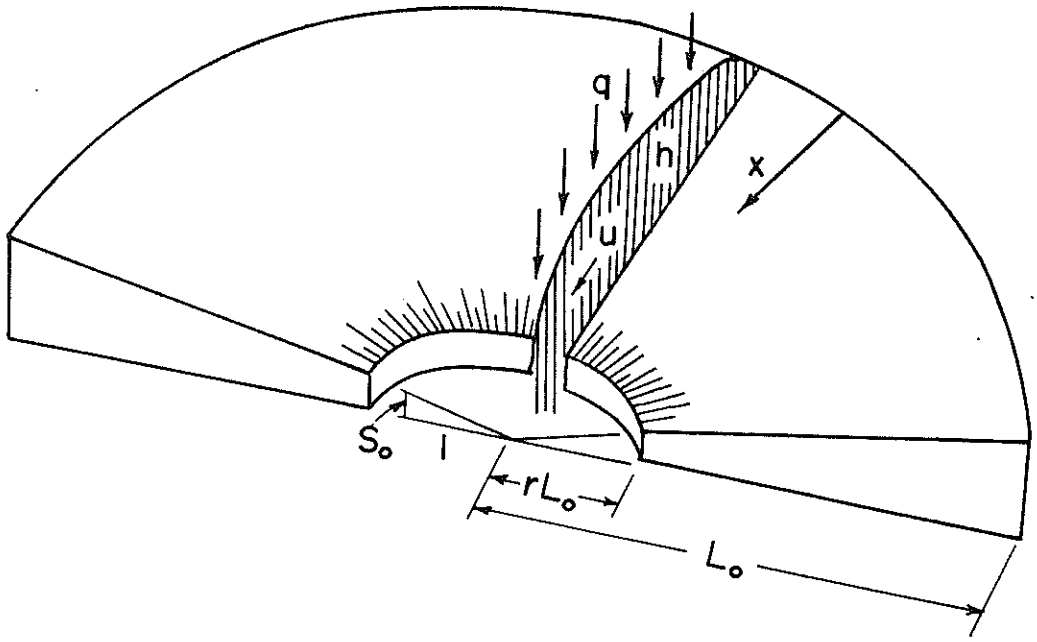

Fig. 4-1. Geometry of a converging section.

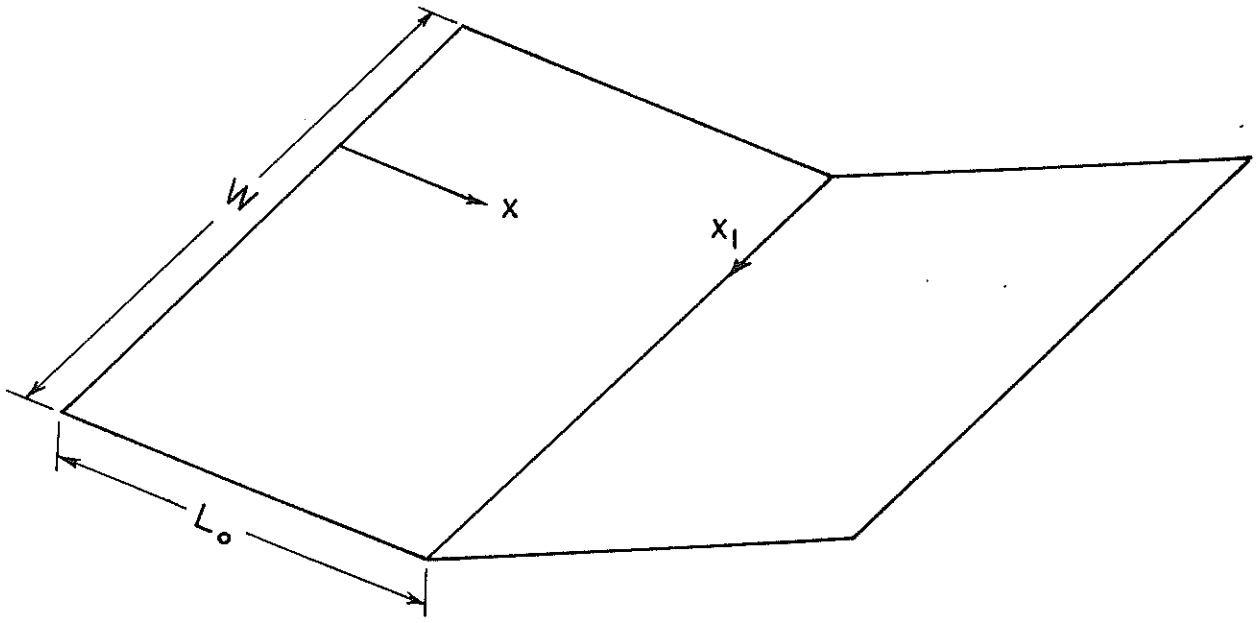

Fig. 4-2. Geometry of Wooding's runoff model.

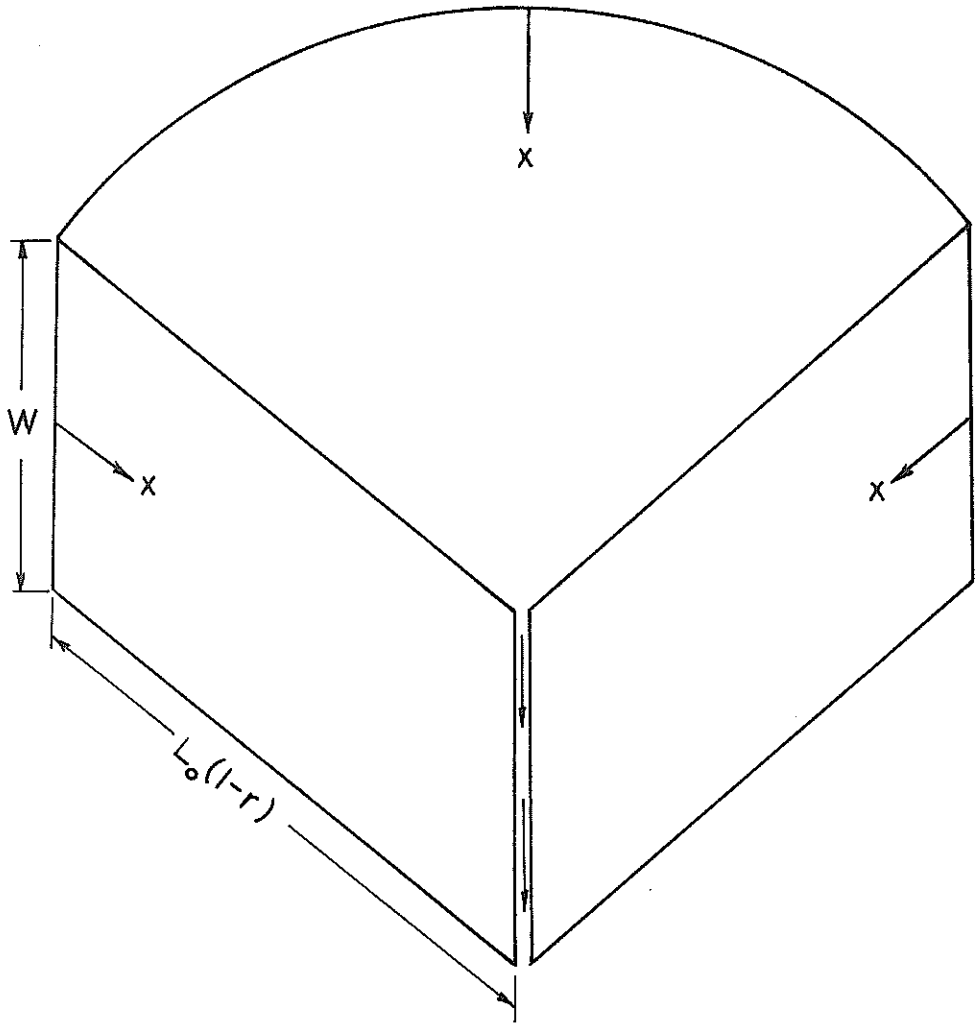

Fig. 4-3. Geometry of a composite section model.

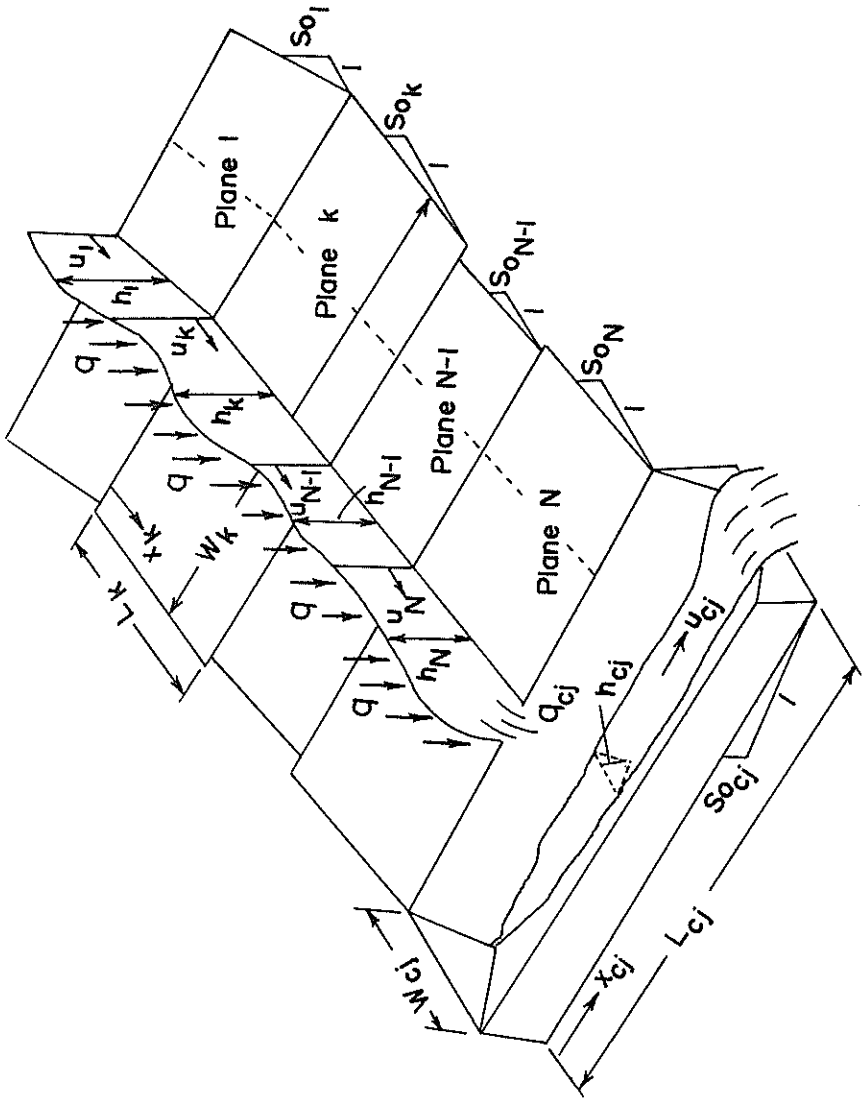

Fig. 4-4. Geometry of a cascade of N planes discharging into the jth channel.

The cascade network geometry can even be made so complex as to provide an almost perfect representation of the watershed geometry. Allowing the parameter α to vary from one element to another will make the cascade model as a quasi-distributed model.

A consideration of watershed runoff dynamics will suggest that the watershed surface roughness characteristics have more predominant influence on the runoff generation process than the geometry as such. In the present context, the roughness characteristics are being represented by the parameter α . It then follows that the above geometric configurations have been advanced primarily to better represent the spatial distribution of the parameter α ; and that the necessity of a complex geometric configuration can be eliminated by simply allowing the parameter α to vary continuously in space. By so doing, the resulting model will be simple and completely distributed. It is interesting to note that this concept of parameter variability is not artificial, but is consistent with runoff dynamics. This is the hypothesis that the proposed study attempts to develop and test by considering its application to natural agricultural watersheds. It must, however, be made clear that by no means we are suggesting here that geometric details will have no influence on runoff process at all.

4.2 DISTRIBUTED KINEMATIC WAVE MODELS

The kinematic wave equations of continuity and momentum can be rewritten in most general one-dimensional form as:

$$\frac{\partial h}{\partial t} + u \frac{\partial h}{\partial x} + h \frac{\partial u}{\partial x} = q(x,t) \tag{4-3}$$

$$Q = \alpha(x,t)\ h^n \tag{4-4}$$

Here the parameter α is a function of both space and time. For a specified rainfall duration T, $q(x,t) = 0$ when $t > T$. We assume $n > 1$. Substituting

Eq. (4-4) into Eq. (4-3) we obtain:

$$\frac{\partial h}{\partial t} + h^n \frac{\partial \alpha(x,t)}{\partial x} + \alpha(x,t)\ n\ h^{n-1} \frac{\partial h}{\partial x} = q(x,t) \qquad (4\text{-}5)$$

Equation (4-5) holds in $S = \{0 < x < L_o,\ t > 0\}$. Depending upon the distributional characteristics of $\alpha(x,t)$ and $q(x,t)$ we can have sixteen special cases of Eq. (4-5):

When $\alpha(x, t) = \alpha$, a constant then

(1) $q(x,t) = q$, a constant

(2) $q(x,t) = q(x)$

(3) $q(x,t) = q(t)$

(4) $q(x,t)$

When $\alpha(x,t) = \alpha(x)$, then

(5) $q(x,t) = q$

(6) $q(x,t) = q(x)$

(7) $q(x,t) = q(t)$

(8) $q(x,t)$

When $\alpha(x,t) = \alpha(t)$, then

(9) $q(x,t) = q$

(10) $q(x,t) = q(x)$

(11) $q(x,t) = q(t)$

(12) $q(x,t)$

When $\alpha(x,t) = \alpha(x,t)$, then

(13) $q(x,t) = q$

(14) $q(x,t) = q(x)$

(15) $q(x,t) = q(t)$

(16) $q(x,t)$

However, it may be interesting to note the two special cases:

1. When the parameter α is constant then Eq. (4-5) becomes:

$$\frac{\partial h}{\partial t} + n\alpha h^{n-1} \frac{\partial h}{\partial x} = q(x,t) \tag{4-6}$$

This is the familiar case which has been extensively investigated.

2. When the parameter α is a function of space only, then Eq.(4-5) takes the form:

$$\frac{\partial h}{\partial t} + h^n \frac{\partial \alpha(x)}{\partial x} + n\,\alpha(x)\, h^{n-1} \frac{\partial h}{\partial x} = q(x,t) \tag{4-7}$$

This case has not been investigated before. The present study attempts to investigate it. It is obvious that the former case given by Eq. (4-6) is also a special case of the latter given by Eq. (4-7).

4.3 MATHEMATICAL SOLUTIONS OF NONLINEAR WATERSHED DYNAMICS

We desire solution to Eq. (4-7). In the context of watershed surface runoff problem it is reasonable to assume the following boundary conditions:

$$\begin{aligned} h(o,t) &= o \ , \ o \leq t \leq T \\ h(x,o) &= o \ , \ o \leq x \leq L_o \end{aligned} \tag{4-8}$$

These conditions represent an initially dry surface. It is physically plausible that $h(o,t)$ should not be specified for $t > T$, that is, the solution of Eq. (4-5) in S below $t = T$ subject to Eq. (4-8) should extend into S above $t = T$. This will be seen to be true in the ensuing mathematical discussion.

It must be pointed out that here $q(x,t)$ forms input to the model. Its hydrological significance is twofold:

(1) Rainfall or any other source of lateral inflow will directly contribute to input. This implies that the watershed surface is impervious, and infiltration is disregarded. This is true for parking lots, highways, runways, etc.

(2) Rainfall-excess forms the input to the model. Here infiltration is considered, and subtracted from rainfall to yield rainfall-excess. An important

implication of this notion of rainfall-excess is that infiltration is allowed to take place only during the period of rainfall. As soon as rainfall ceases to exist, infiltration is assumed to cease simultaneously. This assumption, although far from reality, has been and continues to be utilized in most studies on hydrologic modeling.

In developing solutions to Eqs. (4-7) and (4-8) we employ the method of characteristics. According to this method, the characteristic curves of Eq. (4-7) are the solutions of:

$$\frac{dt}{ds} = 1$$

$$\frac{dx}{ds} = n\,\alpha(x)h^{n-1}$$

$$\frac{dh}{ds} = q(x,t) - h^n \frac{d\alpha(x)}{dx}$$

where s is a parameter.

Through each point of space (x,t,h) there passes a unique characteristic curve. Therefore the solution of Eqs. (4-7) and (4-8) is the surface formed by all the characteristic curves passing through the segment $t = o,\ o \leq x \leq L_o$ and and the segment $x = o,\ o \leq t \leq T$ (in appendix A we show that this solution extends into all of S above $t = T$). Figure 4-5 shows the projections of these characteristic curves onto the (x,t) plane. To obtain the surface formed by characteristic curves we may prefer to take x, instead of s, as independent parameter. Then we may write:

$$\frac{dt}{dx} = \frac{1}{n\,\alpha(x)\,h^{n-1}} \tag{4-9}$$

$$\frac{dh}{dx} = \frac{q(x,t)}{n\,\alpha(x)\,h^{n-1}} - \frac{h^n}{\alpha(x)\,n\,h^{n-1}} \frac{d\alpha(x)}{dx} \tag{4-10}$$

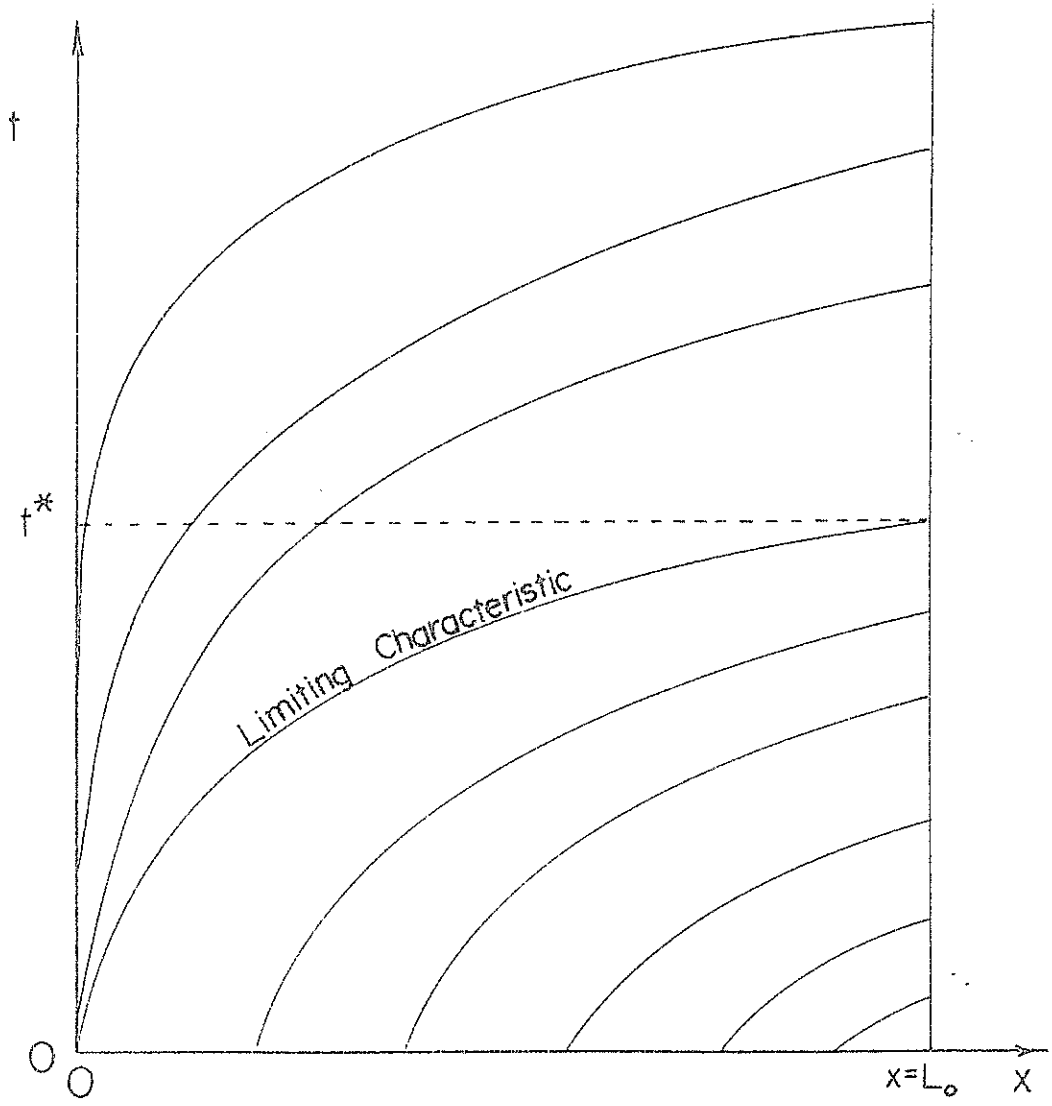

Fig. 4-5. Kinematic wave diagram.

The initial conditions are:

$t(o) = t_o$; $h(o) = o$

or

$t(x_o) = o$; $h(x_o) = o$

The solutions of Eqs. (4-9) and (4-10) will be the solutions of Eq. (4-7). To obtain the solutions of Eqs.(4-9) and (4-10) we distinguish two cases:

1. Case A. The characteristic curve $t = t(x,o)$ through the origin (o,o) intersects $x = L_o$ (the downstream boundary) before it intersects $t = T$ (the duration of rainfall $q(x,t)$). This case will result in equilibrium hydrograph, and is shown in Fig. 4-6. Thus $t^* \leq T$. The characteristic issuing from the origin is called as the limiting characteristic. Here t^* is identical to watershed equilibrium time.
2. Case B. The characteristic curve $t = t(x,o)$ through the origin (o,o) intersects $t = T$ before it intersects the downstream boundary $x = L_o$. This case will result in partial equilibrium hydrograph, and is shown in Fig. 4-7. Thus $t^* > T$ for this case. Here t^* will depend on T, and is not equal to t^* of Case A.

The solutions to these two cases will completely characterize the surface runoff hydrograph. We will develop mathematical solutions to these two cases.

4.3.1 Case A: Equilibrium Situation

We can write the input $q(x,t)$ as:

$$q(x,t) = \begin{cases} q(x,t) & o \leq t \leq T \quad ; \quad T \geq t^* \\ o & t > T \end{cases}$$

where T = rainfall duration, and t^* = time taken by the characteristic to travel from the origin to the downstream boundary. It must be noted that here t^* is independent of T , and may be characterized as the watershed equilibrium time. For this case we divide the solution domain into four subdomains as

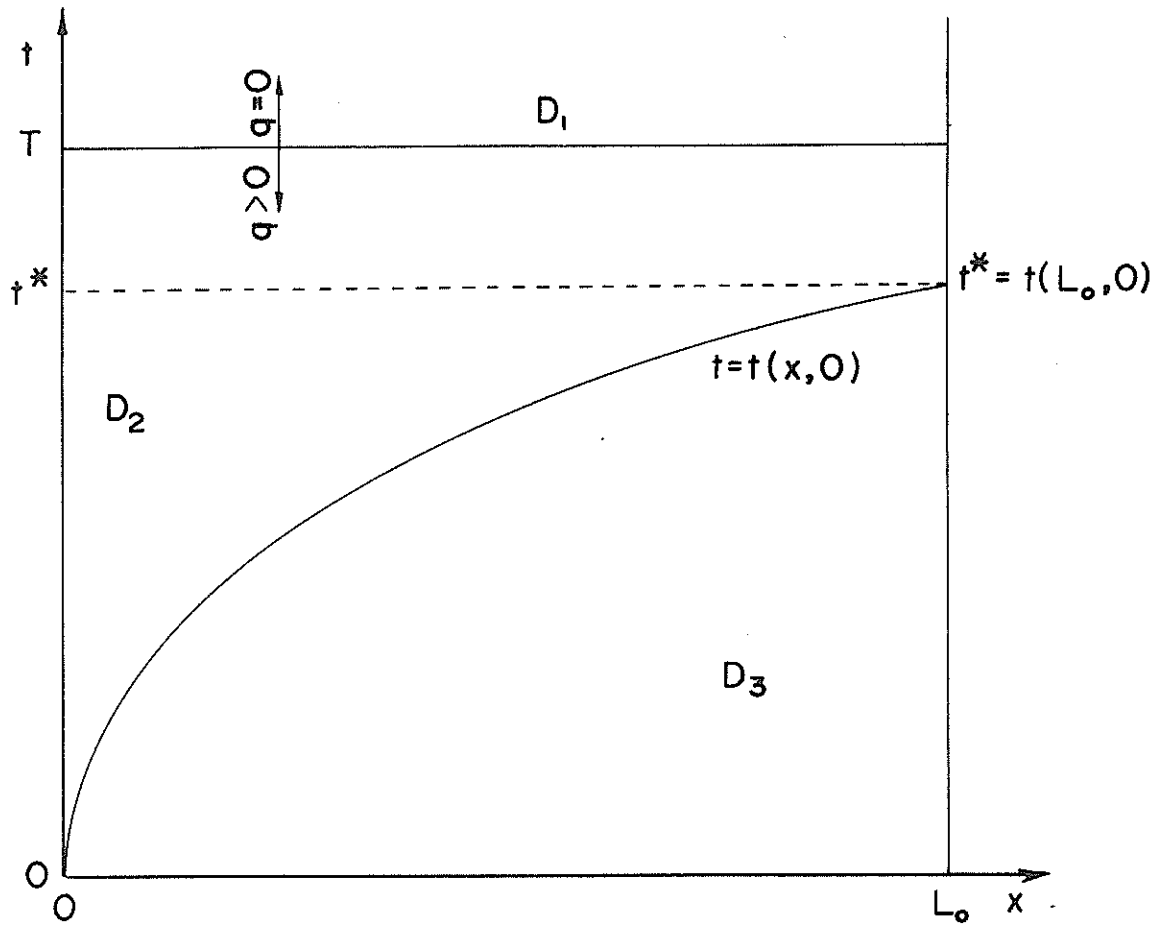

Fig. 4-6. Solution domain for equilibrium hydrograph.

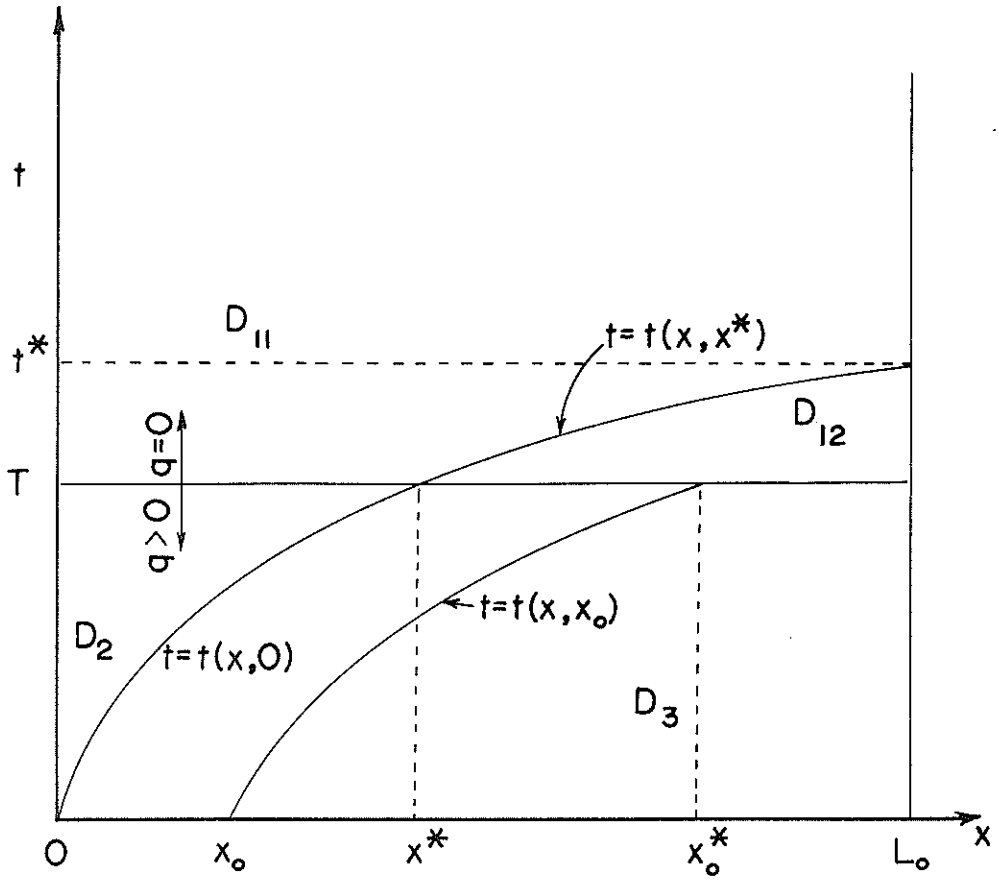

Fig. 4-7. Solution domain for partial equilibrium hydrograph.

as shown in Fig. 4-6. First we wish to obtain the surface formed by the characteristics passing through the t-axis. We have:

Domain D_2. For this domain we can write our initial conditions as:

$t(o) = t_o \quad , \quad 0 \leq t_o \leq T$

$h(o) = 0$

The solution surface is then expressed in terms of x and t_o where:

$t = t(x,t_o)$

$h = h(x,t_o)$

$x = x$

We will assume that, under appropriate conditions on $\alpha(x)$ and $q(x,t)$, the curves $t = t(x,t_o)$ do not, for distinct values of t_o, intersect in S. It will be seen in appendix B that this is true for $q(x,t) = q$, a constant. $t(x,t_o)$ is an increasing function of x for fixed t_o since $h(x) > o$ in S (from Eq.(4-12) below) and, by our nonintersection assumption, it is an increasing function of t_o. Thus we can solve for t_o in $t = t(x,t_o)$ and we can, therefore, express h as a function of x and t.

We can write Eq. (4-10) as:

$$\frac{d(\alpha(x)\ h^n)}{dx} = q(x,t)$$

Integrating and using the condition $h(o) = o$ we obtain:

$$\alpha(x)\ h^n = \int_o^x q(\xi,t(\xi,t_o))\ d\xi$$

Thus we have:

$$h(x,t_o) = \left\{\frac{1}{\alpha(x)} \int_o^x q(\xi,t(\xi,t_o))\ d\xi\right\}^{\frac{1}{n}} \tag{4-12}$$

Inserting Eq. (4-12) into Eq. (4-9):

$$\frac{dt}{dx} = \frac{1}{n\ \alpha(x)} \left\{\frac{1}{\alpha(x)} \int_o^x q(\xi,t(\xi,t_o))\ d\xi\right\}^{\frac{1-n}{n}}$$

or

$$t(x,t_o) = t_o + \frac{1}{n}\int_o^x \left[\frac{1}{\alpha(\eta)}\right]^{\frac{1}{n}} \left\{\int_o^\eta q(\xi,t(\xi,t_o))\, d\xi\right\}^{\frac{1-n}{n}} d\eta \qquad (4\text{-}13)$$

Equation (4-13) is a nonlinear integral equation for $t(x,t_o)$ whose solution will depend on the functional form of α in space and that of q in time and space. Inserting the solution of Eq. (4-13) into Eq. (4-12) we get $h(x,t_o)$. We now examine seven special cases:

1. If $q(x,t)$ is constant then we get explicit solutions:

$$h(x,t_o) = \left\{\frac{qx}{\alpha(x)}\right\}^{\frac{1}{n}} \qquad (4\text{-}14)$$

$$t(x,t_o) = t_o + \frac{q}{n}^{\frac{1-n}{n}} \int_o^x \left\{\frac{1}{\alpha(\xi)}\right\}^{\frac{1}{n}} \left\{\xi\right\}^{\frac{1-n}{n}} d\xi \qquad (4\text{-}15)$$

2. If $q(x,t)$ varies in space only, then we obtain:

$$h(x,t_o) = \left\{\frac{1}{\alpha(x)}\int_o^x q(\xi)\, d\xi\right\}^{\frac{1}{n}} \qquad (4\text{-}16)$$

$$t(x,t_o) = t_o + \frac{1}{n}\int_o^x \left[\frac{1}{\alpha(\eta)}\right]^{\frac{1}{n}} \left\{\int_o^\eta q(\xi)\, d\xi\right\}^{\frac{1-n}{n}} d\eta \qquad (4\text{-}17)$$

3. If $q(x,t)$ varies in time only, then we obtain:

$$h(x,t_o) = \left\{\frac{1}{\alpha(x)}\int_o^x q(t(\xi,t_o))\, d\xi\right\}^{\frac{1}{n}} \qquad (4\text{-}18)$$

$$t(x,t_o) = t_o + \frac{1}{n}\int_o^x \left[\frac{1}{\alpha(\eta)}\right]^{\frac{1}{n}} \left\{\int_o^\eta q(t(\xi,t_o))\, d\xi\right\}^{\frac{1-n}{n}} d\eta \qquad (4\text{-}19)$$

4. If $\alpha(x)$ and $q(x,t)$ both are constant then we get:

$$h(x,t_o) = \left\{\frac{qx}{\alpha}\right\}^{\frac{1}{n}} \tag{4-20}$$

$$t(x,t_o) = t_o + q^{\frac{1-n}{n}} \left(\frac{x}{\alpha}\right)^{\frac{1}{n}} \tag{4-21}$$

5. If $\alpha(x)$ is constant but $q(x,t)$ varies in both time and space, then we get:

$$h(x,t_o) = \left\{\frac{1}{\alpha} \int_o^x q(\xi,t(\xi,t_o))\ d\xi\right\}^{\frac{1}{n}} \tag{4-22}$$

$$t(x,t_o) = t_o + \frac{1}{n} \left(\frac{1}{\alpha}\right)^{\frac{1}{n}} \int_o^x \left\{ \int_o^\eta q(\xi,t(\xi,t_o))\ d\xi \right\}^{\frac{1-n}{n}} d\eta \tag{4-23}$$

6. If $\alpha(x)$ is constant but $q(x,t)$ varies in space only, then we obtain:

$$h(x,t_o) = \left\{\frac{1}{\alpha} \int_o^x q(\xi)\ d\xi\right\}^{\frac{1}{n}} \tag{4-24}$$

$$t(x,t_o) = t_o + \frac{1}{n} \left(\frac{1}{\alpha}\right)^{\frac{1}{n}} \int_o^x \left\{ \int_o^\eta q(\xi)\ d\xi \right\}^{\frac{1-n}{n}} d\eta \tag{4-25}$$

7. If $\alpha(x)$ is constant but $q(x,t)$ varies in time only, then we get:

$$h(x,t_o) = \left\{\frac{1}{\alpha} \int_o^x q(t(\xi,t_o))\ d\xi\right\}^{\frac{1}{n}} \tag{4-26}$$

$$t(x,t_o) = t_o + \frac{1}{n} \left(\frac{1}{\alpha}\right)^{\frac{1}{n}} \int_o^x \left\{ \int_o^\eta q(t(\xi,t_o))\ d\xi \right\}^{\frac{1-n}{n}} d\eta \tag{4-27}$$

From the above discussion it is clear that in the strip $\{o \le x \le L_o$, $t(x,o) \le t \le T\} \equiv D_2$, the surface h, as a function of x and t, depends only on x if $q(x,t)$ is constant or varies in space only regardless of the functional form of $\alpha(x)$. Also, the characteristics issuing from the t-axis will have t-axis as their tangent. This is implied by Eq. (4-9), that is, $\frac{dt}{dx} \to \infty$ at $x = o$, $t_o = o$.

Domain D_3. To obtain the surface containing the x-axis, that is h in D_3, we solve Eqs. (4-9) and(4-10) subject to the boundary conditions:

$t(x_o) = o \quad , \quad o \leq x_o \leq L_o$

$h(x_o) = o$

Then the solution surface is expressed in terms of x and x_o:

$t = t(x,x_o)$

$h = h(x,x_o)$

$x = x$

We again assume that the curves $t = t(x,x_o)$ do not intersect for distinct values of x_o. Thus $t(x,x_o)$ is, for fixed x_o, an increasing function of x and, for fixed x, a decreasing function of x_o. This nonintersection property will be proved in appendix B under the condition $q(x,t)$ a constant and $\alpha(x)$ an increasing function of x.

The solution of Eqs. (4-9) and (4-10) subject to the above specified boundary conditions is:

$$h(x,x_o) = \left\{\frac{1}{\alpha(x)} \int_{x_o}^{x} q(\xi,t(\xi,x_o))\, d\xi\right\}^{\frac{1}{n}} \tag{4-28}$$

$$t(x,x_o) = \frac{1}{n} \int_{x_o}^{x} \left(\frac{1}{\alpha(\eta)}\right)^{\frac{1}{n}} \left\{\int_{x_o}^{\eta} q(\xi,t(\xi,x_o))\, d\xi\right\}^{\frac{1-n}{n}} d\eta \tag{4-29}$$

Equation (4-29) is a nonlinear integral equation for $t(x,x_o)$. We get $h(x,x_o)$ by inserting the solution of Eq. (4-29) into Eq.(4-28). For this domain the seven special cases are:

1. If $q(x,t)$ is constant then we get explicit solutions:

$$h(x,x_o) = \left\{\frac{q(x-x_o)}{\alpha(x)}\right\}^{\frac{1}{n}} \tag{4-30}$$

$$t(x,x_o) = \frac{q}{n}^{\frac{1-n}{n}} \int_{x_o}^{x} \left\{\frac{1}{\alpha(\eta)}\right\}^{\frac{1}{n}} (\eta-x_o)^{\frac{1-n}{n}} \, d\eta \tag{4-31}$$

2. If $q(x,t)$ varies in space only, then we get:

$$h(x,x_o) = \left\{\frac{1}{\alpha(x)} \int_{x_o}^{x} q(\xi) \, d\xi\right\}^{\frac{1}{n}} \tag{4-32}$$

$$t(x,x_o) = \frac{1}{n} \int_{x_o}^{x} \left(\frac{1}{\alpha(\eta)}\right)^{\frac{1}{n}} \left\{\int_{x_o}^{\eta} q(\xi) \, d\xi\right\}^{\frac{1-n}{n}} d\eta \tag{4-33}$$

3. If $q(x,t)$ varies in time only, then we get:

$$h(x,x_o) = \left\{\frac{1}{\alpha(x)} \int_{x_o}^{x} q(t(\xi,x_o)) \, d\xi\right\}^{\frac{1}{n}} \tag{4-34}$$

$$t(x,x_o) = \frac{1}{n} \int_{x_o}^{x} \left\{\frac{1}{\alpha(\eta)}\right\}^{\frac{1}{n}} \left\{\int_{x_o}^{\eta} q(t(\xi,x_o) \, d\xi\right\}^{\frac{1-n}{n}} d\eta \tag{4-35}$$

4. If $\alpha(x)$ and $q(x,t)$ both are constant then we obtain:

$$h(x,x_o) = \left\{\frac{q}{\alpha} (x-x_o)\right\}^{\frac{1}{n}} \tag{4-36}$$

$$t(x,x_o) = \left\{\frac{x-x_o}{\alpha}\right\}^{\frac{1}{n}} q^{\frac{1-n}{n}} \tag{4-37}$$

5. If $\alpha(x)$ is constant but $q(x,t)$ varies in time and space, then we obtain:

$$h(x,x_o) = \left\{\frac{1}{\alpha} \int_{x_o}^{x} q(\xi,t(\xi,x_o)) \, d\xi\right\}^{\frac{1}{n}} \tag{4-38}$$

$$t(x,x_o) = \frac{1}{n} \left(\frac{1}{\alpha}\right)^{\frac{1}{n}} \int_{x_o}^{x} \left\{\int_{x_o}^{\eta} q(\xi,t(\xi,x_o)) \, d\xi\right\}^{\frac{1-n}{n}} d\eta \tag{4-39}$$

6. If $\alpha(x)$ is constant but $q(x,t)$ varies in space only, then we obtain:

$$h(x,x_o) = \left\{\frac{1}{\alpha}\int_{x_o}^{x} q(\xi)\ d\xi\right\}^{\frac{1}{n}} \tag{4-40}$$

$$t(x,x_o) = \frac{1}{n}\left(\frac{1}{\alpha}\right)^{\frac{1}{n}}\int_{x_o}^{x}\left\{\int_{x_o}^{\eta} q(\xi)\ d\xi\right\}^{\frac{1-n}{n}} d\eta \tag{4-41}$$

7. If $\alpha(x)$ is constant but $q(\xi,t)$ varies in time only, then we obtain:

$$h(x,x_o) = \left\{\frac{1}{\alpha}\int_{x_o}^{x} q(t(\xi,x_o))\ d\xi\right\}^{\frac{1}{n}} \tag{4-42}$$

$$t(x,x_o) = \frac{1}{n}\left(\frac{1}{\alpha}\right)^{\frac{1}{n}}\int_{x_o}^{x}\left\{\int_{x_o}^{x} q(t(\xi,x_o))\ d\xi\right\}^{\frac{1-n}{n}} d\eta \tag{4-43}$$

It is clear from the above discussion that h, as a function of x and t, now depends on both x and t.

Domain D_1. We must modify Eqs. (4-9) and (4-10) subject to $q(x,t) = o$ for $t > T$. Thus we have:

$$\frac{dt}{dx} = \frac{1}{n\ \alpha(x)\ h^{n-1}} \tag{4-44}$$

$$\frac{dh}{dx} = -\frac{h}{n\ \alpha(x)}\frac{d\alpha(x)}{dx} \tag{4-45}$$

$$t(x_o^*) = T \tag{4-46}$$

$$h(x_o^*) = h(x_o^*,T) = h_o \tag{4-47}$$

where $h(x_o^*)$ is obtained from Eqs. (4-11) and (4-12). The solution in domain D_1 will be expressed in terms of x and x_o^*:

$t = t(x,x_o^*)$

$h = h(x,x_o^*)$

$x = x$

The solution to Eqs. (4-44) - (4-47) is:

$$h(x,x_o^*) = \left\{h_o{}^n \frac{\alpha(x_o^*)}{\alpha(x)}\right\}^{\frac{1}{n}} \tag{4-48}$$

$$t(x,x_o^*) = T+h_o{}^{1-n}\left\{\frac{1}{\alpha(x_o^*)}\right\}^{\frac{n-1}{n}} \frac{1}{n} \int_{x_o^*}^{x} \left\{\frac{1}{\alpha(\eta)}\right\}^{\frac{1}{n}} d\eta \tag{4-49}$$

By substituting the solution of Eq. (4-49) into Eq. (4-48) we obtain $h(x,x_o^*)$.

We now examine the seven special cases:

1. If $q(x,t)$ is constant then the solution is:

$$h_o = \left\{\frac{q\ x_o^*}{\alpha(x_o^*)}\right\}^{\frac{1}{n}} \tag{4-50}$$

$$h(x,x_o^*) = \left\{h_o{}^n \frac{\alpha(x_o^*)}{\alpha(x)}\right\}^{\frac{1}{n}} = \left\{\frac{q\ x_o^*}{\alpha(x)}\right\}^{\frac{1}{n}} \tag{4-51}$$

$$t(x,x_o^*) = T + \frac{(qx_o^*)^{\frac{1-n}{n}}}{n} \int_{x_o^*}^{x} \left\{\frac{1}{\alpha(\eta)}\right\}^{\frac{1}{n}} d\eta \tag{4-52}$$

2. If $q(x,t)$ varies in space only, then the solution becomes:

$$h_o = \left\{\frac{1}{\alpha(x_o^*)} \int_o^{x_o^*} q(\xi)\ d\xi\right\}^{\frac{1}{n}} \tag{4-53}$$

$$h(x,x_o^*) = \left\{h_o{}^n \frac{\alpha(x_o^*)}{\alpha(x)}\right\}^{\frac{1}{n}} = \left\{\frac{1}{\alpha(x)} \int_o^{x_o^*} q(\xi)\ d\xi\right\}^{\frac{1}{n}} \tag{4-54}$$

$$t(x,x_o^*) = T + \frac{1}{n}\left\{\int_o^{x_o^*} q(\xi)\ d\xi\right\}^{\frac{1-n}{n}} \int_{x_o^*}^{x} \left\{\frac{1}{\alpha(\eta)}\right\}^{\frac{1}{n}} d\eta \tag{4-55}$$

3. If $q(x,t)$ varies in time only, then we get:

$$h_o = \left\{\frac{1}{\alpha(x_o^*)} \int_o^{x_o^*} q(t(\xi,t_o))\ d\xi\right\}^{\frac{1}{n}} \tag{4-56}$$

$$h(x,x_o^*) = \left\{\frac{1}{\alpha(x)} \int_o^{x_o^*} q(t(\xi,t_o))\ d\xi\right\}^{\frac{1}{n}} \tag{4-57}$$

$$t(x,x_o^*) = T + \frac{1}{n} \int_{x_o^*}^{x} \left\{\frac{1}{\alpha(\eta)}\right\}^{\frac{1}{n}} \left\{\int_o^{x_o} q(t(\xi,t_o))\ d\xi\right\}^{\frac{1-n}{n}} d\eta \tag{4-58}$$

4. If $\alpha(x)$ and $q(x,t)$ both are constant then we obtain:

$$h_o = \left\{\frac{q\ x_o^*}{\alpha}\right\}^{\frac{1}{n}} \tag{4-59}$$

$$h(x,x_o^*) = h_o = \left\{\frac{q\ x_o^*}{\alpha}\right\}^{\frac{1}{n}} \tag{4-60}$$

$$t(x,x_o^*) = T + \left\{\frac{\alpha}{q\ x_o^*}\right\}^{\frac{n-1}{n}} \frac{(x-x_o^*)}{\alpha n} \tag{4-61}$$

5. If $\alpha(x)$ is constant but $q(x,t)$ varies in both time and space, we get:

$$h_o = \left\{\frac{1}{\alpha} \int_o^{x_o^*} q(\xi,t(\xi,t_o))\ d\xi\right\}^{\frac{1}{n}} \tag{4-62}$$

$$h(x,x_o^*) = h_o \tag{4-63}$$

$$t(x,x_o^*) = T + \frac{1}{\alpha n} \left\{\frac{1}{\alpha} \int_o^{x_o^*} q(\xi,t(\xi,t_o))\ d\xi\right\}^{\frac{1-n}{n}} (x-x_o^*) \tag{4-64}$$

6. If $\alpha(x)$ is constant but $q(x,t)$ varies in space only, then we get:

$$h_o = \left\{\frac{1}{\alpha} \int_o^{x_o^*} q(\xi)\ d\xi\right\}^{\frac{1}{n}} \tag{4-65}$$

$$h(x,x_o^*) = h_o \tag{4-66}$$

$$t(x,x_o^*) = T + \frac{(x-x_o^*)}{\alpha n} \left\{\frac{1}{\alpha} \int_o^{x_o^*} q(\xi)\ d\xi\right\}^{\frac{1-n}{n}} \tag{4-67}$$

7. If $\alpha(x)$ is constant but $q(x,t)$ varies in time only, then we obtain:

$$h_o = \left\{\frac{1}{\alpha}\int_o^{x_o^*} q(t(\xi,t_o))\, d\xi\right\}^{\frac{1}{n}} \tag{4-68}$$

$$h(x,x_o^*) = h_o \tag{4-69}$$

$$t(x,x_o^*) = T + \frac{(x-x_o^*)}{\alpha n}\left\{\frac{1}{\alpha}\int_o^{x_o^*} q(t(\xi,t_o))\, d\xi\right\}^{\frac{1-n}{n}} \tag{4-70}$$

It is clear from the above discussion that in domain D_1, h depends on both x and t. The curves $t=t(x,x_o)$ fill out the entire domain D_1 as x_o^* ranges from o to L_o. We now summarize the case A, $t^* \leq T$.

(1) In domain D_3 the solution is given by Eqs. (4-28) and (4-29). Here the parameter x_o assumes values on the segment $o \leq x \leq L_o$, $t = o$.

(2) In domain D_2 the solution is given by Eqs. (4-12) and (4-13). Here the parameter t_o assumes values on the segment $x = o$, $o \leq t \leq T$.

(3) In domain D_1 the solution is given by Eqs. (4-48) and (4-49). Here the parameter x_o^* assumes values on the segment $o \leq x \leq L_o$, $t = T$.

We consider now, in case A with $q(x,t) = q$, h as a function of t for fixed x, that is, we want to know the appearance of the curve cut out of the surface $h(x,t)$ by a plane perpendicular to the x-axis. In domain D_3 we have:

$$\frac{\partial h(x,t)}{\partial t} = \frac{\partial h(x,x_o)}{\partial x_o}\,\frac{\partial x_o}{\partial t} = \frac{\partial h(x,x_o)/\partial x_o}{\partial t(x,x_o)/\partial x_o}$$

From Eqs. (4-30) and (4-31) we see that $\frac{\partial h(x,x_o)}{\partial x_o} < o$. From these equations it also follows, although the discussion is more complicated, that $\frac{\partial t(x,x_o)}{\partial x_o} < o$. Thus $\frac{\partial h(x,t)}{\partial t} > o$ if $(x,t) \in D_3$. In domain D_2 $h(x,t)$ is independent of t for time-invariant input, and for space-variant input. In domain D_1 we have, from Eqs. (4-51) and (4-52), $\frac{\partial h(x,x_o^*)}{\partial x_o^*} > o$

and $\frac{\partial t(x,x_o^*)}{\partial x_o^*} < o$, hence $\frac{\partial h(x,t)}{\partial t} < o$. From Eq. (4-52) $t \to \infty$ for fixed x is equivalent to $x_o^* \to o$ for fixed x , and from Eq. (4-51) $h(x,t) \to o$ as $t \to \infty$. It then follows that, for a fixed value of x , the function $h(x,t)$, due to a pulse input, has the appearance as shown in Fig. 4-8. We may obtain the approximate behaviour of $h(x,t)$ for large (and therefore small x_o^*) by setting $x_o^* = o$ in the integral in Eq. (4-52) and the eliminating x_o^* between Eqs. (4-51) and (4-52):

$$t(x,x_o^*) = T + \frac{(qx_o^*)^{\frac{1-n}{n}}}{n} \int_o^x \left(\frac{1}{\alpha(\eta)}\right)^{\frac{1}{n}} d\eta$$

Then we obtain:

$$x_o^* = \frac{1}{q} \left\{ \frac{(t-T)^n}{\int_o^x \left(\frac{1}{\alpha(\eta)}\right)^{\frac{1}{n}} d\eta} \right\}^{\frac{n}{1-n}}$$

Substituting for x_o^* into Eq. (4-51) we obtain $h(x,t)$:

$$h(x,t) = \frac{\Psi(n)}{(t-T)^{\frac{1}{n-1}}}$$

where

$$\psi(x) = \frac{\left\{\int_o^x (\alpha(\eta))^{\frac{1}{n}} d\eta\right\}^{\frac{1}{n-1}}}{n^{\frac{1}{n-1}} (\alpha(x))^{\frac{1}{n}}}$$

We note that the decline of h to o as $t \to \infty$ is not exponential. Thus if $n = 1.5$, $h(x,t)$ goes to zero as t^{-2} . In Table 4-1 we summarize the conditions leading to explicit analytical solutions.

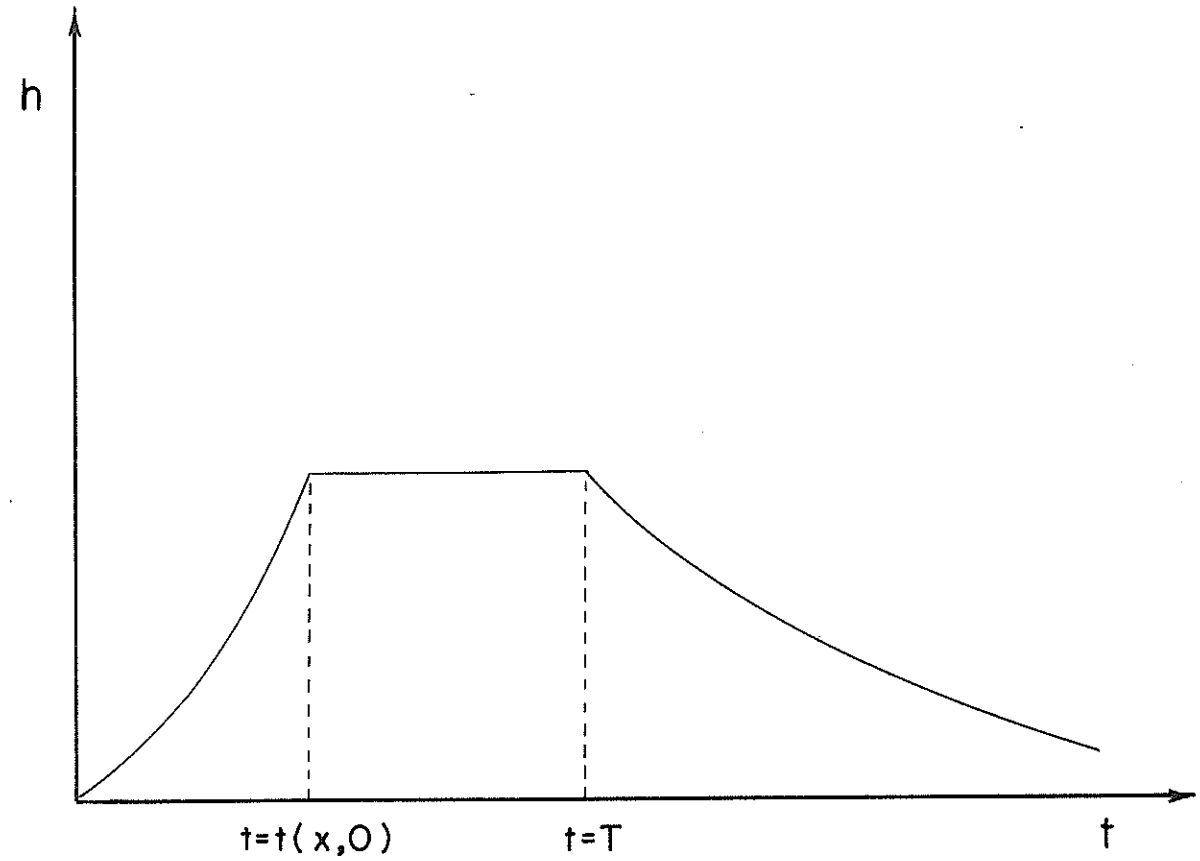

Fig. 4-8. A typical hydrograph of depth of flow for equilibrium case due to steady input.

Table 4-1. Conditions leading to analytical solutions for equilibrium and partial equilibrium hydrographs

Case number	Parameter $\alpha(x)$		Input $q(x,t)$				Analytical Solutions		Remarks
	Constant	Varying in space	Constant	Varying in space only	Varying in time only	Varying in both space and time	Complete	Part	
1		X				X		X	The functional forms of $\alpha(x)$ and $q(x,t)$ will determine the form of solutions
2		X	X				X		The functional form of $\alpha(x)$ will determine the form of solutions
3		X		X				X	The functional forms of $\alpha(x)$ and $q(x)$ will determine the form of solutions
4		X			X			X	The functional forms of $\alpha(x)$ and $q(t)$ will determine the form of solutions
5	X					X		X	The functional form of $q(x,t)$ will determine the form of solutions
6	X		X				X		
7	X			X				X	The functional form of $q(x)$ will determine the form of solutions
8	X				X			X	The functional form of $q(t)$ will determine the form of solutions

It may be instructive at this point to determine the equilibrium time and the equilibrium depth; these quantities will be given when the characteristic curve $t(x,o)$ passing through the origin (o,o) intersects the downstream boundary $x = L_o$. For case A equilibrium time will be the same as t^* in Fig. 4-6, and will be independent of the rainfall pattern and duration. Thus we have:

$$h_e = \left\{\frac{1}{\gamma}\int_o^{L_o} q(\xi,t(\xi))\ d\xi\right\}^{\frac{1}{n}} \tag{4-71}$$

$$t_e = \frac{1}{n\gamma}\left\{\frac{1}{\gamma}\int_o^{L_o} q(\xi,t(\xi))\ d\xi\right\}^{\frac{1-n}{n}} \tag{4-72}$$

where γ = the value of $\alpha(x)$ when $x=L_o$, h_e = equilibrium depth, and t_e = equilibrium time. Let us now consider the seven special cases:

1. If $q(x,t)$ is constant then we obtain:

$$h_e = \left\{\frac{q\ L_o}{\gamma}\right\}^{\frac{1}{n}} \tag{4-73}$$

$$t_e = \frac{q^{\frac{1-n}{n}}}{n}\int_o^{L_o} \left\{\frac{1}{\alpha(\xi)}\right\}^{\frac{1}{n}}\left(\xi\right)^{\frac{1-n}{n}}\ d\xi \tag{4-74}$$

2. If $q(x,t)$ varies in space only, then we obtain:

$$h_e = \left\{\frac{1}{\gamma}\int_o^{L_o} q(\xi)\ d\xi\right\}^{\frac{1}{n}} \tag{4-75}$$

$$t_e = \frac{1}{n}\int_o^{L_o} \left\{\frac{1}{\alpha(\eta)}\right\}^{\frac{1}{n}}\left\{\int_o^{\eta} q(\xi)\ d\xi\right\}^{\frac{1-n}{n}} d\eta \tag{4-76}$$

3. If $q(x,t)$ varies in time only, then we obtain:

$$h_e = \left\{\frac{1}{\gamma}\int_o^{L_o} q(t(\xi))\ d\xi\right\}^{\frac{1}{n}} \tag{4-77}$$

$$t_e = \frac{1}{n}\int_o^{L_o} \left\{\frac{1}{\alpha(\eta)}\right\}^{\frac{1}{n}}\left\{\int_o^{\eta} q(t(\xi)\ d\xi\right\}^{\frac{1-n}{n}} d\eta \tag{4-78}$$

4. If $\alpha(x)$ and $q(x,t)$ both are constant then we get:

$$h_e = \left\{\frac{q\ L_o}{\alpha}\right\}^{\frac{1}{n}} \tag{4-79}$$

$$t_e = q^{\frac{1-n}{n}} \left(\frac{L_o}{\alpha}\right)^{\frac{1}{n}} \tag{4-80}$$

5. If $\alpha(x)$ is constant but $q(x,t)$ varies in time and space then we get:

$$h_e = \left\{\frac{1}{\alpha} \int_o^{L_o} q(\xi, t(\xi))\ d\xi\right\}^{\frac{1}{n}} \tag{4-81}$$

$$t_e = \frac{1}{n} \left(\frac{1}{\alpha}\right)^{\frac{1}{n}} \int_o^{L_o} \left\{ \int_o^{\eta} q(\xi, t(\xi))\ d\xi \right\}^{\frac{1-n}{n}} d\eta \tag{4-82}$$

6. If $\alpha(x)$ is constant but $q(x,t)$ varies in space only, then we obtain:

$$h_e = \left\{\frac{1}{\alpha} \int_o^{L_o} q(\xi)\ d\xi\right\}^{\frac{1}{n}} \tag{4-83}$$

$$t_e = \frac{1}{n} \left(\frac{1}{\alpha}\right)^{\frac{1}{n}} \int_o^{L_o} \left\{ \int_o^{\eta} q(\xi)\ d\xi \right\}^{\frac{1-n}{n}} d\eta \tag{4-84}$$

7. If $\alpha(x)$ is constant but $q(x,t)$ varies in time only, then we obtain:

$$h_e = \left\{\frac{1}{\alpha} \int_o^{L_o} q(t(\xi))\ d\xi\right\}^{\frac{1}{n}} \tag{4-85}$$

$$t_e = \frac{1}{n} \left(\frac{1}{\alpha}\right)^{\frac{1}{n}} \int_o^{L_o} \left\{ \int_o^{\eta} q(\xi)\ d\xi \right\}^{\frac{1-n}{n}} d\eta \tag{4-86}$$

4.3.2 Case B: Partial Equilibrium Situation

We can write the input as:

$$q(x,t) = \begin{cases} q(x,t) & o \leq t \leq T\ ,\quad T < t^* \\ o & \text{otherwise} \end{cases}$$

This case is somewhat more complicated. The quantity t^* will depend on T. The solution domain is shown in Fig. 4-7, and is divided into four parts.

Let x^* be the solution of $T = t(x,o)$. Let D_{11} be the domain above the line $t = T$ and above the curve $t = t(x,x^*)$. The curve $t = t(x,x^*)$ is just the propagation of $t = t(x,o)$ beyond $t = T$. Let D_{12} be the domain bounded by $t = t(x,x^*)$, $t = T$, and $x = L_o$. The domain D_2 is bounded by $t = T$, $x = o$ and the curve $t = t(x,o)$. The domain D_3 is bounded by $t = t(x,o)$, $t = T$, $t = o$, and $x = L_o$.

Domain D_2. The solution is given by Eqs. (4-12) and (4-13).

Domain D_3. The solution is given by Eqs. (4-28) and 4-29).

Domain D_{11}. Let $o < x_o^* \leq x^*$, $t = T$, then the solution is given by Eqs. (4-48) and (4-49).

Domain D_{12}. Let x_o^* be the solution of $T = t(x,x_o)$, that is, the value of x where the curve $t = t(x,x_o)$ given by Eq. (4-29) intersects the line $t = T$. Then along the segment $x^* < x_o^* < L_o$, $t = T$, we have, from Eq. (4-28):

$$h(x_o^*,x_o) = \left\{\frac{1}{\alpha(x_o^*)} \int_{x_o}^{x_o^*} q(\xi,t(\xi,x_o))\, d\xi\right\}^{\frac{1}{n}} \tag{4-87}$$

Now we solve the two differential equations given by Eqs. (4-44) and (4-45) subject to the initial conditions:

$$t(x_o^*) = T \tag{4-88}$$

$$h(x_o^*) = h(x_o^*,x_o)$$

Then the solution follows:

$$h(x;x_o^*,x_o) = h(x_o^*,x_o)\left\{\frac{\alpha(x_o^*)}{\alpha(x)}\right\}^{\frac{1}{n}} = \left\{\int_{x_o}^{x_o^*} q(\xi,t(\xi,x_o))\, d\xi\right\}^{\frac{1}{n}}\left\{\frac{1}{\alpha(x)}\right\}^{\frac{1}{n}} \tag{4-89}$$

$$t(x;x_o^*,x_o) = T + \frac{1}{n}\left\{h(x_o^*,x_o)\right\}^{1-n}\left\{\frac{1}{\alpha(x_o^*)}\right\}^{\frac{n-1}{n}} \int_{x_o^*}^{x} \left\{\alpha(\eta)\right\}^{-\frac{1}{n}} d\eta \tag{4-90}$$

Here x_o^* and x_o are bounded by the relation:

$$T = \frac{1}{n} \int_{x_o}^{x_o^*} \left(\frac{1}{\alpha(\eta)}\right)^{\frac{1}{n}} \left\{ \int_{x_o}^{\eta} q(\xi, t(\xi, x_o))\, d\xi \right\}^{\frac{1-n}{n}} d\eta \tag{4-91}$$

Thus, in Eqs. (4-89) and (4-90) we may think of x_o^* as the parameter, in which case we have to replace x_o which appears in these equations by its solution in Eq. (4-91) in terms of x_o^*. On the other hand we may think of x_o as the parameter in Eqs. (4-89) and (4-90); in that case we have to replace x_o^* in these equations by its solution in Eq. (4-91). Since, in Eq. (4-91) x_o^* is an increasing function of x_o, the correspondence between x_o^* and x_o is one to one. Now we examine the seven special cases:

1. If $q(x,t)$ is constant then we obtain:

$$h(x_o^*, x_o) = \left\{ \frac{q(x_o^* - x_o)}{\alpha(x_o^*)} \right\}^{\frac{1}{n}} \tag{4-92}$$

$$h(x; x_o^*, x_o) = \left\{ \frac{q(x_o^* - x_o)}{\alpha(x)} \right\}^{\frac{1}{n}} \tag{4-93}$$

$$t(x; x_o^*, x_o) = T + \frac{1}{n} \left\{ q(x_o^* - x_o) \right\}^{\frac{1-n}{n}} \int_{x_o^*}^{x} \left\{ \frac{1}{\alpha(\eta)} \right\}^{\frac{1}{n}} d\eta \tag{4-94}$$

2. If $q(x,t)$ varies in space only, then we obtain:

$$h(x_o^*, x_o) = \left\{ \frac{1}{\alpha(x_o^*)} \int_{x_o}^{x_o^*} q(\xi)\, d\xi \right\}^{\frac{1}{n}} \tag{4-95}$$

$$h(x; x_o^*, x_o) = \left\{ \frac{1}{\alpha(x)} \int_{x_o}^{x_o^*} q(\xi)\, d\xi \right\}^{\frac{1}{n}} \tag{4-96}$$

$$t(x; x_o^*, x_o) = T + \frac{1}{n} \left\{ \int_{x_o}^{x_o^*} q(\xi)\, d\xi \right\}^{\frac{1-n}{n}} \int_{x_o^*}^{x} \left\{ \frac{1}{\alpha(\eta)} \right\}^{\frac{1}{n}} d\eta \tag{4-97}$$

3. If $q(x,t)$ varies in time only, then we obtain:

$$h(x_o^*,x_o) = \left\{\frac{1}{\alpha(x_o^*)} \int_{x_o}^{x_o^*} q(t(\xi,x_o))\ d\xi\right\}^{\frac{1}{n}} \tag{4-98}$$

$$h(x;x_o^*) = \left\{\frac{1}{\alpha(x)} \int_{x_o}^{x_o^*} q(t(\xi,x_o))\ d\xi\right\}^{\frac{1}{n}} \tag{4-99}$$

$$t(x;x_o^*,x_o) = T + \frac{1}{n}\left\{\int_{x_o}^{x_o^*} q(t(\xi,t_o))\ d\xi\right\}^{\frac{1-n}{n}} \int_{x_o^*}^{x} \left(\frac{1}{\alpha(\eta)}\right)^{\frac{1}{n}} d\eta \tag{4-100}$$

4. If $\alpha(x)$ and $q(x,t)$ both are constant then we obtain:

$$h(x_o^*,x_o) = \left\{\frac{q}{\alpha}\ (x_o^* - x_o)\right\}^{\frac{1}{n}} \tag{4-101}$$

$$h(x;x_o^*,x_o) = h(x_o^*,x_o) \tag{4-102}$$

$$t(x;x_o^*,x_o) = T + \frac{1}{n}\left(\frac{1}{\alpha}\right)^{\frac{1}{n}} \left\{q(x_o^* - x_o)\right\}^{\frac{1-n}{n}}\ (x - x_o^*) \tag{4-103}$$

5. If $\alpha(x)$ is constant but $q(x,t)$ varies in time and space then we obtain:

$$h(x_o^*,x_o) = \left\{\frac{1}{\alpha} \int_{x_o}^{x_o^*} q(\xi,t(\xi,x_o))\ d\xi\right\}^{\frac{1}{n}} \tag{4-104}$$

$$h(x;x_o^*,x_o) = h(x_o^*,x_o) \tag{4-105}$$

$$t = T + \frac{1}{n}\left\{\int_{x_o}^{x_o^*} q(\xi)\ d\xi\right\}^{\frac{1-n}{n}}\ (x - x_o^*)\ \left(\frac{1}{\alpha}\right)^{\frac{1}{n}} \tag{4-106}$$

6. If $\alpha(x)$ is constant but $q(x,t)$ varies in space only, then we get:

$$h(x_o^*,x_o) = \left\{\frac{1}{\alpha} \int_{x_o}^{x_o^*} q(\xi)\ d\xi\right\}^{\frac{1}{n}} \tag{4-107}$$

$$h(x;x_o^*,x_o) = h(x_o^*,x_o) \tag{4-108}$$

$$t(x;x_o^*,x_o) = T + \frac{1}{n}\left\{\int_{x_o}^{x_o^*} q(\xi)\, d\xi\right\}^{\frac{1-n}{n}} (x - x_o^*) \left(\frac{1}{\alpha}\right)^{\frac{1}{n}} \tag{4-109}$$

7. If $\alpha(x)$ is constant but $q(x,t)$ varies in space only, then we get:

$$h(x_o^*,x_o) = \left\{\frac{1}{\alpha}\int_{x_o}^{x_o^*} q(t(\xi,x_o))\, d\xi\right\}^{\frac{1}{n}} \tag{4-110}$$

$$h(x;x_o^*,x_o) = h(x_o^*,x_o) \tag{4-111}$$

$$t(x;x_o^*,x_o) = T + \frac{1}{n}\left\{\int_{x_o}^{x_o^*} q(t(\xi,x_o))\, d\xi\right\}^{\frac{1-n}{n}} (x-x_o^*) \left(\frac{1}{\alpha}\right)^{\frac{1}{n}} \tag{4-112}$$

We summarize the case B , $t^* > T$:

(1) In domain D_3 the solution is given by Eqs. (4-28) and (4-29). Here the parameter x_o assumes values on the segment $o \leq x \leq L_o$, $t = o$.

(2) In domain D_2 the solution is given by Eqs. (4-12) and (4-13). Here the parameter t_o assumes values on the segment $x = o$, $o \leq t \leq T$.

(3) In domain D_{11} the solution is given by Eqs. (4-48) and (4-49) where x_o is replaced in these equations by x_o^* . The parameter x_o^* assumes values on the segment $o \leq x_o^* \leq x^*$, $t = T$.

(4) In domain D_{12} the solution is given by Eqs. (4-89) and (4-90). Here we may regard x_o or x_o^* as the parameter.

As in case A, we consider h as a function of t for fixed x when $q(x,t) = q$. In case B this behavior of $h(x,t)$ is the same as in case A for $o < x < x^*$ as shown in Fig. 4-9 . If $x^* \leq x \leq L_o$ then $h(x,t)$ is an increasing function of t if $(x,t) \in D_3$, and it is a decreasing function of t if $(x,t) \in D_{11}$; the arguments are the same as in case A. It remains

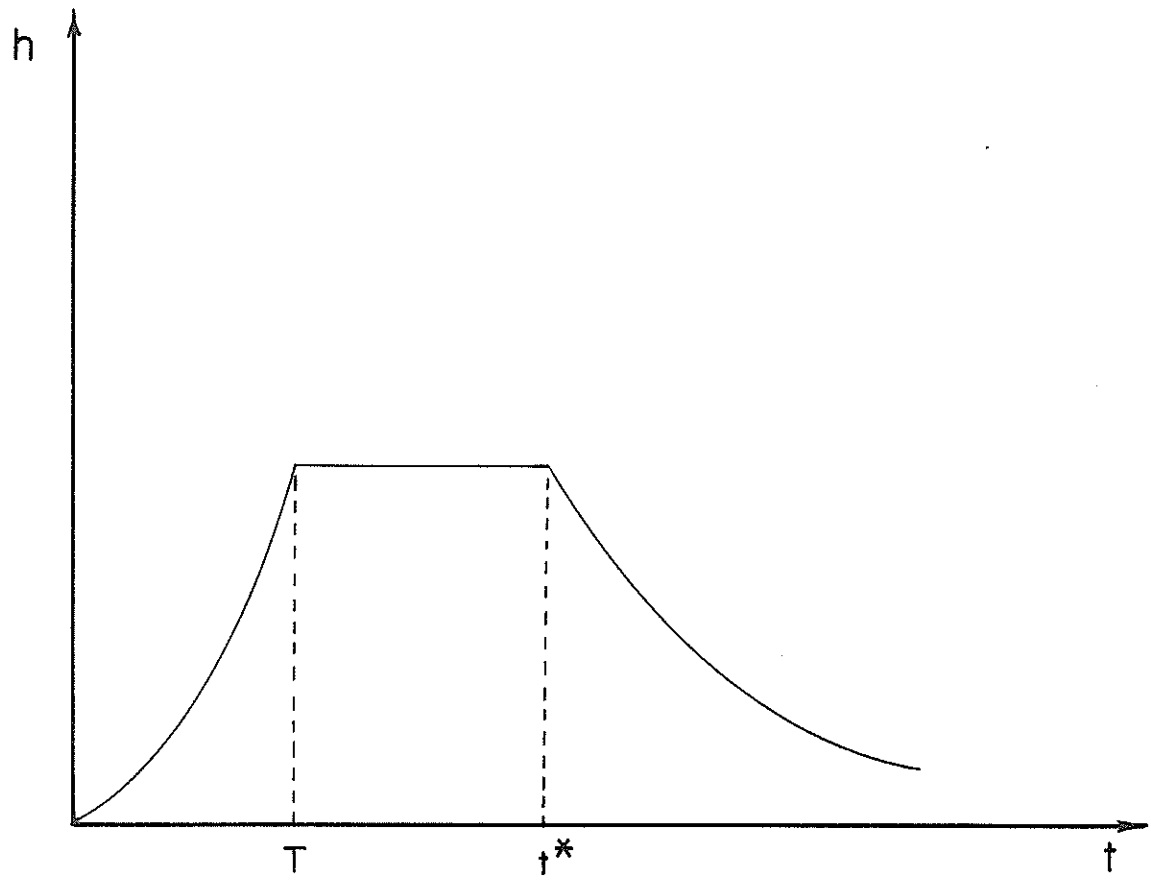

Fig. 4-9. A typical hydrograph of depth of flow for partial equilibrium case due to steady input.

to consider the behavior of $h(x,t)$ when x is fixed and $(x,t) \in D_{12}$; the maximum of $h(x,t)$, for x fixed, will occur in D_{12} , possibly on $t = T$ or on $t = t(x,x^*)$. We have:

$$\frac{\partial h(x,t)}{\partial t} = \frac{\partial h(x;x_o^*(x_o),x_o)}{\partial x_o} \frac{\partial x_o}{\partial t} \tag{4-113}$$

We can write in a more compact form:

$$h_t(x,t) = h_{x_o}(x;x_o^*(x_o),x_o)/t_{x_o}(x;x_o^*(x_o),x_o) \tag{4-114}$$

We can also write:

$$h_{x_o}(x;x_o^*(x_o),x_o) = h_{x_o^*}(x;x_o^*,x_o) \frac{dx_o^*}{dx_o} + h_{x_o}(x;x_o^*,x_o) \tag{4-115}$$

To demonstrate the above it will be more useful to consider a special case when $q(t,t)$ is constant. Then from Eq. (4-93):

$$h_{x_o}(x;x_o^*(x_o),x_o) = q^{\frac{1}{n}} \left\{\frac{x_o^* - x_o}{\alpha(x)}\right\}^{\frac{1}{n}-1} \frac{1}{n} \frac{1}{\alpha(x)} \left\{-\frac{dx_o^*}{dx_o} + 1\right\} \tag{4-116}$$

Thus the sign of $h_{x_o}(x;x_o^*(x_o),x_o)$, and therefore also the sign of $h_t(x,t)$, is determined by

$$\left\{1 - \frac{dx_o^*}{dx_o}\right\}$$

The value of the derivative dx_o^*/dx_o will depend on the functional form of $\alpha(x)$. If $\alpha(x)$ is taken as constant, it is easy to show that the maximum of $h(x,t)$ will occur on $t = T$. Table 1 summarizes the conditions leading to analytical solutions for this case B.

We must, however, determine x^* before we can hope to determine the partial equilibrium hydrograph. This quantity can be determined by solving for the limiting characteristic curve $t(x,o)$, passing through the origin, at the point in (x,t) plane where it intersects the segment $t = T$.

That is,

$$T = \frac{1}{n} \int_0^{x^*} \left(\frac{1}{\alpha(\eta)}\right)^{\frac{1}{n}} \left\{ \int_0^{\eta} q(\xi, t(\xi)) d\xi \right\}^{\frac{1-n}{n}} d\eta \tag{4-117}$$

We shall now consider all the seven special cases:

1. If $q(x,t)$ is constant then we obtain:

$$T = \frac{q^{\frac{1-n}{n}}}{n} \int_0^{x^*} \left(\frac{1}{\alpha(\eta)}\right)^{\frac{1}{n}} \left(\eta\right)^{\frac{1-n}{n}} d\eta \tag{4-118}$$

2. If $q(x,t)$ varies in space only, then we obtain:

$$T = \frac{1}{n} \int_0^{x^*} \left(\frac{1}{\alpha(\eta)}\right)^{\frac{1}{n}} \left\{ \int_0^{\eta} q(\xi) d\xi \right\}^{\frac{1-n}{n}} d\eta \tag{4-119}$$

3. If $q(x,t)$ varies in time only, then we obtain:

$$T = \frac{1}{n} \int_0^{x^*} \left(\frac{1}{\alpha(\eta)}\right)^{\frac{1}{n}} \left\{ \int_0^{\eta} q(t(\xi)) d\xi \right\}^{\frac{1-n}{n}} d\eta \tag{4-120}$$

4. If both $\alpha(x)$ and $q(x,t)$ are constant then we get:

$$T = q^{\frac{1-n}{n}} \left(\frac{1}{\alpha}\right)^{\frac{1}{n}} x^{*\frac{1}{n}} \tag{4-121}$$

5. If $\alpha(x)$ is constant but $q(x,t)$ varies in both time and space, then we get:

$$T = \frac{1}{n} \left(\frac{1}{\alpha}\right)^{\frac{1}{n}} \int_0^{x^*} \left\{ \int_0^{\eta} q(\xi, t(\xi)) d\xi \right\}^{\frac{1-n}{n}} d\eta \tag{4-122}$$

6. If $\alpha(x)$ is constant but $q(x,t)$ varies in space only, then we obtain:

$$T = \frac{1}{n} \left(\frac{1}{\alpha}\right)^{\frac{1}{n}} \int_0^{x^*} \left\{ \int_0^{\eta} q(\xi) d\xi \right\}^{\frac{1-n}{n}} \tag{4-123}$$

7. If $\alpha(x)$ is constant but $q(x,t)$ varies in time only then we obtain:

$$T = \frac{1}{n} \left(\frac{1}{\alpha}\right)^{\frac{1}{n}} \int_0^{x^*} \left\{ \int_0^{\eta} q(t(\xi)) d\xi \right\}^{\frac{1-n}{n}} d\eta \tag{4-124}$$

In the beginning of this case we indicated that t^* depends on T, and is not exactly equal to t^* of case A. We will try to establish the functional relationship between t^* and T. From Fig. 4-7 we see that $t^* = T + \Delta t$ where Δt is the difference between t^* and T, or the time of propagation of $t(x,o)$ beyond $t = T$ until the downstream boundary. Hence our interest is in the determination of Δt. Thus we have from Eq. (4-49):

$$t^* = T + \frac{1}{n}\left\{\int_o^{x^*} q(\xi,t(\xi))d\xi\right\}^{\frac{1-n}{n}} \int_{x^*}^{L_o}\left(\frac{1}{\alpha(\eta)}\right)^{\frac{1}{n}} d\eta \qquad (4\text{-}125)$$

We shall give the quantity t^* for all seven cases:

1. If $q(x,t)$ is constant then the solution is:

$$t^* = T + \frac{(qx^*)^{\frac{1-n}{n}}}{n} \int_{x^*}^{L_o}\left(\frac{1}{\alpha(\eta)}\right)^{\frac{1}{n}} d\eta \qquad (4\text{-}126)$$

2. If $q(x,t)$ varies in space only, then we obtain:

$$t^* = T + \frac{1}{n}\left\{\int_o^{x^*} q(\xi)d\xi\right\}^{\frac{1-n}{n}} \int_{x^*}^{L_o}\left(\frac{1}{\alpha(\eta)}\right)^{\frac{1}{n}} d\eta \qquad (4\text{-}127)$$

3. If $q(x,t)$ varies in time only, then we obtain:

$$t^* = T + \frac{1}{n}\left\{\int_o^{x^*} q(t(\xi))d\xi\right\}^{\frac{1-n}{n}} \int_{x^*}^{L_o}\left(\frac{1}{\alpha(\eta)}\right)^{\frac{1}{n}} d\eta \qquad (4\text{-}128)$$

4. If both $\alpha(x)$ and $q(x,t)$ are constant then we obtain:

$$t^* = T + \left(\frac{\alpha}{qx^*}\right)^{\frac{n-1}{n}} \frac{(L_o - x^*)}{\alpha n} \qquad (4\text{-}129)$$

5. If $\alpha(x)$ is constant but $q(x,t)$ varies in both time and space, then we get:

$$t^* = T + \frac{1}{n}\left(\frac{1}{\alpha}\right)^{\frac{1}{n}}\left\{\int_o^{x^*} q(\xi,t(\xi))d\xi\right\}^{\frac{1-n}{n}} (L_o - x^*) \qquad (4\text{-}130)$$

6. If $\alpha(x)$ is constant but $q(x,t)$ varies in space only, then we get:

$$t^* = T + \frac{(L_o - x^*)}{n} \left(\frac{1}{\alpha}\right)^{\frac{1}{n}} \left\{ \int_o^{x^*} q(\xi)d\xi \right\}^{\frac{1-n}{n}} \tag{4-131}$$

7. If $\alpha(x)$ is constant but $q(x,t)$ varies in time only, then we obtain:

$$t^* = T + \frac{(L_o - x^*)}{n} \left(\frac{1}{\alpha}\right)^{\frac{1}{n}} \left\{ \int_o^{x^*} q(\xi,t(\xi))d\xi \right\}^{\frac{1-n}{n}} \tag{4-132}$$

4·3·3 Criterion to Distinguish Equilibrium and Partial Equilibrium Situations

One question arises: how can we distinguish cases A and B beforehand? It turns out that there is a simple criterion, when $q(x,t) = q$, which distinguishes cases A and B. From Eq. (4-15) we obtain, by setting $t_o = o$ and the left side equal to T,

$$T = \frac{q}{n}^{\frac{1-n}{n}} \int_o^x \left(\frac{1}{\alpha(\xi)}\right)^{\frac{1}{n}} \left(\xi\right)^{\frac{1-n}{n}} d\eta \tag{4-133}$$

Equation (4-133) has a root x^* between o and L_o in case B and does not have a root in case A. Since the right side, $F(x)$, of Eq. (4-133) is an increasing function of x, it is sufficient to determine the value of F at $x = L_o$: $F(L_o) \leq T$, case A; $F(L_o) > T$, case B.

4·3·4 Definition of t^*

We define t^* as the time of intersection of $t = t(x,o)$ with $x = L_o$ in case A, and as the intersection of $t = t(x,x^*)$ with $x = L_o$ in case B. Thus t^* is a function of T. Let $q(x,t) = q$, and define $T_o = F(L_o)$; here $F(x)$ is the right side of Eq. (4-133). Then $t^*(T) = T_o$ when $T \geq T_o$ and when $T < T_o$, $t^*(T)$ is defined through x^* by $T = F(x^*)$.

We have:

$$t^* = F(x^*) + \frac{1}{n} \left\{qx^*\right\}^{\frac{1-n}{n}} \int_{x^*}^{L_o} \left\{\frac{1}{\alpha(\eta)}\right\}^{\frac{1}{n}} d\eta \qquad (4\text{-}134)$$

Since

$$\frac{dt^*}{dT} = \frac{dt^*}{dx^*} \frac{dx^*}{dT} \qquad (4\text{-}135)$$

and since $dx^*/dT > o$, the sign of dt^*/dT is the same as the sign of dt^*/dx^* . It is easily checked that $dt^*/dx^* \lesseqgtr o$. Thus $t^*(T)$ is a decreasing function of T when $o < T < T_o$. As $T \to o$, $x^* \to o$, and we see from Eq. (4-134) that $t^* \to \infty$, as shown in Fig. 4-10.

Two application examples are worked out in appendix C to show how the above mathematical development can be utilized in computing surface runoff hydrograph. Both equilibrium and partial equilibrium cases are considered.

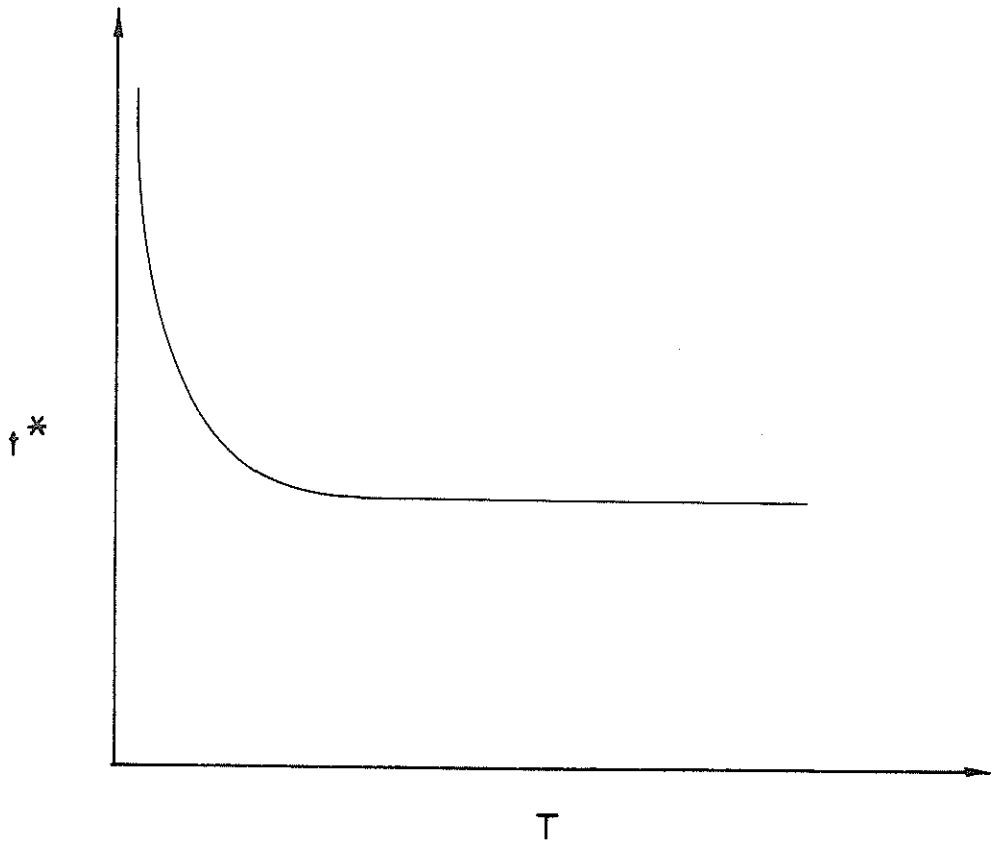

Fig. 4-10. Variation of the time, when the characteristic issuing from the origin intersects the downstream boundary, with rainfall duration.

CHAPTER 5

KINEMATIC WAVE MODELS FOR INFILTRATING WATERSHEDS

5.1 GENERAL REMARKS

The overland flow and infiltration have been extensively studied as separate components of hydrologic cycle (Woolhiser and Ligget, 1967; Woolhiser, 1969; Kibler and Woolhiser, 1970; Singh, 1974; Lane, 1975; Philip, 1967; Hanks and Bowers, 1962; Whisler and Klute, 1965; Rubin, 1966). A combined study of these phases is required for modeling overland flow. Barring a few exceptions, notably the work by Smith (1970) and Smith and Woolhiser (1971), the conventional approach (Wooding, 1965; Eagleson, 1972; Singh, 1975f) to combine these phases has been through the familiar notion of so-called rainfall-excess. In this approach infiltration is independently determined and subtracted from rainfall; the residual is termed as rainfall-excess, which forms input to overland flow model. It seems that this concept of rainfall-excess is more of an artifice than a reality. The processes of infiltration and runoff occur simultaneously in nature during and after the occurrence of rainfall and, therefore, warrant a combined study. In this chapter we develop a combined treatment of infiltration and overland flow. The combined treatment will be useful in studying the effect of infiltration on nonlinear watershed runoff dynamics. It goes without saying that unlike the conventional approach, the present approach does not require an independent, apriori determination of infiltration; rather by specifying an infiltration function, infiltration and overland flow are simultaneously determined. Interestingly enough, this evolves into a free boundary problem.

5.2 MATHEMATICAL SOLUTIONS FOR OVERLAND FLOW ON INFILTRATING PLANE SURFACES

In the previous chapter, infiltration of water through the ground surface was either disregarded or considered through rainfall-excess. Now we treat infiltration and overland flow simultaneously. Let $f(x,t)$ be the rate of infiltration per unit area; f is dependent on the depth of flow, h, in the following sense:

$f(x,t) > o$ if $h(x,t) > o$

$f(x,t) = o$ if $h(x,t) = o$

We will assume further that

$$q(x,t) > f(x,t) \quad , \quad o \leqq t \leqq T \quad , \quad o \leqq x \leqq L_o$$

where q = lateral inflow per unit area, T = duration of q, L_o = length of plane surface, and x and t are space and time coordinates. Then the continuity and momentum equations are:

$$\frac{\partial h}{\partial t} + \frac{\partial (uh)}{\partial x} = q(x,t) - f(x,t) \tag{5-1}$$

$$u = \alpha(x)\, h^{n-1} \tag{5-2}$$

where u = local mean velocity and α and n are kinematic wave parameters. As before $q(x,t) = o$ when $t > T$, and $n > 1$. The boundary conditions are:

$$h(x,o) = o \ , \quad o \leqq x \leqq L_o \ ; \quad h(o,t) = o \ , \quad o \leqq t \leqq T \tag{5-3}$$

It is plausible on physical grounds that there will be a curve $t = t^o(x)$ in $\{t \geqq T \ , \ o \leqq x \leqq L_o\}$, starting at $x = o$, $t = T$, and such that $h(x,t^o(x)) = o$. This curve gives the time history of the water edge as it recedes from $x = o$ to $x = L_o$. The equations (5-1) and (5-2) are satisfied in the region $S = \{o < t < t^o(x), \ o < x < L_o\}$. Thus $t = t^o(x)$ is a free boundary, and Eqs. (5-1) to (5-3), and $h(x,t^o(x)) = o$ form a free boundary problem. In the domain above the curve $t = t^o(x)$,

$h(x,t) = o$. The determination of the free boundary $t = t^o(x)$ is, as we will see, relatively simple when q and f are constant (see Fig. (5-1)); in this study we will discuss only that case in detail.

Eliminating u between Eqs. (5-1) and (5-2) we get:

$$\frac{\partial h}{\partial t} + n\alpha(x)\, h^{n-1} \frac{\partial h}{\partial x} + h^n \frac{\partial \alpha(x)}{\partial x} = q(x,t) - f(x,t) \tag{5-4}$$

The characteristic equations of Eq. (5-4) are:

$$\frac{dt}{ds} = 1$$

$$\frac{dx}{ds} = n\alpha(x)\, h^{n-1}$$

$$\frac{dh}{ds} = q(x,t) - f(x,t) - \alpha'(x)\, h^n$$

where s = parameter, and $\alpha'(x) = \frac{\partial \alpha(x)}{\partial x} \equiv \frac{d\alpha(x)}{dx}$

The solution of Eqs. (5-4) and (5-3) is the surface $h(x,t)$ formed by all the characteristic curves through the segment $t = o$, $o \leq x \leq L_o$ and the segment $x = o$, $o \leq t \leq T$. The free boundary $t = t^o(x)$ is the locus $h(x,t) = o$ in the (x,t) plane. If we take x as parameter then the characteristic curves are given by:

$$\frac{dt}{dx} = \frac{1}{n\alpha(x)\, h^{n-1}} \tag{5-5}$$

$$\frac{dh}{dx} = \frac{q(x,t) - f(x,t)}{n\alpha(x)\, h^{n-1}} - \frac{\alpha'(x)h}{n\alpha(x)} \tag{5-6}$$

and the initial conditions are:

$$h(x) = t_o \quad , \quad h(o) = o \quad , \quad o \leq t_o \leq T \tag{5-7}$$

or

$$t(x_o) = o \quad , \quad h(x_o) = o \quad , \quad o \leq x_o \leq L_o \tag{5-8}$$

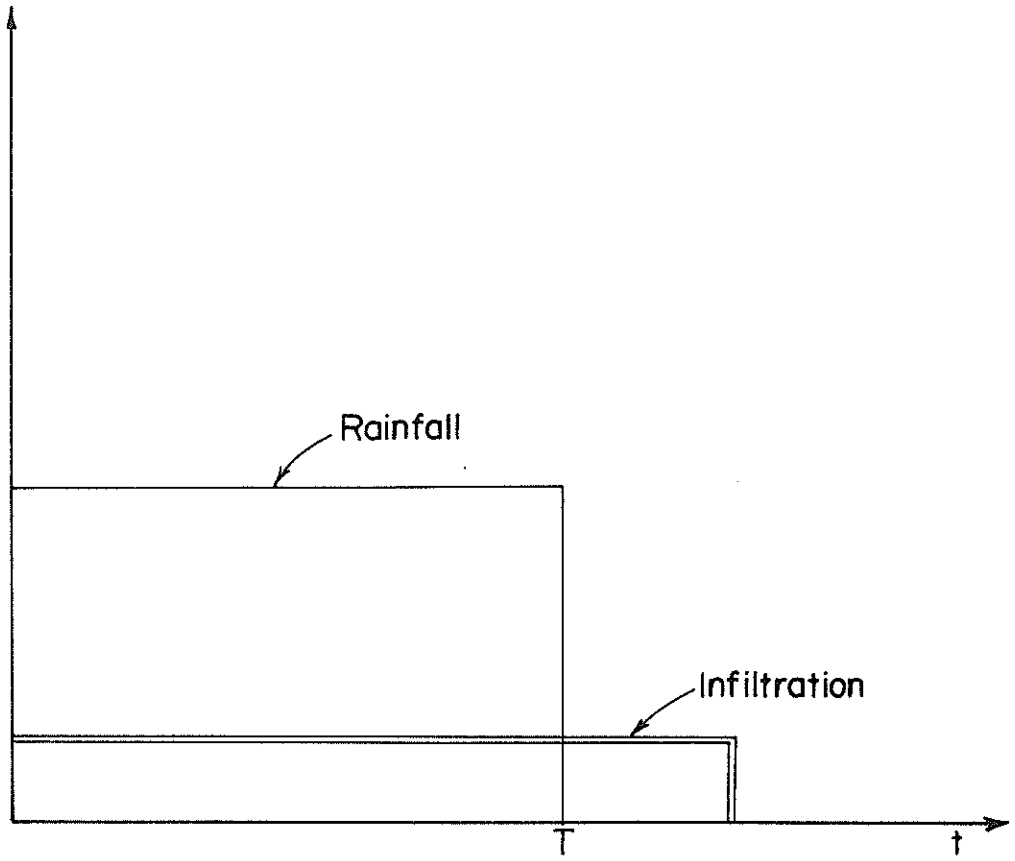

Fig. 5-1. Rainfall and infiltration, constant in time and space.

We assume that the curves $t = t(x,t_o)$, which are the solutions of Eqs. (5-5) to (5-7), do not intersect for distinct values of t_o . Similarly we assume that the curves $t = t(x,x_o)$, which are the solutions of Eqs. (5-5), (5-6) and (5-8), do not intersect for distinct values of x_o . This is true when q and f are constant; it is known from chapter 4 when $t \leq T$, i.e. in domains D_2 and D_3 (Fig. 5-2), and, when $t > T$, it is proved in appendix D.

We distinguish three cases A, B_1 and B_2 which depend on the relative disposition of the three curves $t = t^o(x)$, $t = T$, and $t = t(x,o)$ ($t = t(x,x^*)$ is the prolongation of $t = t(x,o)$ to the right of $x = x^*$) , as shown in Figs. 5-2 - 5-4.

Case A: $t^o(x) > T > t(x,o)$, $o < x \leq L_o$.

Case B_1: $t^o(x) > T$ and $t^o(x) > t(x,o)$, but $t = T$ and $t = t(x,o)$ intersect at $x = x^*$, i.e., $T = t(x^*,o)$ and $o < x^* < L_o$.

Case B_2: $t^o(x) > T$, but $t = T$ and $t = t(x,o)$ intersect at $x = x^*$ and $t = t^o(x)$ and $t = t(x,x^*)$ intersect at $x = \bar{x}$, i.e., $t^o(\bar{x}) = t(\bar{x},x^*)$ and $o < \bar{x} < L_o$.

Since $t^o(x)$ and $t(x,o)$ are not known until we have solved the problem, it appears that we cannot distinguish these cases beforehand. But in the special case which we consider in this study, $q(x,t)$ and $f(x,t)$ both constant, we can distinguish these cases beforehand. The domains D_1, D_2, and D_3 in case A, and the domains D_{11}, D_{12}, D_2, and D_3 in cases B_1 and B_2 are indicated in Figs. 5-2 - 5-4.

5.2.1 Case A: Equilibrium Situation

In case A the solutions in domains D_2 and D_3, when q and f are constant, are obtained from discussion in chapter 4. Then in domain D_2

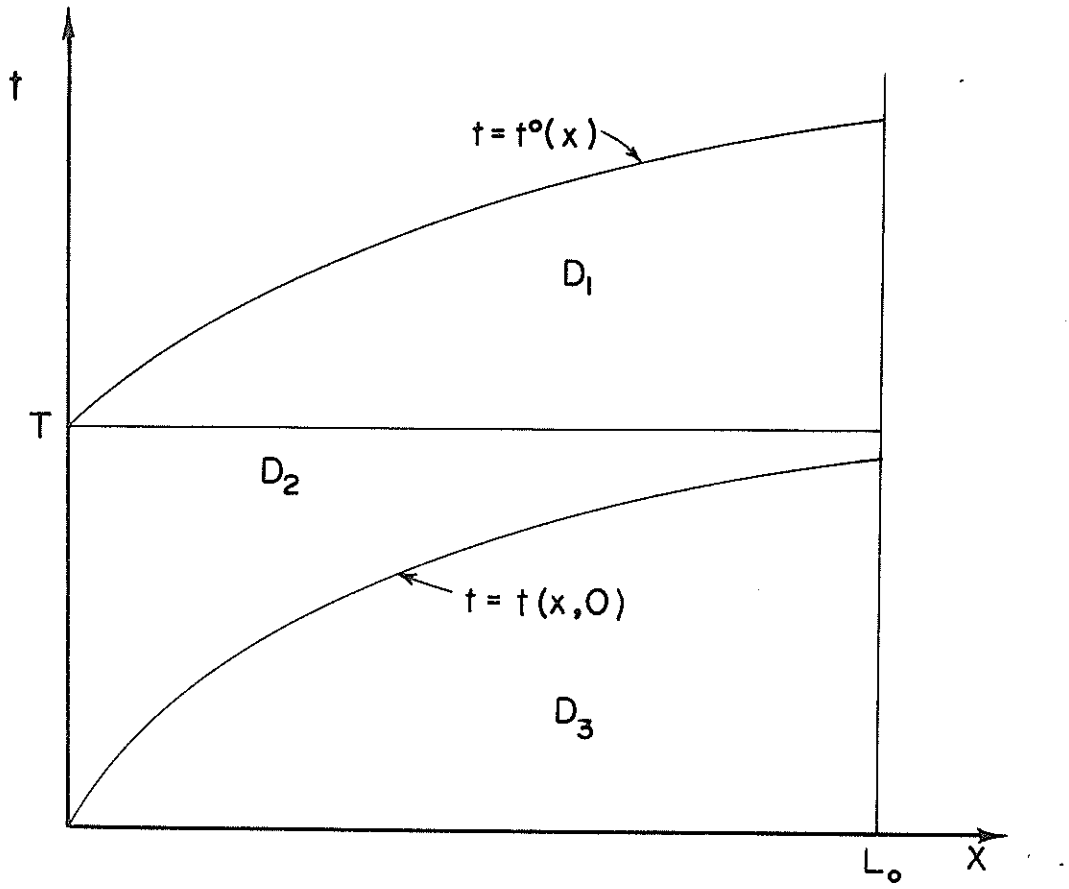

Fig. 5-2. Solution domain for case A.

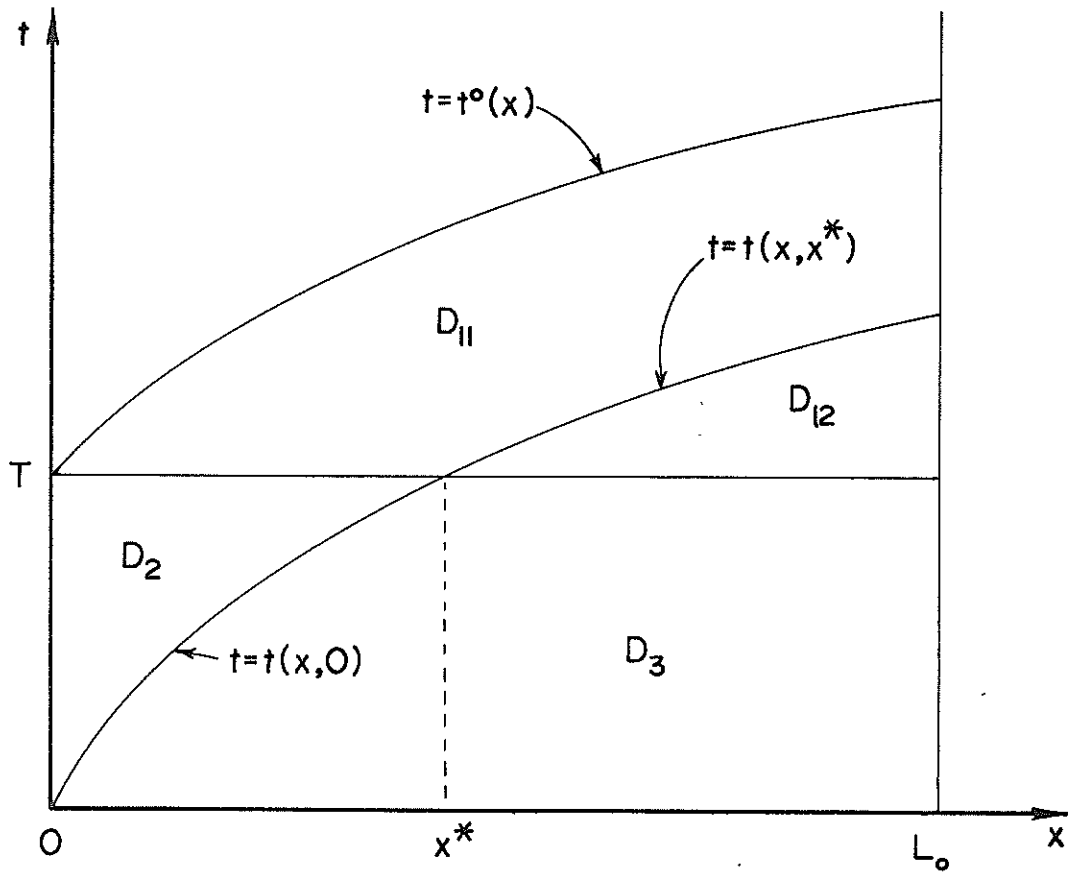

Fig. 5-3. Solution domain for case B_I.

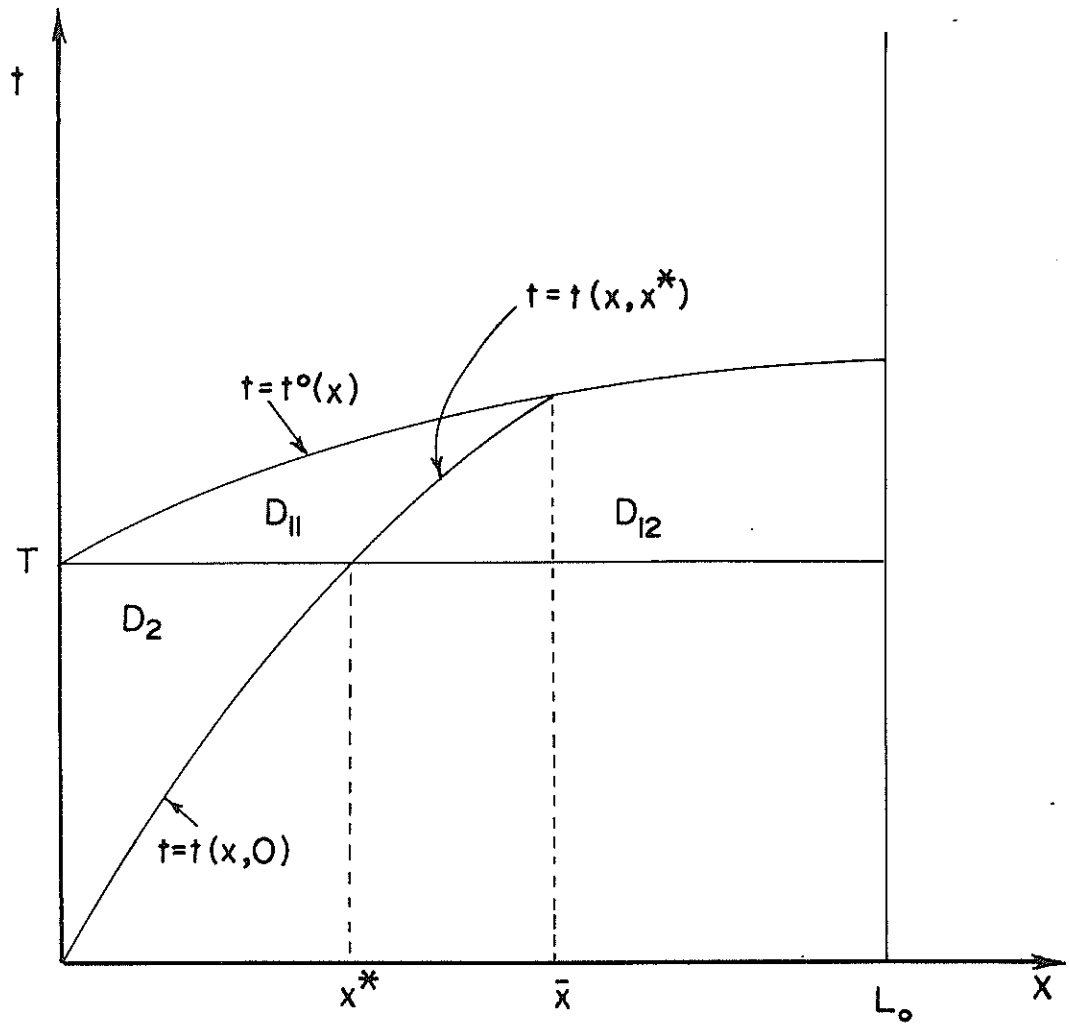

Fig. 5-4. Solution domain for case B_2.

the solution is given by Eqs. (4-14) and (4-15), with q replaced by $(q-f)$:

$$h(x,t_o) = \left\{\frac{(q-f)\,x}{\alpha(x)}\right\}^{\frac{1}{n}} \tag{5-9}$$

$$t(x,t_o) = t_o \left(q-f\right)^{\frac{1-n}{n}} \frac{1}{n} \int_o^x \left(\frac{1}{\alpha(\eta)}\right)^{\frac{1}{n}} \left(\eta\right)^{\frac{1-n}{n}} d\eta \tag{5-10}$$

If $\alpha(x) = \alpha$, a constant, then we have:

$$h(x,t_o) = \left\{\frac{(q-f)x}{\alpha}\right\}^{\frac{1}{n}} \tag{5-11}$$

$$t(x,t_o) = t_o + \left(q-f\right)^{\frac{1-n}{n}} \left(\frac{x}{\alpha}\right)^{\frac{1}{n}} \tag{5-12}$$

In domain D_3 the solution is given by Eqs. (4-30) and (4-31), with q replaced by $(q-f)$:

$$h(x,t_o) = \left\{\frac{(q-f)(x-x_o)}{\alpha(x)}\right\}^{\frac{1}{n}} \tag{5-13}$$

$$t(x,x_o) = \left(q-f\right)^{\frac{1-n}{n}} \frac{1}{n} \int_{x_o}^x \left\{\frac{1}{\alpha(\eta)}\right\}^{\frac{1}{n}} \left(\eta - x_o\right)^{\frac{1-n}{n}} d\eta \tag{5-14}$$

If $\alpha(x) = \alpha$, a constant, then we get:

$$h(x,t_o) = \left\{\frac{(q-f)(x-x_o)}{\alpha}\right\}^{\frac{1}{n}} \tag{5-15}$$

$$t(x,x_o) = \left(q-f\right)^{\frac{1-n}{n}} \left\{\frac{x-x_o}{\alpha}\right\}^{\frac{1}{n}} \tag{5-16}$$

In domain D_1 we solve Eqs. (5-5) and (5-6), with $q(x,t) = o$ and $f(x,t) = f$, subject to

$$t(x_o^*) = T \ , \ h(x_o^*) = h(x_o^*,T) = \left\{\frac{(q - f)x_o^*}{\alpha(x_o^*)}\right\}^{\frac{1}{n}} \tag{5-17}$$

Then the solution is:

$$h(x,x_o^*) = \left\{\frac{qx_o^* - fx}{\alpha(x)}\right\}^{\frac{1}{n}} \tag{5-18}$$

$$t(x,x_o^*) = T + \frac{1}{n} \int_{x_o^*}^{x} \left(\frac{1}{\alpha(\eta)}\right)^{\frac{1}{n}} \left\{qx_o^* - f\,\eta\right\}^{\frac{1-n}{n}} d\eta \tag{5-19}$$

If $\alpha(x) = \alpha$, then we obtain:

$$h(x,x_o^*) = \left\{\frac{qx_o^* - fx}{\alpha}\right\}^{\frac{1}{n}} \tag{5-20}$$

$$t(x,x_o^*) = T + \frac{1}{f} \left\{\frac{(qx_o^* - fx) - (x_o^*(q - f))^{\frac{1}{n}}}{\alpha^{\frac{1}{n}}}\right\}$$

The curves $t = t(x,x_o^*)$ do not intersect in domain D_1; the curves $t = t(x,t_o)$ do not intersect in domain D_2; and the curves $t = t(x,x_o)$ do not intersect in domain D_3 (appendix B). The free boundary $t = t^o(x)$ is now determined by:

$$qx_o^* - fx = o \tag{5-21}$$

and Eq. (5-18). Eliminating x_o^* between Eqs. (5-18) and (5-21) we get:

$$t^o(x) = T + \frac{f}{n}^{\frac{1-n}{n}} \int_{\psi(x)}^{x} \left(\frac{1}{\alpha(\eta)}\right)^{\frac{1}{n}} \left\{x - \eta\right\}^{\frac{1-n}{n}} d\eta \tag{5-22}$$

where $\psi(x) = \frac{fx}{q}$

As in chapter 4, for fixed x, $h(x,t)$ is an increasing function of t in domain D_3, independent of t in domain D_2, and a decreasing function of t in domain D_1 (see Fig. 5-5).

The criterion for distinguishing between case A and cases B_1 and B_2 is, as in chapter 4, obtained from:

$$T = \frac{(q - f)}{n}^{\frac{1-n}{n}} \int_0^x \left(\frac{1}{\alpha(\eta)}\right)^{\frac{1}{n}} \left(\eta\right)^{\frac{1-n}{n}} d\eta \tag{5-23}$$

If $\alpha(x) = \alpha$, then we obtain:

$$T = \left(q - f\right)^{\frac{1-n}{n}} \left(\frac{x}{\alpha}\right)^{\frac{1}{n}} \tag{5-24}$$

If Eq. (5-23) does not have a root between o and L_o then we are in case A; if there is such a root x^* then we are in case B_1 or B_2. If $F(x)$ is the right side of Eq. (5-24) then case A occurs if and only if $F(L_o) \leq T$, and case B_1 or B_2 occurs if and only if $F(L_o) > T$. To distinguish between cases B_1 and B_2 we note, referring to Eq. (5-17), that

$$qx^* - fx = o \tag{5-25}$$

does not have a root between o and L_o in case B_1 and does have such a root $\bar{x}$ in case B_2. In case B_2 the intersection of the curves $t = t(x,x^*)$ and $t = t^o(x)$ occurs at:

$$\bar{x} = \frac{q}{f} x^* \tag{5-26}$$

$$\bar{t} = T + \frac{f}{n}^{\frac{1-n}{n}} \int_{x^*}^{\bar{x}} \left(\frac{1}{\alpha(\eta)}\right)^{\frac{1}{n}} \left\{x - \eta\right\}^{\frac{1-n}{n}} d\eta \tag{5-27}$$

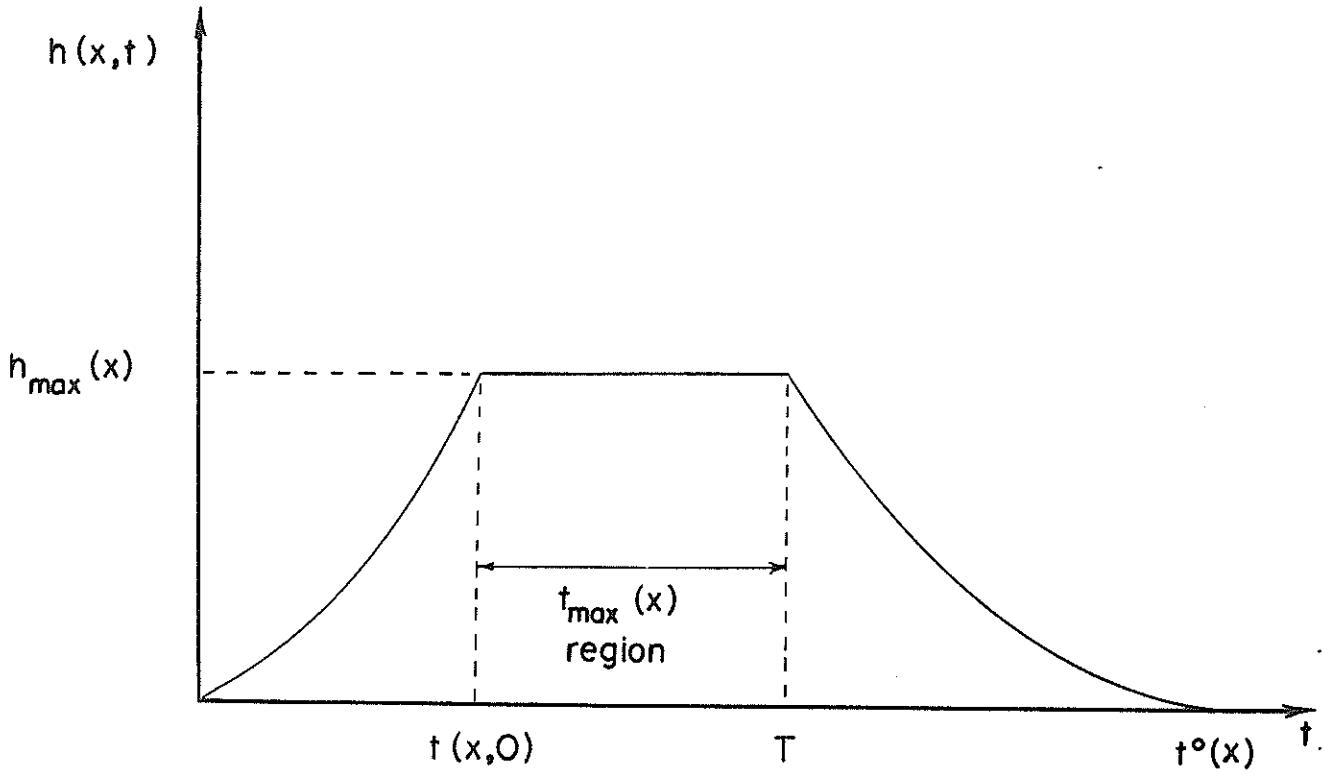

Fig. 5-5. The depth of flow, h(x,t), as a function of t for fixed x for case A.

5.2.2 Cases B_1 and B_2: Partial Equilibrium Situation

In both cases the solution in domain D_{11} is given by Eqs. (5-18) and (5-19), in domain D_2 by Eqs. (5-9) and (5-10), and in domain D_3 by Eqs. (5-13) and (5-14). It remains to determine the solution in domain D_{12}. As in chapter 4, we define x_o^* by $T = t(x_o^*, x_o)$; here $x^* \leq x_o^* \leq L_o$.

Thus from Eq. (5-14),

$$T = \frac{(q - f)}{n}^{\frac{1-n}{n}} \int_{x_o}^{x_o^*} \left(\frac{1}{\alpha(\eta)}\right)^{\frac{1}{n}} \left(\eta - x_o\right)^{\frac{1-n}{n}} d\eta \tag{5-28}$$

If $\alpha(x) = \alpha$, then we obtain:

$$T = \left(q - f\right)^{\frac{1-n}{n}} \left(\frac{x_o^* - x_o}{\alpha}\right)^{\frac{1}{n}} \tag{5-29}$$

Then from Eqs. (4-93) and (4-94) we obtain:

$$h(x; x_o^*, x_o) = \left\{\frac{q(x_o^* - x_o) + f(x_o - x)}{\alpha(x)}\right\}^{\frac{1}{n}} \tag{5-30}$$

$$t(x; x_o^*, x_o) = T + \frac{1}{n} \int_{x_o^*}^{x} \left(\frac{1}{\alpha(\eta)}\right)^{\frac{1}{n}} \left\{q(x_o^* - x_o) + f(x_o - \eta)\right\}^{\frac{1-n}{n}} d\eta \tag{5-31}$$

If $\alpha(x) = \alpha$, then we get:

$$h(x; x_o^*, x_o) = \left\{\frac{q(x_o^* - x_o) + f(x_o - x)}{\alpha}\right\}^{\frac{1}{n}} \tag{5-32}$$

$$t(x; x_o^*, x_o) = T + \left(\frac{1}{\alpha}\right)^{\frac{1}{n}} \left[\left\{q(x_o^* - x_o) + f(x_o - x)\right\}^{\frac{1}{n}} - \left\{q(x_o^* - x_o) + f(x_o - x_o^*)\right\}^{\frac{1}{n}}\right] \tag{5-33}$$

It is proved in appendix D that the curves defined by Eqs. (5-30) and (5-31) do not intersect in domain D_{12}.

In case B_2 part of the boundary of domain D_{12} is $t = t^o(x)$. This is obtained by eliminating x_o and x_o^* between Eqs. (5-28) and (5-31) and from Eq. (5-30),

$$q(x_o^* - x_o) + f(x_o - x) = o \tag{5-34}$$

From Eq. (5-26) we obtain:

$$x_o^* = \psi(x,x_o) = x_o - \frac{f}{q}(x_o - x) \tag{5-35}$$

Thus $t = t^o(x)$ is defined by:

$$T = \frac{(q-f)^{\frac{1-n}{n}}}{n} \int_{x_o}^{\psi(x,x_o)} \left(\frac{1}{\alpha(\eta)}\right)^{\frac{1}{n}} \left(\eta - x_o\right)^{\frac{1-n}{n}} d\eta \tag{5-36}$$

$$t(x,x_o) = T + \frac{1}{n} \int_{\psi(x,x_o)}^{x} \left(\frac{1}{\alpha(\eta)}\right)^{\frac{1}{n}} \left\{f(x_o - \eta) - f(x_o - x)\right\}^{\frac{1-n}{n}} d\eta \tag{5-37}$$

In Eqs. (5-36) and (5-37) $\bar{x} \leq x \leq L_o$; when $o \leq x \leq \bar{x}$, $t^o(x)$ is defined by Eq. (5-21).

The behavior of $h(x,t)$ as a function of t for fixed x , $o < x < x^*$, is the same in cases B_1 and B_2, as in case A (Fig. 5-5). In cases B_1 and B_2 $h_t(x,t) > o$ when $(x,t) \in D_3$ and $h_t(x,t) < o$ when $(x,t) \in D_{11}$; the arguments are the asme as in case A. The maximum of $h(x,t)$ occurs therefore when $(x,t) \in D_{12}$ (Fig. 5-6), but it can occur on the boundary of domain D_{12} as in chapter 4.

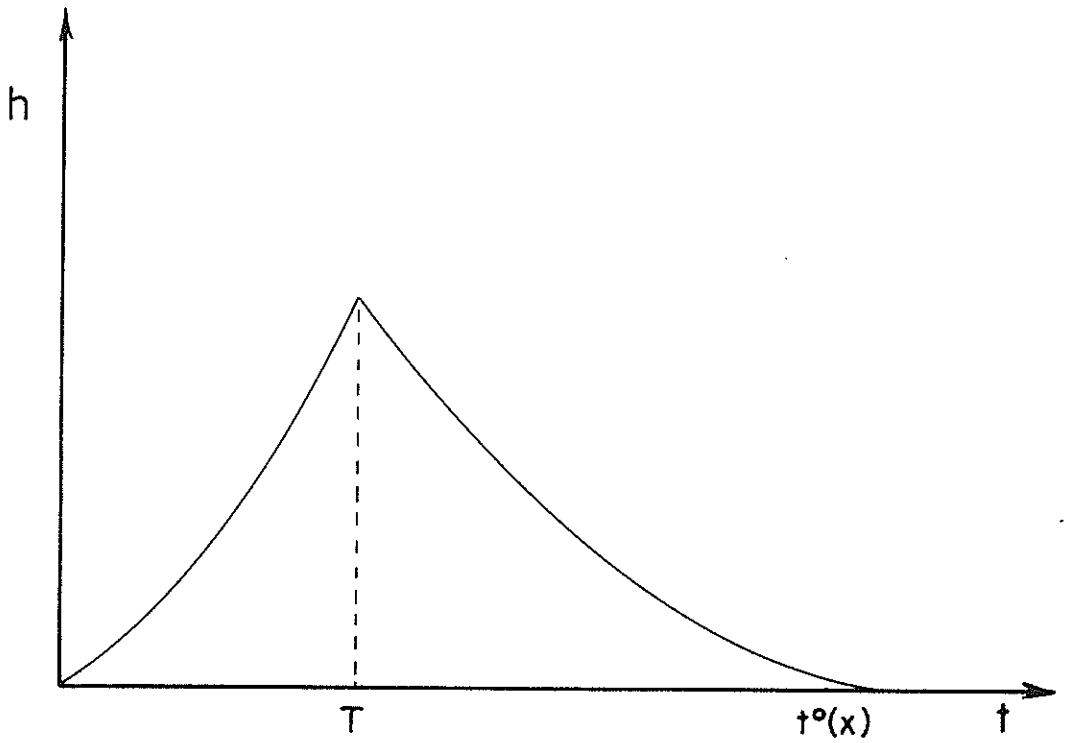

Fig. 5-6. Depth of flow, $h(x,t)$, as a function of t for fixed x for cases B_1 and B_2.

CHAPTER 6

SOLUTION TECHNIQUES

6.1 GENERAL REMARKS

Since its formulation by Lighthill and Whitham (1955), its application to watershed modeling by Henderson and Wooding (1964) and Wooding (1965a, 1965b, 1966), and the subsequent demonstration of its applicability, in general, to problems of hydrologic significance by Woolhiser and Ligget (1967), the kinematic wave theory has been increasingly utilized in numerous investigations on watershed modeling (Brakensiek, 1967; Woolhiser, 1963; Woolhiser, et al, 1970; Eagleson, 1972; Singh, 1974). Depending upon the type of input (rainfall pattern) and representation of watershed geometry, two types of solutions to kinematic wave equations have been developed in these investigations: (1) analytical, and (2) numerical. Analytical solutions have been obtained for time invariant (steady or pulse) input, and simple geometric configurations (for example, rectangular plane section). The assumptions leading to analytical solutions are so restrictive that their practical utility is greatly diminished. Numerical solutions, even though applicable to a wide spectrum of input and geometric configurations, are time-consuming. In this chapter we attempt to develop an approach called "hybrid approach" which is part numerical and part analytical. The fusion of numerical and analytical solutions combines in this approach their individual advantages. The hybrid approach is, therefore, useful where analytical solutions are not feasible, and computationally far more efficient than a numerical approach. We will formulate the current kinematic wave models of watershed runoff in terms of the proposed approach. Finally, this approach will be applied to a set of rainfall-runoff events on a natural agricultural watershed to demonstrate its computational efficiency.

6.2 KINEMATIC WAVE MODELS OF WATERSHED RUNOFF

The development of a kinematic wave model will depend on the type of input and the representation of watershed geometry.

6.2.1 Input Pattern

Rainfall-excess usually forms input to the model. It may be of two types:

6.2.1.1 Time-Invariant. Rainfall-excess is constant in time. It is also referred to as steady rainfall, and may be of either pulse or impulse type.

6.2.1.2 Time-Variant. Rainfall-excess changes in time, and is typically in the form of a hyetograph. It is made up of a combination of pulses of varying magnitudes. It is also referred to as unsteady, or complex rainfall-excess. It is this type of input that we are primarily concerned with in the present study.

6.2.2 Representation of Natural Watershed Geometry

Normally, the geometric structure of a natural watershed is very complex. The only perfect representation of watershed geometry is, of course, the watershed itself. It is, therefore, necessary to transform the complex geometry into a simpler one having a similar hydrologic response. In recent years, four alternate forms of geometric configurations have been proposed to represent a given watershed geometry, and have been incorporated in kinematic wave models of watershed runoff, as described in the previous chapter.

It is apparent from Figs. 4-1 to 4-4 that these alternate, simplified configurations are formed by combinations of the following three elemental sections: (a) linearly converging section of a cone, (b) rectangular plane, and (c) channel.

It will be convenient to develop the hybrid approach for these elemental sections and point out the conditions leading to analytical solutions for them.

6.3 DEVELOPMENT OF HYBRID APPROACH FOR PLANE

The hybrid approach is part analytical and part numerical. The rising limb of runoff hydrograph is computed numerically while the recession limb analytically. Numerical solutions will be based on a simple-step, second-order, explicit, Lax-Wendroff finite difference scheme (Houghton and Kasahara, 1968) which has been found satisfactory in many investigations on kinematic wave modeling (Woolhiser, 1969; Kibler and Woolhiser, 1970; Singh, 1974, 1975e, 1975f, 1975h).

For a detailed mathematical treatment of this numerical scheme for all the elemental sections see the reference by Singh (1974). We will present both dimensional and dimensionless solutions for the special case when $\alpha(x,t) = \alpha$, a constant.

6.3.1 Dimensional Solutions

The kinematic equations for the plane section are:

the continuity equation

$$\frac{\partial h}{\partial t} + u \frac{\partial h}{\partial x} + h \frac{\partial u}{\partial x} = q \qquad (6\text{-}1)$$

and the kinematic momentum equation

$$Q = uh = \alpha h^n \qquad (6\text{-}2)$$

The solution to the above system of equations will characterize the overland flow over the plane. For rainfall of pulse type analytical solutions have been obtained (Wooding, 1965b; Kibler and Woolhiser, 1970; Singh, 1974, 1975h). However, for complex rainfall analytical solutions are not feasible. The hybrid approach is, therefore, formulated.

6.3.1.1 The Rising Hydrograph. The Lax-Wendroff scheme (Houghton and Kasahara, 1968) can be easily derived for the kinematic wave equations. Combining Eqs. (6-1) and (6-2) we obtain:

$$\frac{\partial h}{\partial t} + \alpha n h^{n-1} \frac{\partial h}{\partial x} = q \tag{6-3}$$

The depth of flow, h, is a function of both space and time coordinates.

Exapanding h by Taylor series in time:

$$h(x,t + \Delta t) = h(x,t) + \frac{\partial h}{\partial t} \Delta t + \frac{\partial^2 h}{\partial t^2} \frac{(\Delta t)^2}{2} + \text{HOT} \tag{6-4}$$

where HOT denotes higher order terms.

We can obtain $\frac{\partial h}{\partial t}$ directly from Eq. (6-3) as:

$$\frac{\partial h}{\partial t} = - \alpha n h^{n-1} \frac{\partial h}{\partial x} + q \tag{6-5}$$

Differentiating Eq. (6-5) with respect to t we obtain $\frac{\partial^2 h}{\partial t^2}$ as

$$\frac{\partial^2 h}{\partial t^2} = - \alpha \frac{\partial}{\partial x} \left(n h^{n-1} \frac{\partial h}{\partial t} \right) + \frac{\partial q}{\partial t} \tag{6-6}$$

Substituting Eqs. (6-5) and (6-6) in Eq. (6-4), neglecting HOT, and rearranging the terms we obtain:

$$h(x,t + \Delta t) = h(x,t) + \Delta t \left\{ - \alpha n h^{n-1} \frac{\partial h}{\partial x} + q \right\} + \frac{(\Delta t)^2}{2} \left\{ - \alpha \frac{\partial}{\partial x} \left(n h^{n-1} \frac{\partial h}{\partial t} \right) + \frac{\partial q}{\partial t} \right\} \tag{6-7}$$

We can further write:

$$h(x,t + \Delta t) = h(x,t) + \Delta t \left\{ - \alpha n h^{n-1} \frac{\partial h}{\partial x} + q \right\} + \frac{(\Delta t)^2}{2} \left\{ - \alpha \frac{\partial}{\partial x} \left(n h^{n-1} \left[- \alpha n h^{n-1} \frac{\partial h}{\partial x} + q \right] \right) + \frac{\partial q}{\partial t} \right\} \tag{6-8}$$

Following the notation in Fig. 6-1, Eq. (6-8) can be written in the finite difference form as:

$$h_j^{i+1} = h_j^i - \Delta t \left\{ \alpha \frac{h_{j+1}^{i\,n} - h_{j-1}^{i\,n}}{2\Delta x} - q_j^i \right\} + \frac{(\Delta t)^2}{2} \left[\frac{n\alpha}{\Delta x} \left(\frac{h_{j+1}^{i\,(n-1)} + h_j^{i\,(n-1)}}{2} \right) \right.$$

$$\left\{\alpha\left[\frac{h_{j+1}^{i^n} - h_j^{i^n}}{\Delta x}\right] - \left[\frac{q_{j+1}^i + q_j^i}{2}\right]\right\} - \frac{\alpha n}{\Delta x}\left[\frac{h_j^{i^{(n-1)}} + h_{j-1}^{i^{(n-1)}}}{2}\right]\left\{\alpha\left[\frac{h_j^{i^n} - h_{j-1}^{i^n}}{\Delta x}\right]\right.$$

$$\left. - \left[\frac{q_j^i + q_{j-1}^i}{2}\right]\right\} + \frac{q_j^{i+1} - q_j^i}{\Delta t}\Bigg] \qquad (6\text{-}9)$$

Consider N nodal points along the x-axis at which the depth of flow is to be computed. The boundary conditions are:

$h(x,o) = o$

$h(o,t) = o$

Equation (6-9) will give, when used in conjunction with the boundary conditions, the depth of flow at the nodal points $j = 1, 2, 3, \ldots (N-1)$. The depth of flow at the outlet $(j = N)$ can be obtained using the first order difference scheme:

$$h_N^{i+1} = h_N^i + \Delta t\left\{-\alpha\frac{h_N^{i^n} - h_{N-1}^{i^n}}{\Delta x} + q_N^i\right\} \qquad (6\text{-}10)$$

6.3.1.2 The Recession Hydrograph. The lateral inflow, q , will be zero for the recession hydrograph. Equation (6-3) can then be written as:

$$\frac{\partial h}{\partial t} + \alpha n h^{n-1}\frac{\partial h}{\partial x} = o \qquad (6\text{-}11)$$

Although Eq. (6-11) is a nonlinear partial differential equation, it can be solved analytically by standard procedure of the separation of variables. Consider:

$$h = X(x)\ T(t) \qquad (6\text{-}12)$$

Substituting Eq. (6-12) in Eq. (6-11) and rearranging the terms we get:

$$\frac{1}{T^n}\frac{dT}{dt} + \alpha n\ X^{n-2}\frac{dX}{dx} = o \qquad (6\text{-}13)$$

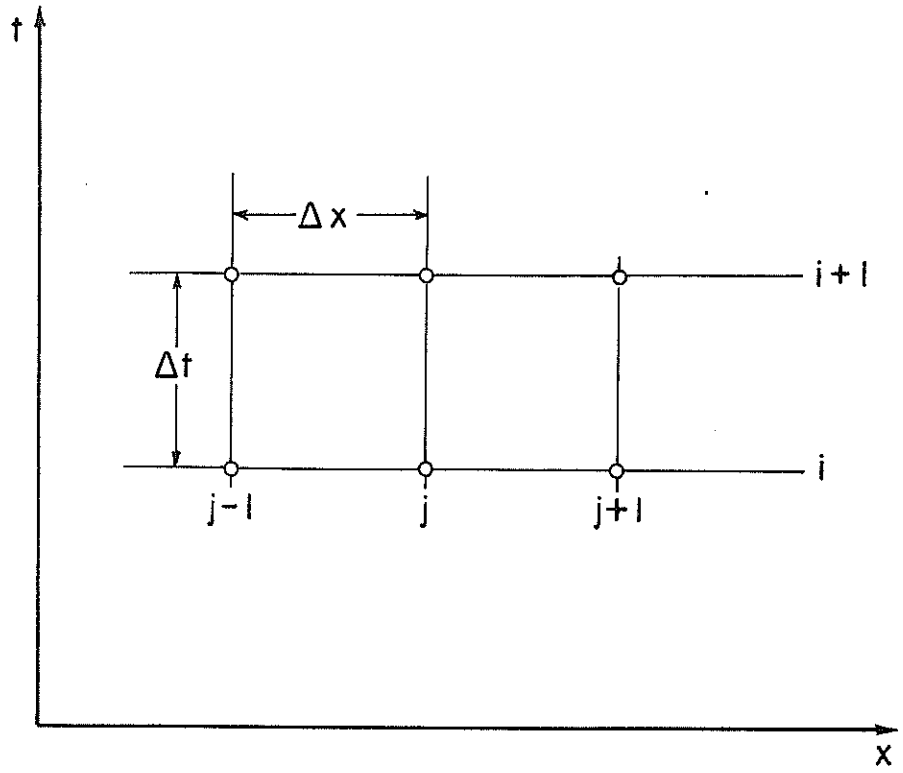

Fig. 6-1. Notation for finite difference scheme.

Writing Eq. (6-13) as:

$$\frac{1}{T^n}\frac{dT}{dt} = -\alpha n\, X^{n-2}\frac{dX}{dx} = -\mu^2 \tag{6-14}$$

where μ^2 is some constant which mathematically can take negative, zero or positive values. In our case it can only take positive values, to be consistent with physical realism of the problem Thus we have:

$$\frac{1}{T^n}\frac{dT}{dt} + \mu^2 = o \tag{6-15}$$

$$\alpha n\, X^{n-1}\frac{dX}{dx} - \mu^2 = o \tag{6-16}$$

This system of equations can now be easily solved. Thus we obtain:

$$T = \left\{(1 - n)\ (C_1 - \mu^2 t)\right\}^{\frac{1}{1-n}} \tag{6-17}$$

$$X = \left\{\left(\frac{n-1}{\alpha n}\right)\ (C_1 + \mu^2 x)\right\}^{\frac{1}{n-1}} \tag{6-18}$$

where C_1 and C_2 are the constants of integration. The following boundary conditions can be utilized to solve for these constants:

$h(o,t) = o$

$h(L_o,t_o) = h_o$

The quantities, t_o and h_o, will be obtained from the rising hydrograph and will correspond to the point where recession starts, that is, h_o will equal the peak runoff depth and t_o the peak runoff time in a single peaked hydrograph. Then we have:

$$h = \left\{\frac{(n-1)\ (C_1 + \mu^2 x)}{(1-n)\ \alpha n\ (C_1 - \mu^2 t)}\right\}^{\frac{1}{n-1}} \tag{6-19}$$

Substituting the boundary conditions we obtain:

$$C_1 = \left\{ \mu^2 t_o - \frac{\mu^2 L_o}{h_o^{n-1}\ \alpha n} \right\}$$

$$C_2 = o$$

Then we get:

$$h = h_o \left\{ \frac{x}{L_o + (t - t_o)\alpha n h_o^{n-1}} \right\}^{\frac{1}{n-1}} \qquad (6\text{-}20)$$

6.3.2 Dimensionless Equations and Solutions

One of the advantages of normalized solutions is that the number of parameters is reduced. The following normalizing quantities for the plane section can be defined:

$X_o = L_o$

$T_o = \left(\frac{1}{q_{max}}\right)^{\frac{(n-1)}{n}} \left(\frac{L_o}{\alpha}\right)^{\frac{1}{n}}$, where q_{max} is the maximum spatially uniform lateral inflow rate. T_o is the time required to traverse the distance X_o at the velocity V_o corresponding to the normalizing depth H_o ; $V_o = \alpha H_o^{n-1}$.

$Q_o = H_o V_o = q_{max} L_o$, total steady state outflow from the section divided by the mean width of the section.

$$V_o = \frac{L_o}{T_o}$$

$$q_o = \frac{H_o V_o}{L_o}$$

$$q_{max} = q_o$$

The dimensionless variables, designated with asterisks, are thus given by:

$$h_* = \frac{h}{H_o} \ ; \ q_* = \frac{q}{q_o} \ ; \ t_* = \frac{t}{T_o} \ ; \ x_* = \frac{x}{X_o} \ ; \ u_* = \frac{u}{V_o} \ ; \ Q_* = \frac{Q}{Q_o}$$

Substituting these dimensionless quantities in Eqs. (6-1) and (6-2) we obtain:

$$\frac{\partial h}{\partial t}_* + u_* \frac{\partial h}{\partial x}_* + h_* \frac{\partial u}{\partial x}_* = q_* \tag{6-21}$$

$$Q_* = u_* h_* = h_*^n \tag{6-22}$$

Equations (6-21) and (6-22) are the dimensionless form of Eqs. (6-1) and (6-2). Note that the parameter α no longer appears in the dimensionless equations. Now we present derivation of the normalizing quantities.

6.3.2.1 Definition of q_o . Substituting the normalized quantities in Eq. (6-1) and simplifying we obtain:

$$\frac{\partial h}{\partial t}_* + u_* \frac{\partial h}{\partial x}_* + h_* \frac{\partial u}{\partial x}_* = q_* \frac{q_o X_o}{H_o V_o} \tag{6-23}$$

In Eq. (6-23) if we choose $q_o = \frac{H_o V_o}{X_o}$, then the normalizing quantities will be eliminated and its dimensionless form will be given by Eq. (6-21).

6.3.2.2 Definition of T_o . According to its definition, $T_o = \frac{L_o}{V_o}$. We know that $V_o = \alpha H_o^{n-1}$, and $H_o V_o = q_{max} L_o$. Then we can write:

$$H_o = \left\{\frac{q_{max} L_o}{\alpha}\right\}^{\frac{1}{n}}$$

$$V_o = \alpha\left\{\frac{q_{max} L_o}{\alpha}\right\}^{\frac{n-1}{n}}$$

Then we have:

$$T_o = \left(\frac{1}{q_{max}}\right)^{\frac{n-1}{n}} \left\{\frac{L_o}{\alpha}\right\}^{\frac{1}{n}}$$

6.3.2.3 Definition of q_{max} . We know that

$$q_{max} = \frac{Q_o}{L_o} = \frac{H_o V_o}{L_o}$$

and hence

$q_{max} = q_o$

6.3.2.4 Definition of Q_o . The area of plane per unit width is L_o . Then the steady state discharge per unit mean width at $x_* = 1$ is $q_{max} L_o$. For the plane $Q_o = H_o V_o$.

6.3.2.5 Dimensionless Solutions. Following the same procedure as outlined for the dimensional solutions we obtain the numerical solution for the rising hydrograph as:

$$h_{*_j}^{i+1} = h_{*_j}^{i} - \Delta t_* \left\{ \frac{h_{*_{j+1}}^{i^n} - h_{*_{j-1}}^{i^n}}{2\Delta x_*} + q_{*_j}^{i} \right\} + \frac{(\Delta t_*)^2}{2} \left[\frac{n}{\Delta x_*} \left(\frac{h_{*_{j+1}}^{i^n} + h_{*_j}^{i^n}}{2} \right) \left\{ \left(\frac{h_{*_{j+1}}^{i^n} - h_{*_j}^{i^n}}{\Delta x_*} \right) - \left(\frac{q_{*_{j+1}}^{i} - q_{*_j}^{i}}{2} \right) \right\} - \frac{n}{\Delta x_*} \left(\frac{h_{*_j}^{i^n} + h_{*_{j-1}}^{i^n}}{2} \right) \left\{ \left(\frac{h_{*_j}^{i^n} - h_{*_{j-1}}^{i^n}}{\Delta x_*} \right) - \left(\frac{q_{*_j}^{i} + q_{*_{j-1}}^{i}}{2} \right) \right\} + \left(\frac{q_{*_j}^{i+1} - q_{*_j}^{i}}{\Delta t_*} \right) \right] \quad (6\text{-}24)$$

for $j = 1,2,\ldots (N-1)$.

$$h_{*_N}^{i+1} = h_{*_N}^{i} - \Delta t_* \left\{ \frac{h_{*_{N-1}}^{i} - h_{*_N}^{i}}{\Delta x_*} + q_{*_N}^{i} \right\} \quad (6\text{-}25)$$

for $j = N$

For the recession hydrograph the analytical solution takes the form:

$$h_* = h_{*_o} \left\{ \frac{x_*}{1 + (t_* - t_{*_o})\, n\, h_{*_o}^{n-1}} \right\} \quad (6\text{-}26)$$

where h_{*_o} and t_{*_o} correspond to the dimensionless peak depth of flow and the peak time, and will be given by the solutions of the rising hydrograph.

6.4 DEVELOPMENT OF HYBRID APPROACH FOR CONVERGING SECTION

The kinematic wave equations for the converging section, as derived by Singh (1974), are:

the continuity equation

$$\frac{\partial h}{\partial t} + u\frac{\partial h}{\partial x} + h\frac{\partial u}{\partial x} = q + \frac{uh}{(L_o - x)} \tag{6-27}$$

and the kinematic momentum equation

$$Q = uh = \alpha h^{n-1} \tag{6-28}$$

where L_o is radius of flow region, and other symbols retain their same meaning. The solution to the above system of equations will completely characterize the overland flow over the converging surface. For pulse lateral inflow, q, analytical solutions have been obtained by Woolhiser (1969) and Singh (1974), but for complex lateral inflow analytical solutions do not seem tractable. The hybrid approach is, therefore, formulated.

6.4.1 The Rising Hydrograph

Following the same procedure as outlined for the plane section the Lax-Wendroff scheme for the converging section can be easily derived: Using the notation in Fig. 6-1, it can be written as:

$$h_j^{i+1} = h_j^i - \left\{ \alpha \left(\frac{{h_{j+1}^i}^n - {h_{j-1}^i}^n}{2\Delta x} \right) - q_j^i - \frac{\alpha {h_j^i}^n}{(L_o - x_j^i)} \right\} \left\{ \Delta t + \frac{(\Delta t)^2 \alpha n h_j^i}{2(L_o - x_j^i)} \right\}$$

$$+ \frac{(\Delta t)^2}{2} \frac{n\alpha}{\Delta x} \left(\frac{{h_{j+1}^i}^{(n-1)} - {h_j^i}^{(n-1)}}{2} \right) \left\{ \alpha \left(\frac{{h_{j+1}^i}^n - {h_j^i}^n}{\Delta x} \right) - \left(\frac{q_{j+1}^i + q_j^i}{2} \right) - \alpha \right.$$

$$\left.\left.\left.\left.\frac{h_{j+1}^{i^n} + h_j^{i^n}}{2L_o - (x_{j+1}^i + x_j^i)}\right)\right\} - \frac{n\alpha}{\Delta x}\left[\frac{h_j^{i^{(n-1)}} + h_{j-1}^{i^{(n-1)}}}{2}\right]\left\{\left[\alpha\ \frac{h_j^{i^n} - h_{j-1}^{i^n}}{\Delta x}\right] -\right.\right.\right.$$

$$\left.\left.\left.\left[\frac{q_j^i + q_{j-1}^i}{2}\right] - \frac{\alpha\left(h_j^{i^n} + h_{j+1}^{i^n}\right)}{2L_o - (x_j^i + x_{j-1}^i)}\right\} + \frac{q_j^{i+1} + q_j^i}{\Delta t}\right]\right. \qquad (6\text{-}29)$$

for $j = 1, 2, \ldots (N-1)$. The boundary conditions are:

$h(x,o) = o$

$h(o,t) = o$

Equation (6-29) will give, when used in conjunction with the boundary conditions, the depth of flow at the nodal points $j = 1,2,3,\ldots (N-1)$. The depth of flow at the outlet $(j=N)$ will be given by the first order scheme:

$$h_{NK}^i = h_{NK}^i + \Delta t\left\{ - \left[\frac{h_N^{i^n} - h_{N-1}^{i^n}}{\Delta x}\right] + q_N^i + \frac{\alpha\, h_N^{i^n}}{(L_o - x_N^i)}\right\} \qquad (6\text{-}30)$$

6.4.2 The Recession Hydrograph

For the recession hydrograph $q = o$, and the boundary conditions are:

$h(o,t) = o$

$h(L_o(1-r),\ t_o) = h_o$

where r denotes the degree of convergence, and $L_o(1-r)$ the length of flow. Then the solution for the recession hydrograph is:

$$h = h_o \left\{\frac{r^{(n-1)/n}\ (L_o^{(2n-1)/n} - (L_o - x)^{(2n-1)/n})}{(L_o-x)^{(n-1)/n}\ (L_o(1-r^{(2n-1)/n}) + (t-t_o)\ \alpha\ r^{(n-1)/n}(2n-1)\ h_o^{n-1})}\right\}^{\frac{1}{(n-1)}} \qquad (6\text{-}31)$$

For an elaborate discussion of these solutions see the reference by Singh (1975e).

6.4.3 Dimensionless Solutions

Equations (6-27) and (6-28) can be written in dimensionless form as:

$$\frac{\partial h_*}{\partial t_*} + h_* \frac{\partial u_*}{\partial x_*} + u_* \frac{\partial h_*}{\partial x_*} = q_* + \frac{u_* h_*}{(1 - x_*)} \tag{6-32}$$

$$Q_* = u_* h_* = h_*^n \tag{6-33}$$

where the dimensionless variables, designated with asterisks, are given by:

$$h_* = \frac{h}{H_o} \; ; \; q_* = \frac{q}{q_o} \; ; \; t_* = \frac{t}{T_o} \; ; \; x_* = \frac{x}{x_o} \; ; \; Q_* = \frac{Q}{Q_o}$$

For derivation of the normalizing quantities see the reference by Singh (1974). Only their definitions will be presented here.

H_o is the normal depth for a discharge equal to the total steady state outflow from the converging section divided by the mean width of the section.

$$X_o = L_o(1-r)$$

$$T_o = \left(\frac{1}{q_{max}}\right)^{\frac{n-1}{n}} \left\{\frac{L_o(1-r)}{\alpha}\right\}^{\frac{1}{n}}$$

T_o is the time required to traverse the distance X_o at the velocity V_o corresponding to the normalizing depth H_o ; $V_o = \alpha H_o^{n-1}$; and q_{max} is the maximum spatially lateral inflow rate.

$$q_o = \frac{H_o V_o}{L_o(1-r)}$$

$$Q_o = \frac{H_o V_o(1+r)}{2r}$$

Then the dimensionless numerical solution of the rising hydrograph will be expressed by:

$$h_{*_j}^{i+1} = h_{*_j}^{i} - \left\{ \frac{h_{*_{j+1}}^{i^n} - h_{*_{j-1}}^{i^n}}{2\Delta x_*} - q_{*_j}^{i} - \frac{(1-r)\, h_{*_j}^{i^n}}{(1-(1-r)x_{*_j}^{i})} \right\} \left\{ \Delta t_* + \frac{(\Delta t_*)^2}{2} \right.$$

$$\left. \frac{(1-r)\, n\, h_{*_j}^{i^{(n-1)}}}{(1-(1-r)\, x_{*_j})} \right\} + \frac{(\Delta t_*)^2}{2} \left[\frac{n}{\Delta x_*} \left(\frac{h_{*_{j+1}}^{i} + h_{*_j}^{i}}{2} \right)^{n-1} \left\{ \frac{h_{*_{j+1}}^{i^n} - h_{*_j}^{i^n}}{\Delta x_*} - \frac{q_{*_{j+1}}^{i} - q_{*_j}^{i}}{2} - \right. \right.$$

$$\left. \left. \frac{(1-r)\, (h_{*_{j+1}}^{i^n} + h_{*_j}^{i^n})}{(2-(1-r)\, (x_{*_{j+1}}^{i} + x_{*_j}^{i}))} \right\} - \frac{n}{\Delta x_*} \left(\frac{h_{*_j}^{i} + h_{*_{j-1}}^{i}}{2} \right)^{n-1} \left\{ \frac{h_{*_j}^{i^n} - h_{*_{j-1}}^{i^n}}{\Delta x_*} - \frac{q_{*_j}^{i^n} - q_{*_{j-1}}^{i^n}}{2} - \right. \right.$$

$$\left. \left. \frac{(1-r)\, (h_{*_j}^{i^n} + h_{*_{j-1}}^{i^n})}{(2-(1-r)\, (x_{*_j}^{i} + x_{*_{j-1}}^{i}))} \right\} + \frac{q_{*_j}^{i-1} - q_{*_j}^{i}}{\Delta t_*} \right] \qquad (6\text{-}34)$$

for $j=1,2,\ldots(N-1)$, and

$$h_{*_N}^{i+1} = h_{*_N}^{i} - \Delta t_* \left\{ \frac{h_{*_N}^{i^n} - h_{*_{N-1}}^{i^n}}{\Delta x_*} - q_{*_N}^{i} - \frac{(1-r)\, h_{*_N}^{i^n}}{(1-(1-r)x_{*_N}^{i})} \right\} \qquad (6\text{-}35)$$

for $j = N$

The dimensionless analytical solution for the recession hydrograph will take the form:

$$h_* = h_{*_o} \left\{ \frac{r^{(n-1)/n}\, [1-(1-(1-r)x_*)^{\frac{2n-1}{n}}]}{(1-(1-r)x_*)^{(n-1)/n} [(1-r^{(2n-1)/n}) + (t_*-t_{*_o})(2n-1)(1-r)\, h_{*_o}^{n-1}\, r^{(n-1)/n}]} \right\}^{\frac{1}{(n-1)}} \qquad (6\text{-}36)$$

6.5 DEVELOPMENT OF HYBRID APPROACH FOR CHANNEL SECTION

The channel is an important element in the geometric network representing a natural watershed. The lateral inflow to it will always be time dependent.

Hence, the numerical approach is perhaps the most practical way to obtain the solutions. The Lax-Wendroff scheme will be given for the channel geometry as shown in Fig. 6-2 (where a is some arbitrarily chosen constant t_o convert a triangular section into a trapezoidal one).

The kinematic wave equations for the channel section can be written as: the continuity equation

$$\frac{\partial A}{\partial t} + \frac{\partial Q}{\partial x} = q \tag{6-37}$$

and the kinematic momentum equation

$$Q = \alpha\, A(HR)^{n-1} = \alpha\, A^{n}\, (WP)^{1-n} \tag{6-38}$$

Where A = cross-sectional area, HR = hydraulic radius = A/WP , and WP = wetted perimeter. The Lax-Wendroff scheme for the channel can be written as:

$$A_j^{i+1} = A_j^i + \Delta t \left[-\frac{f_1}{2\Delta x} + q_j^i \right] + \frac{(\Delta t)^2}{2} \left[\left\{ \frac{f_2}{2} \left(\frac{f_3}{\Delta x} - q_j^i \right) - \frac{f_4}{2} \left(\frac{f_5}{\Delta x} - q_j^i \right) \right\} + \frac{q_j^{i+1} - q_j^i}{\Delta t} \right] \tag{6-39}$$

where $f_1 = GAF\,(h_{j+1}^i) - GAF\,(h_{j-1}^i)$; $f_2 = DGA\,(h_{j+1}^i) + DGA\,(h_j^i)$;

$f_3 = GAF\,(h_{j+1}^i) - GAF\,(h_j^i)$; $f_4 = DGA\,(h_j^i) + DGA\,(h_{j-1}^i)$; $GAF(h) = Q$;

$DGA(h) = \partial Q/\partial A$; and $DGH(h) = \partial Q/\partial h$.

Equation (6-39) will, in conjunction with the boundary conditions: $h(x,o) = o$, $h(o,t) = g(t)$, input receiving from the upstream plane, will provide the depth of flow at the nodal points $j = 1,2,\ldots(N-1)$. The depth at the outlet $(j = N)$ will be computed by the first order numerical scheme:

$$A_N^{i+1} = A_N^i + \Delta t \left[\frac{q_N^{i+1} + q_N^i}{2} - \left\{ \frac{GAF(h_N^i) - GAF(h_{N-1}^i)}{\Delta x} \right\} \right] \tag{6-40}$$

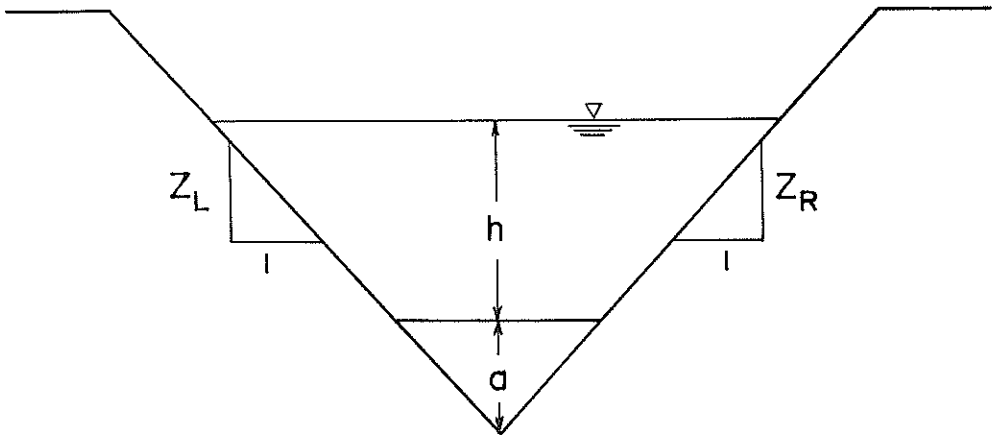

Fig. 6-2. Channel geometry.

The normalizing quantities for the channel section are defined as they are for the plane section. The dimensionless solutions will be identical to those given in Eqs. (6-39) and (6-40) and hence will not be repeated.

6.6 HYBRID FORMULATION OF KINEMATIC WAVE MODELS

In hybrid formulation the main emphasis will be to use analytical solutions wherever and whenever possible. Obviously, it will much depend on the position of a geometric element in a network model under consideration.

6.6.1 The Converging Section Model

The geometry of this model could be taken to represent a watershed of any complexity, or it could be used as a basic element in a network model (Woolhiser, 1969; Singh, 1974), for example, in the composite model. For a given rainfall event the runoff hydrograph will be simulated using numerical solution (Eqs. (6-29) and (6-30))for the rising part and analytical solution (Eq. (6-31)) for the recession part.

6.6.2 The Wooding Model

The hydrograph of each plane will be computed using hybrid approach, that is, the rising limb by Eqs. (6-9) and (6-10), and the recession limb by Eq. (6-11). The hydrographs of the planes will form input to the channel. The two hydrographs must be added together before putting them as input to the channel. The hydrograph at the mouth of the channel will be computed using Eqs. (6-39) and (6-40).

6.6.3 The Composite Model

The geometry of this model is a combination of the geometries of converging section and Wooding's model. The hydrograph for the converging section will be computed as described above, and will form input to the

channel at its upstream boundary. The hydrographs for the planes will be simulated in just the same way as described for Wooding's model, and will form, when added together, lateral input to the channel. The hydrograph at the outlet will be simulated using Eqs. (6-39) and (6-40).

6.6.4 The Cascade Model

The cascade geometry consists of planes and channels. The arrangement of planes and channels will be different for different watersheds. Depending upon this arrangement, numerical and analytical solutions will be utilized. For example, if the arrangement were the one shown in Fig. 4-4, hydrographs of the planes will be simulated using hybrid approach, and channel hydrograph will be simulated using Eq. (6-39) and (6-40).

6.7 APPLICATION OF HYBRID APPROACH TO A NATURAL WATERSHED

To demonstrate the computational efficiency of the hybrid approach the converging overland flow model was considered. Nine rainfall-runoff events were obtained on an experimental agricultural watershed, called SW-17, near Riesel (Waco), Texas. This is a small watershed of about 3 acres in areal extent. For a detailed description of the watershed and rainfall-runoff data thereon see the USDA publication entitled "Hydrologic Data for Experimental Agricultural Watersheds in the United States", published almost every year.

For these events rainfall-excess was estimated (Singh, 1974) using Philip's equation (Philip, 1957). Optimal values of the parameters were found to be: $L_o(1-r) = 400$ ft , $r = 0.01$, $n = 1.5$, and $\alpha = 0.90$. A brief summary of rainfall-runoff data and parameters of Philip's equation are given in Table 6-1. It must be mentioned that the parameter α was optimized on hydrograph peak; more on the optimization will be discussed in the next chapter.

Table 6-1. Parameters of Philip's equation[1] for rainfall-runoff events on watershed SW-17 Riesel (Waco), Texas

Serial Number	Date of Rainfall Event	Rainfall Volume (Inches)	Runoff Volume (Inches)	Observed Hydrograph Peak (Inches/hr.)	Parameter A	Parameter S
1	3-12-1953	0.830	0.695	1.610	0.01	0.3713
2	3-31-1957	0.590	0.240	0.441	0.01	0.9603
3	4-24-1957	1.750	1.730	2.900	0.01	0.0062
4	4-13-1957	1.620	1.360	1.740	0.01	0.1700
5	6-24-1959	1.990	1.520	2.170	0.01	0.5298
6	6-25-1961	1.380	0.350	0.604	0.01	4.0349
7	7-16-1961	1.080	0.280	0.348	0.01	1.0993
8	6-09-1962	2.080	1.670	3.790	0.01	0.5218
9	3-29-1965	4.990	3.5033	2.440	0.01	1.3470

[1]Philip's equation for infiltration is:

$$f = A + S\ t^{-0.5}$$

where f is infiltration in inches/hr., t, time in hours, and A and S are parameters.

Before comparing the computational efficiency of numerical and hybrid approaches, the error behavior of the Lax-Wendroff scheme as related to the number of grid points in space was examined. For an arbitrarily chosen rainfall event of 6/31/1962, the error behavior is shown in Fig. 6-3. Here the error was defined as: (observed runoff peak-estimated runoff peak) x 100/(observed runoff peak). Figure 6-3 gives an idea, however, about a reasonable number of grid points to be chosen in computation if reasonable accuracy is to be acquired. It must be pointed out that because of roundoff and propagation errors that develop in the computing system the error will not go to zero even for a large number of grid points; instead it will start increasing as these errors start dominating the accuracy of the difference scheme.

For all the nine rainfall events hydrographs were simulated, on IBM 360-44 computer, using both numerical and hybrid approaches. Their computational performance is shown in Table 6-2. Figure 6-4 gives the execution time taken by both schemes to perform the same computations. Figure 6-5 gives the cost of execution (computed at the rate of 250×10^{-4} \$/sec). Figure 6-6 gives the total cost (including execution cost, compilation cost, page cost, printing cost, etc.) of running the computer programs. From Table 6-2 and Figs. 6-3--6-5, it is quite evident that hybrid approach is far more efficient than the numerical approach. From these figures it is also clear that the cost of hybrid approach shows a very little increase with increasing number of grid points. This tacitly suggests that it is the recession limb of the hydrograph that requires more computation because of its usually longer duration than the rising limb.

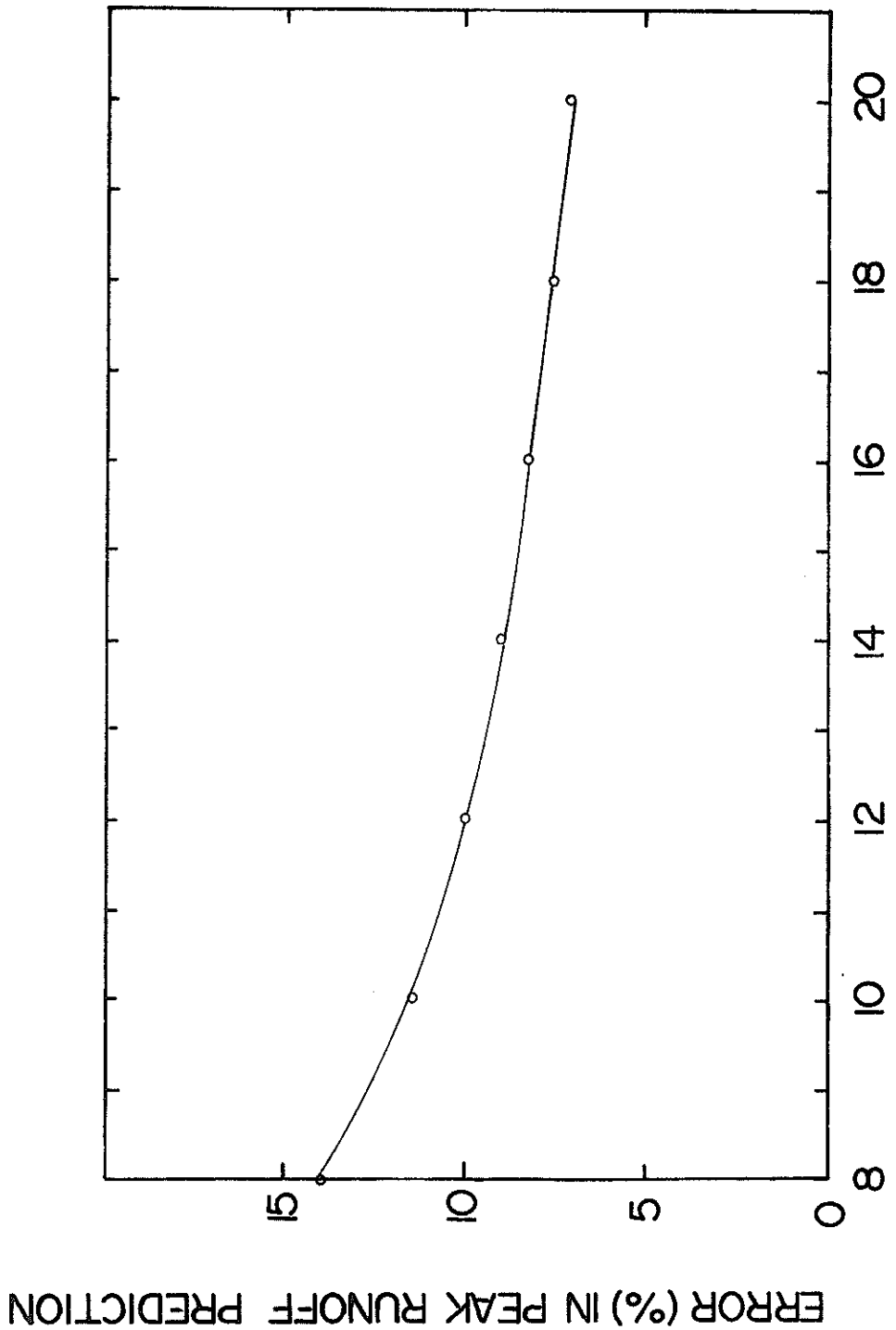

Fig. 6-3. Relationship between relative error and number of grid points for Lax-Wendroff finite-difference scheme.

Table 6-2. Computational efficiency of numerical and hybrid approaches

Grid Points	Numerical Approach			Hybrid Approach			Remarks
	Execution Time (Secs)	Execution Cost (Dollars)	Total Cost (Dollars)	Execution Time (Secs)	Execution Cost (Dollars)	Total Cost (Dollars)	
8	144	3.60	5.25	65	1.63	3.43	Watershed SW-17 Riesel (Waco), Texas.
10	198	4.95	6.73	82	2.05	3.76	
12	270	6.75	8.45	98	2.45	4.29	Number of Rainfall events = 9
14	361	9.03	10.72	115	2.88	4.56	L_o (1-r) = 400'
16	472	11.80	13.52	135	3.38	5.10	r = 0.01 α = 0.90
18	597	14.93	16.70	142	3.55	5.30	
20	749	18.73	20.50	165	4.13	5.85	

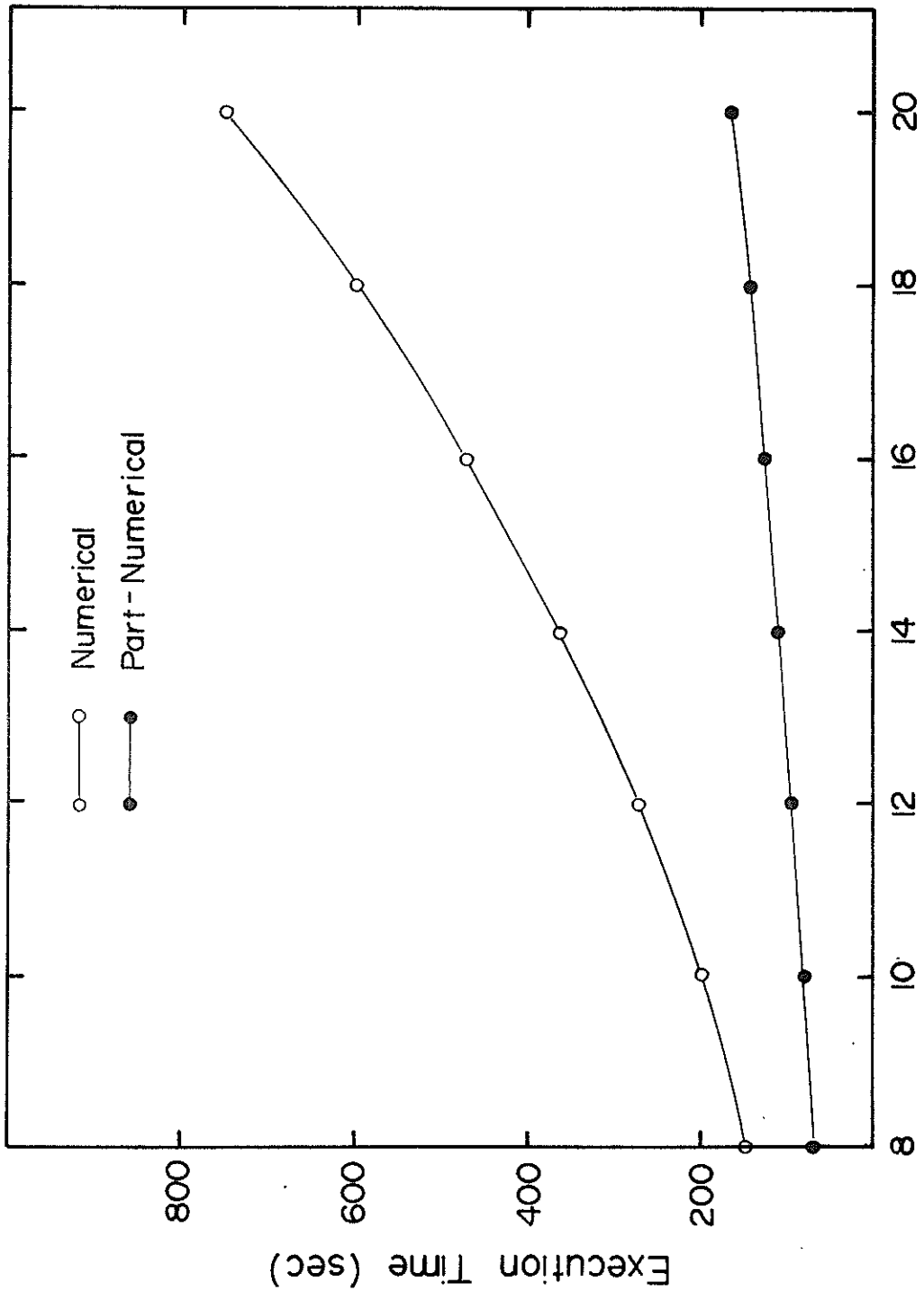

Fig. 6-4. Comparison of execution times of numerical and hybrid approaches for simulating hydrographs for a set of nine rainfall events on watershed SW-17, Riesel (Waco), Texas.

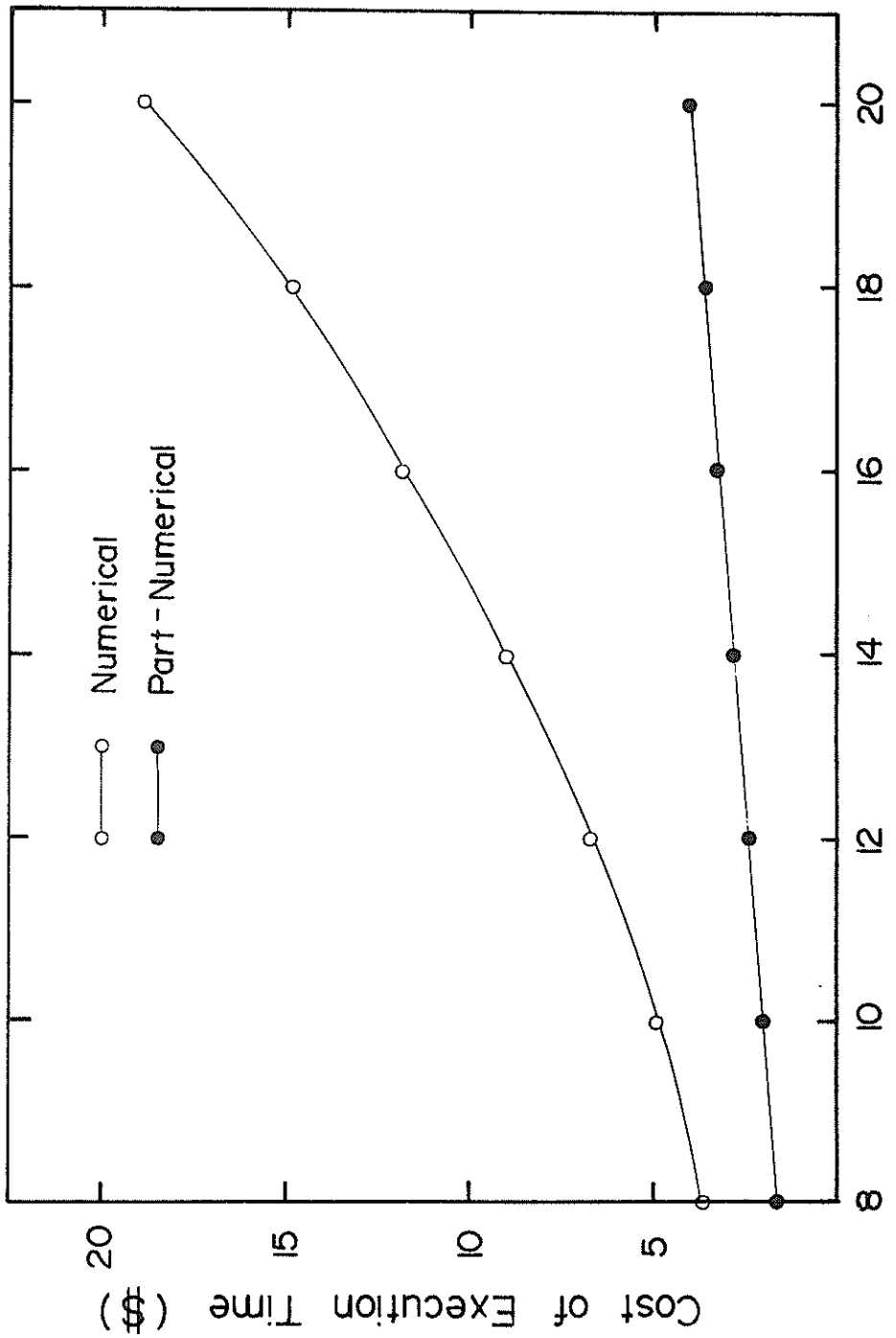

Fig. 6-5. Comparison of execution costs of numerical and hybrid approaches for simulating hydrographs for a set of nine rainfall events on watershed SW-17, Riesel (Waco), Texas.

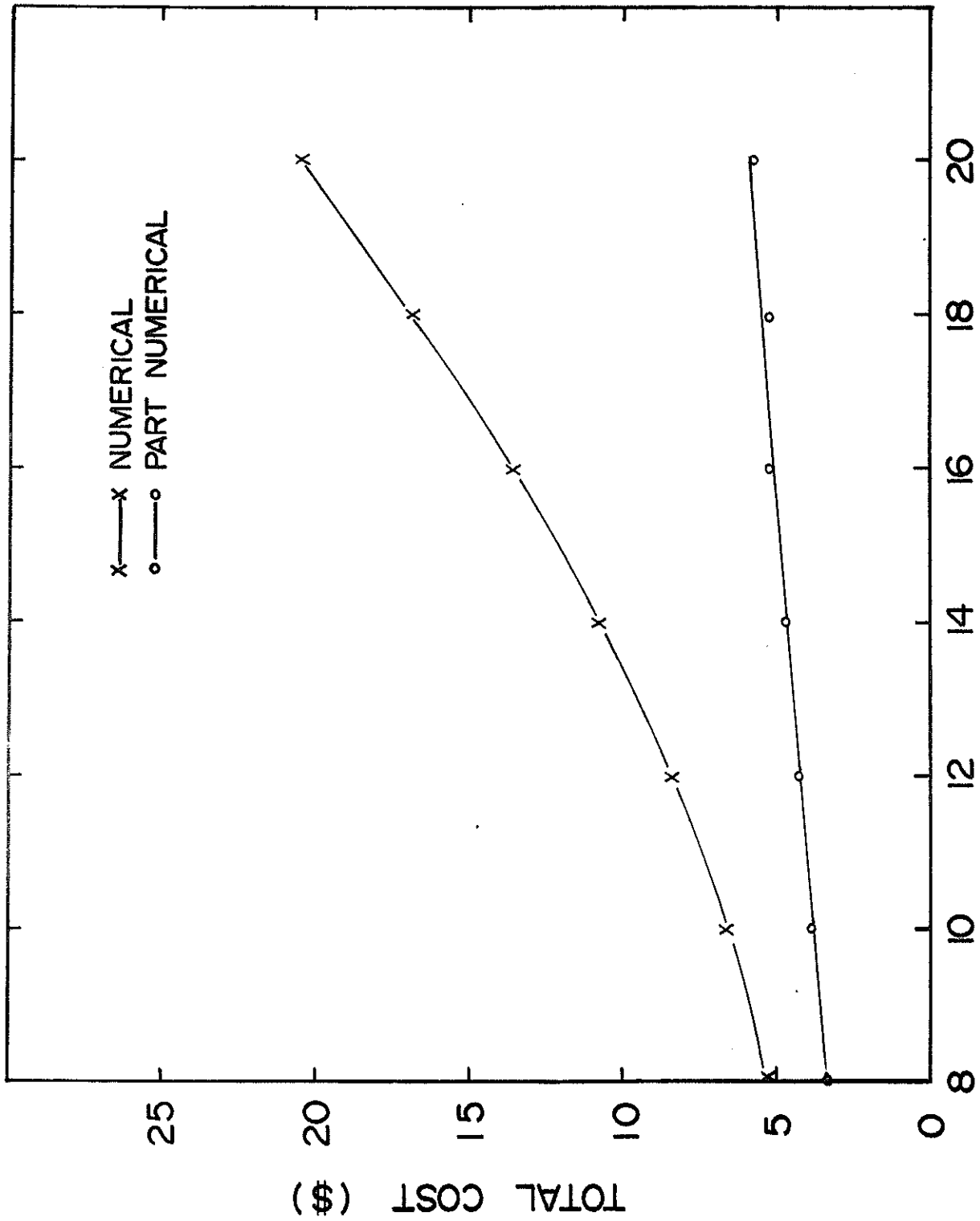

Fig. 6-6. Comparison of total costs of numerical and hybrid approaches for simulating runoff hydrographs for a set of nine rainfall events on watershed SW-17, Riesel (Waco), Texas.

CHAPTER 7

APPLICATION TO NATURAL WATERSHEDS

7.1 GENERAL REMARKS

In the previous chapters we dealt with analytical mathematics of non-linear watershed runoff dynamics by the method of characteristic domains in that conditions were pointed out regarding the feasibility of explicit analytic solutions. In this chapter our objective is to apply the proposed distributed kinematic wave model to predict surface runoff from natural agricultural watersheds, examine its performance and reflect on its potential in simulating watershed surface runoff response.

When analytical solutions are not feasible use is made of hybrid solutions which combine advantages of numerical and analytical solutions. We will briefly present numerical solutions for the distributed model. The coupling of the continuity equation and kinematic approximation to momentum equation yields:

$$\frac{\partial h}{\partial t} + \alpha(x) n\, h^{n-1} \frac{\partial h}{\partial x} + h^n \frac{\partial \alpha(x)}{\partial x} = q(x,t) \tag{7-1}$$

The Lax-Wendroff for Eq. (7-1) can be formulated as:

$$\frac{\partial h}{\partial t} = - \alpha(x)\, h^{n-1}\, n \frac{\partial h}{\partial x} - h^n \frac{\partial \alpha(x)}{\partial x} + q(x,t) \tag{7-2}$$

Expanding $h(x,t+\Delta t)$ by Taylor Series,

$$h(x,t+\Delta t) = h(x,t) + \Delta t \frac{\partial h}{\partial t} + \frac{(\Delta t)^2}{2} \frac{\partial^2 h}{\partial t^2} + \text{HOT} \tag{7-3}$$

where HOT denotes higher order terms. Differentiating Eq.(7-2) with respect to t,

$$\frac{\partial^2 h}{\partial t^2} = - \alpha(x) \frac{\partial}{\partial x} \left\{ \frac{\partial h^n}{\partial t} \right\} - \frac{\partial \alpha(x)}{\partial x} \frac{\partial h^n}{\partial t} + \frac{\partial q(x,t)}{\partial t} \tag{7-4}$$

Substituting Eqs. (7-2) and (7-4) into Eq. (7-3) and neglecting HOT we obtain:

$$h(x,t+\Delta t)= h(x,t) + \Delta t \left\{- \alpha(x)\ n\ h^{n-1} \frac{\partial h}{\partial x} - h^n \frac{\partial \alpha(x)}{\partial x} + q(x,t)\right\} +$$

$$\frac{(\Delta t)^2}{2} \left\{- \alpha(x) \frac{\partial}{\partial x}\left[\frac{\partial h^n}{\partial t}\right] - \frac{\partial \alpha(x)}{\partial x} \frac{\partial h^n}{\partial t} + \frac{\partial q(x,t)}{\partial t}\right\} \qquad (7\text{-}5)$$

Writing Eq. (7-5) in a compact form,

$$h(x,t+\Delta t) = h(x,t) + \left\{- \alpha(x) \frac{\partial h^n}{\partial x} - h^n \frac{\partial \alpha(x)}{\partial x} + q(x,t)\right\} \left\{\Delta t + \frac{(\Delta t)^2}{2}\right.$$

$$\left.\left(- \frac{\partial \alpha(x)}{\partial x}\ n\ h^{n-1}\right)\right\} + \frac{(\Delta t)^2}{2} \left[\frac{\partial q(x,t)}{\partial x} - \alpha(x) \frac{\partial}{\partial x} \left\{n\ h^{n-1} \left[- h^n \frac{\partial \alpha(x)}{\partial x} -\right.\right.\right.$$

$$\left.\left.\left.\alpha(x) \frac{\partial h^n}{\partial x} + q(x,t)\right)\right\}\right] \qquad (7\text{-}6)$$

Following the notation in Fig. 6-1 we can write Eq. (7-6) in finite difference form as:

$$h_j^{i+1} = h_j^i + \left\{-h_j^{i^n} \left(\frac{\alpha_{j+1}^i - \alpha_{j-1}^i}{2\Delta x}\right) - \alpha_j^i \left(\frac{h_{j+1}^{i^n} - h_{j-1}^{i^n}}{2\Delta x}\right) + q_j^i\right\} \left\{\Delta t + \frac{(\Delta t)^2}{2} \left[-\right.\right.$$

$$\left.\left. n\ h_j^{i^{n-1}} \left(\frac{\alpha_{j+1}^i - \alpha_{j-1}^i}{2\Delta x}\right)\right]\right\} + \frac{(\Delta t)^2}{2}\left[\left\{\frac{q_j^{i+1} - q_j^i}{\Delta t}\right\} - \left\{\alpha_j^i \frac{n}{\Delta x} \left[\frac{h_{j+1}^{i^{n-1}} + h_j^{i^{n-1}}}{2}\right]\right.\right.$$

$$\left\{- \left[\frac{h_{j+1}^{i^n} + h_j^{i^n}}{2}\right] \left[\frac{\alpha_{j+1}^i - \alpha_j^i}{\Delta x}\right] - \left[\frac{\alpha_{j+1}^i + \alpha_j^i}{2}\right] \left[\frac{h_{j+1}^{i^n} - h_j^{i^n}}{\Delta x}\right] + \left[\frac{q_{j+1}^i + q_j^i}{2}\right]\right\} -$$

$$\alpha_j^i \frac{n}{\Delta x} \left[\frac{h_j^{i^{n-1}} + h_{j-1}^{i^{n-1}}}{2}\right] \left\{- \left[\frac{h_j^{i^n} + h_{j-1}^{i^n}}{2}\right] \left[\frac{\alpha_j^i - \alpha_{j-1}^i}{\Delta x}\right] - \left[\frac{\alpha_j^i + \alpha_{j-1}^i}{2}\right] \left[\frac{h_j^{i^n} - h_{j-1}^{i^n}}{\Delta x}\right]\right.$$

$$\left.\left.\left.\left.\left.+ \left[\frac{q_j^i + q_{j-1}^i}{2}\right]\right\}\right\}\right] \qquad (7\text{-}7)$$

Assume that the depth of flow is to be determined at N nodal points. Then the depth of flow at nodal points $j = 1,2,\ldots.\ (N-1)$ will be computed by the scheme in Eq. (7-7) in conjunction with the following boundary conditions:

$$h(o,t) = o$$

$$h(x,o) = o \qquad (7\text{-}8)$$

Equation (7-8) represents an initially dry surface. The scheme of Eq. (7-7) is explicit, second order, and single-step. The depth of flow at the downstream boundary (j = N) can be computed by the first order difference scheme; that is,

$$h(x;t + \Delta t) = h(x,t) + \Delta t \frac{\partial h}{\partial t} \tag{7-9}$$

Substituting Eq. (7-2) into Eq. (7-9).

$$h(x;t + \Delta t) = h(x,t) + \Delta t \left\{ - h^n \frac{\partial \alpha(x)}{\partial x} - \alpha(x) \frac{\partial h^n}{\partial x} + q(x,t) \right\} \tag{7-10}$$

Writing the difference form of Eq.

$$h_N^{i+1} = h_N^i + \Delta t \left\{ - h_N^{i^n} \left(\frac{\alpha_N^i - \alpha_{N-1}^i}{\Delta x} \right) - \alpha_N^i \left(\frac{h_N^{i^n} - h_{N-1}^{i^n}}{\Delta x} \right) + q_N^i \right\} \tag{7-11}$$

These numerical solutions can be combined with analytical solutions in an appropriate manner to yield hybrid solutions.

7.2 APPLICATION TO NATURAL WATERSHEDS

The distributed model was applied to three agricultural watersheds near Riesel (Waco), Texas. One of them is SW-12 as shown in Fig. 7-1 small watershed of about 3 acres in area. The other is SW-17 as shown in Fig. 7-2 , also about 3 acres in area, and another is Y-2 as shown in Fig. 7-3 , 132 acres in area. Deep, fine-textured, granular, slowly permeable, alkaline throughout, and slow internal drainage are typical characteristics of soils of these watersheds. The dominance of Houston black clay is notable. These soils are also noted for the formation of large extensive cracks upon drying. Surface drainage is, by and large, good but no well-defined drainage-ways exist on these watersheds. Usually, water is drained by rills and poorly defined field gullies.

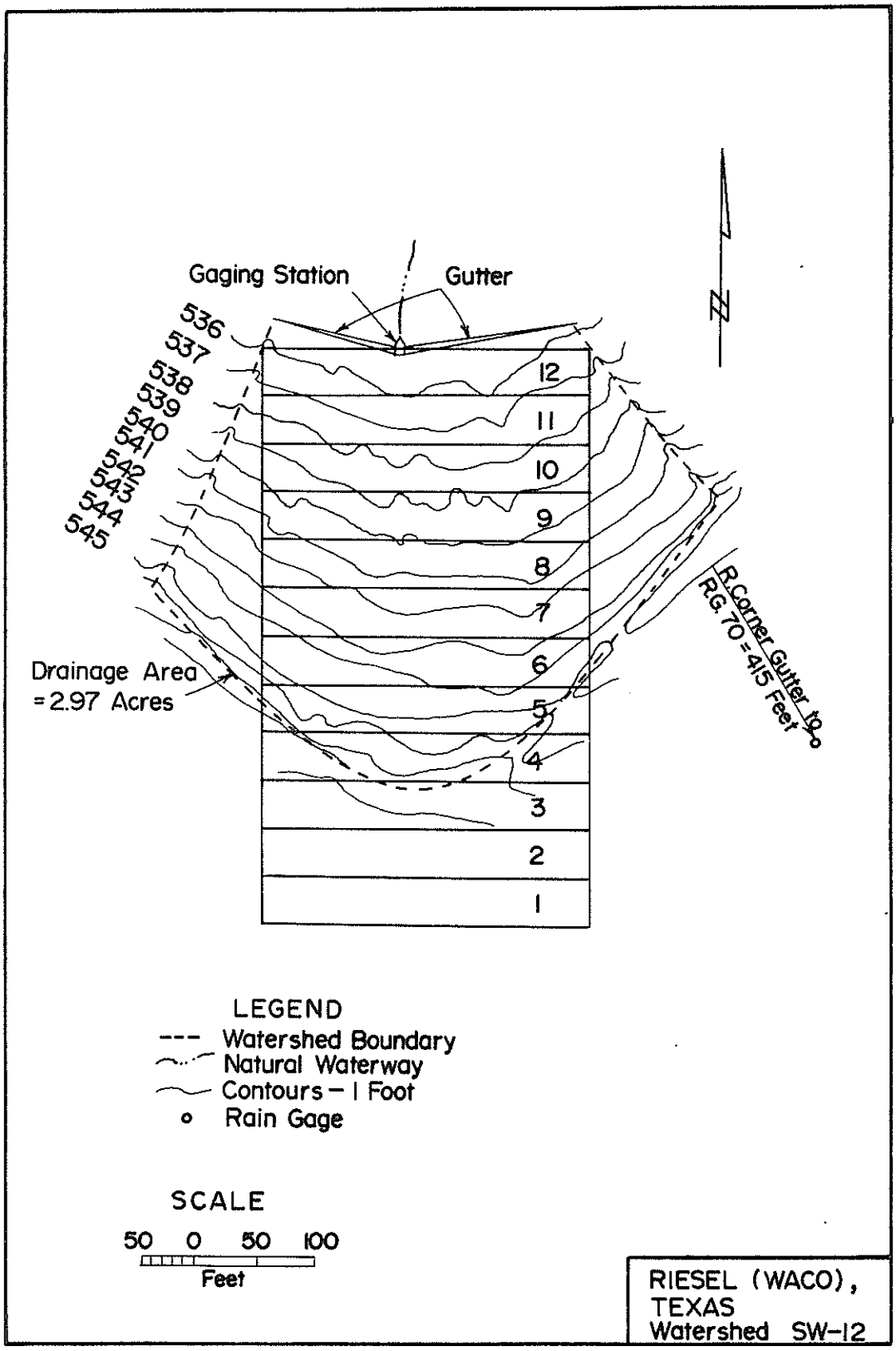

Fig. 7-1. Geometric representation of watershed SW-12, Riesel (Waco), Texas.

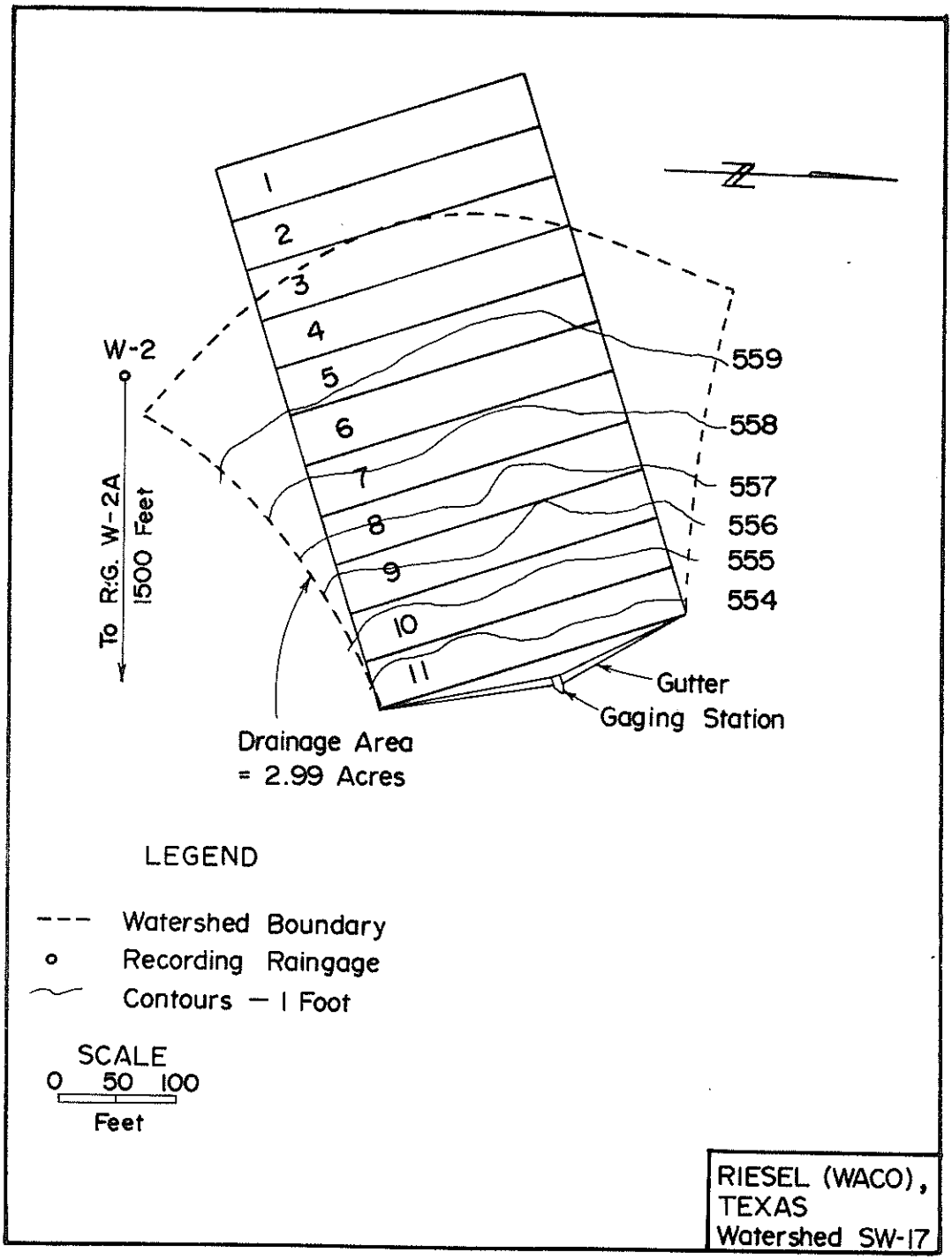

Fig. 7-2. Geometric representation of watershed SW-17, Riesel (Waco), Texas.

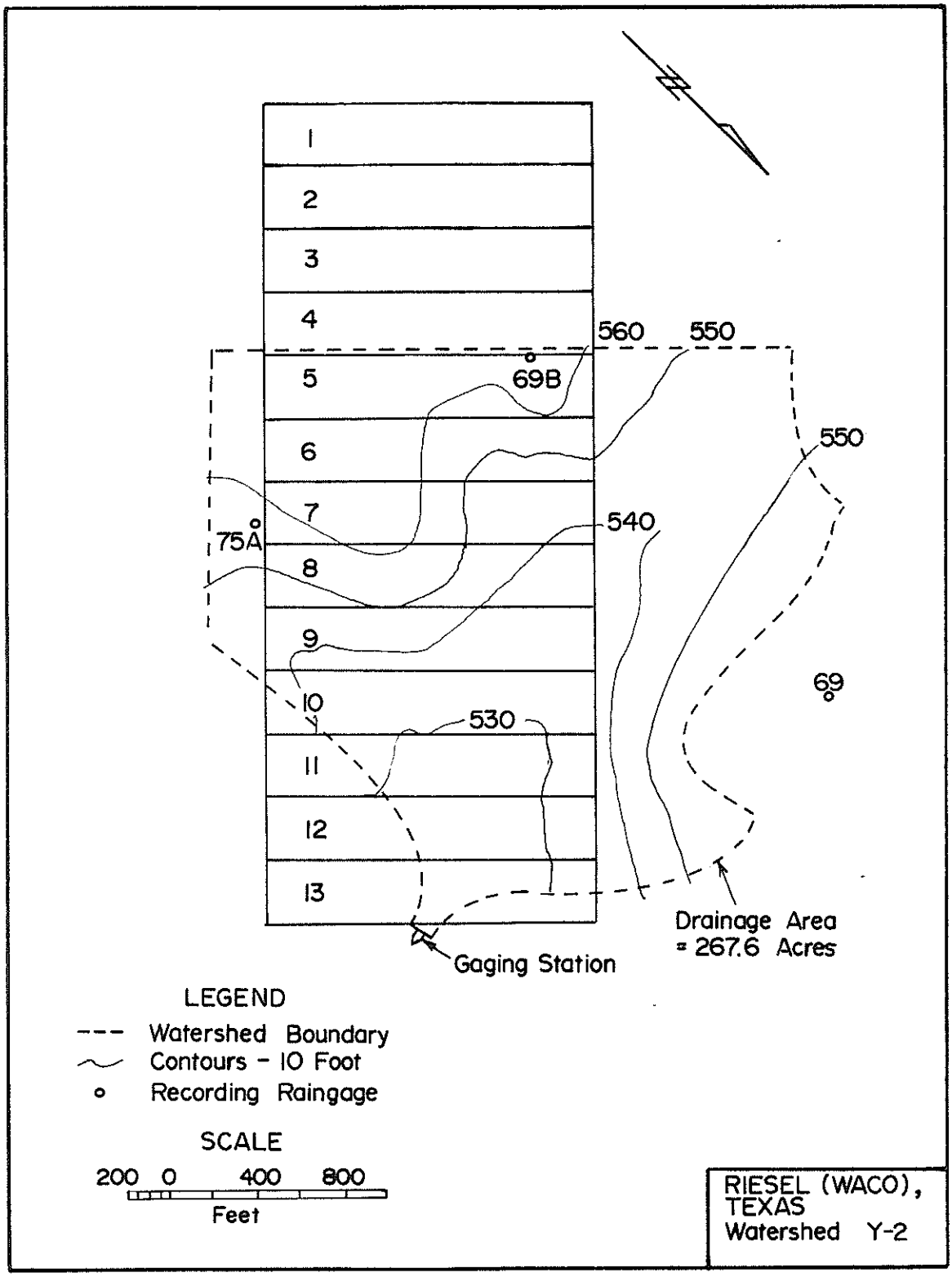

Fig. 7-3. Geometric representation of watershed Y-2, Riesel (Waco), Texas.

Most of the time these watersheds are covered with agricultural crops. Because of low permeability of the soils these watersheds respond rapidly to rainfall, and produce quickly rising hydrographs. For the rainfall events under consideration the major portion of rainfall was observed as surface runoff; and infiltration was only minor. For a more complete discussion of these watersheds and rainfall-runoff data thereon see the USDA publications entitled "Hydrologic Data for Experimental Agricultural Watersheds in the United States". These publications are published almost every year and contain, on an average, one event per watershed.

7.2.1 Determination of Rainfall Excess

Rainfall-excess forms input to the model. Estimating infiltration is essential for determining rainfall-excess. Philip's equation (Philip, 1957) was employed to estimate the infiltration loss. Philip's equation can be written as:

$$f = a + b\, t^{-0.5} \tag{7-12}$$

where f = infiltration loss rate, t = time, and a and b are parameters dependent on soil characteristics and initial moisture conditions. The parameters a and b have the dimensions L/T and $L/\sqrt{T}$ respectively; L denotes length dimension and T time dimension. Note that the parameter a has the same dimension as f. Theoretically the parameters will vary from storm to storm on the same watershed, and from watershed to watershed for the same storm. For practical considerations the parameter a was considered roughly identical to steady infiltration; thus it was determined from physical characteristics of the soil. The parameter b was allowed to vary with each rainfall episode, thus accounting for soil moisture conditions existing prior to its

occurrence. It was estimated for each storm, utilizing Newton's numerical algorithm (Conte, 1965) subject to preserving mass continuity. Tables 7-1 - 7-3 provide values of these parameters for some rainfall events on each watershed. As can be seen the parameter b is quite sensitive to rainfall characteristics and antecedent soil moisture conditions.

7.2.2 Geometric Representation

A simple rectangular section was employed to represent the watershed geometry as shown in Figs. 7-1 - 7-3. The plane section geometry has two parameters L_o and W. L_o represents length of flow and W width. With watershed area known we need to determine only one quantity, that is either L_o or W. Thus a topographic map would suffice to transform the natural geometry into a simple rectangular plane section geometry.

7.2.3 Choice of Objective Function

The following objective function, based on hydrograph peak, was used in this study:

$$F = \min \sum_{j=1}^{M} \left\{ Q_{p_o}(j) - Q_{p_e}(j) \right\}^2 \qquad (7\text{-}13)$$

where F = objective function or error criterion, $Q_{p_o}(j)$ = observed hydrograph peak for the jth event, $Q_{p_e}(j)$ = estimated hydrograph peak for the jth event, and M = number of events in the optimization set. The choice of this objective function is based on findings of Kibler and Woolhiser (1970) and Singh (1974, 1975a, 1975b, 1975e, 1975f). Besides its usefulness in flood studies and its amenability to statistical implications it has an advantage that it does not suffer from timing errors resulting from improper synchronization between rainfall and runoff.

7.2.4 Parameter Optimization

A simple relation between the parameter α and topographic slope was hypothesized:

$$\alpha(x) = C_1 + C_2\sqrt{S(x)} \qquad (7\text{-}14)$$

where $S(x)$ = topographic slope varying in space, and C_1 and C_2 are constants. These constants will supposedly vary from one watershed to another. At present we can only hope to obtain them by the technique of optimization. We must note here that the parameter $\alpha(x)$ varies continuously in space.

For computational purposes the plane geometry was decomposed into several segments, for example, 12 segments for watershed SW-12, 11 segments for watershed SW-17, and 13 segments for watershed Y-2, as shown in Figs. 7-1 - 7-3 respectively. It was assumed that within each segment the surface characteristics would remain unchanged. For each segment weighted slope is known from the topographic map. Two sets of rainfall-runoff events were selected on each of the three watersheds; one set was called as optimization set implying that the events in this set were used for optimization only, and the other set was called as the prediction set implying that the rainfall events were used for hydrograph prediction only. These two sets were mutually exclusive implying that they did not have any event in common. The optimization sets consisted of a set of 3 events on SW-12, a set of 5 events on SW-17, and a set of 5 events on Y-2. The prediction sets consisted of a set of 2 events on SW-12, a set of 4 events on SW-17, and a set of 4 events on Y-2. The constants in Eq. (7-14) were obtained by optimization over the optimization set for each watershed. The optimization was performed by the Rosenbrock-Palmer algorithm (Rosenbrock, 1960; Himmelblau, 1972) utilizing the objective function of

Eq. (7-13). The optimized values of constants for each watershed are:

Watershed	C_1	C_2
SW-12	2.3	2.9
SW-17	2.4	3.0
Y-2	3.6	4.3

7.2.5 Hydrograph Prediction

Utilizing optimized values of the constants C_1 and C_2 hydrograph predictions were made for the events in the prediction set of each watershed. The results of model predictions are shown in Tables 7-1 - 7-3. Predicted hydrographs are shown in sample Figs. 7-4 - 7-7. From the figures and the tables it is evident that on the whole model has performed quite well, especially for its simplicity. However, a few points prompt discussion:

(1) In predicting hydrograph peak relative error has gone as high as about 50% in some cases, for example, for two events 5-13-1957 and 3-29-65 on watershed SW-17. Except for these two instances the relative error has stayed well below 20%. There might be several reasons for high prediction error. Of all two appear to be most prominent: (a) the size of the optimization set is very small and, therefore, we cannot hope to obtain representative values of the constants C_1 and C_2, and (b) there is difficulty in determining rainfall-excess which, in fact, generated observed runoff. The determination of rainfall-excess seems to be the major problem in all rainfall-runoff models. Philip's equation is too simple to accurately predict time-distribution of infiltration and then there is the difficulty of estimating its parameters.

(2) Figures 7-4 - 7-7 indicate that the model predicts time-distribution of runoff fairly well. We must note that the optimization of constants C_1 and C_2 utilized an objective function based on hydrograph peak

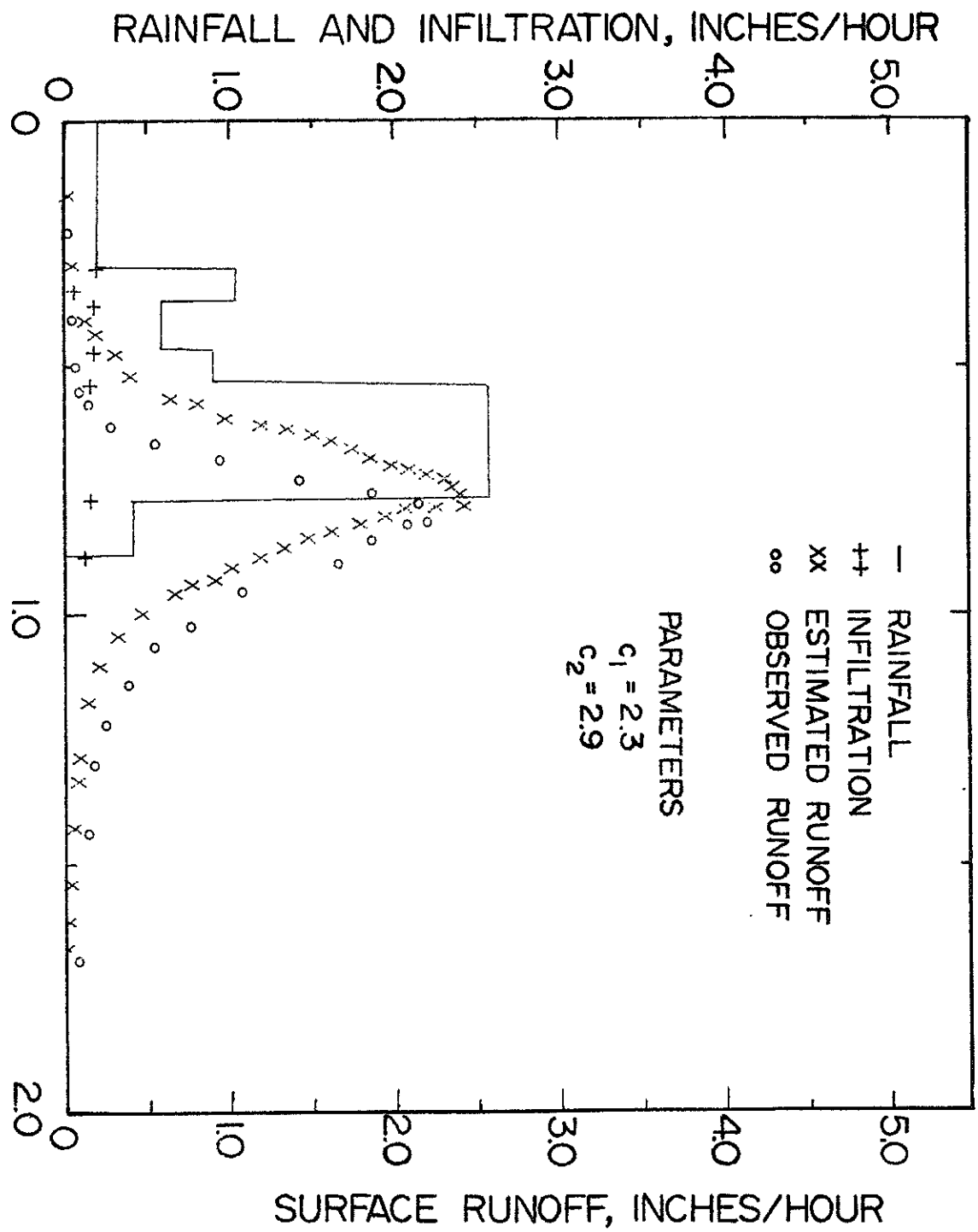

Fig. 7-4. Hydrograph prediction by distributed kinematic wave model for rainfall event of 3-12-1953 on watershed SW-12, Riesel (Waco), Texas.

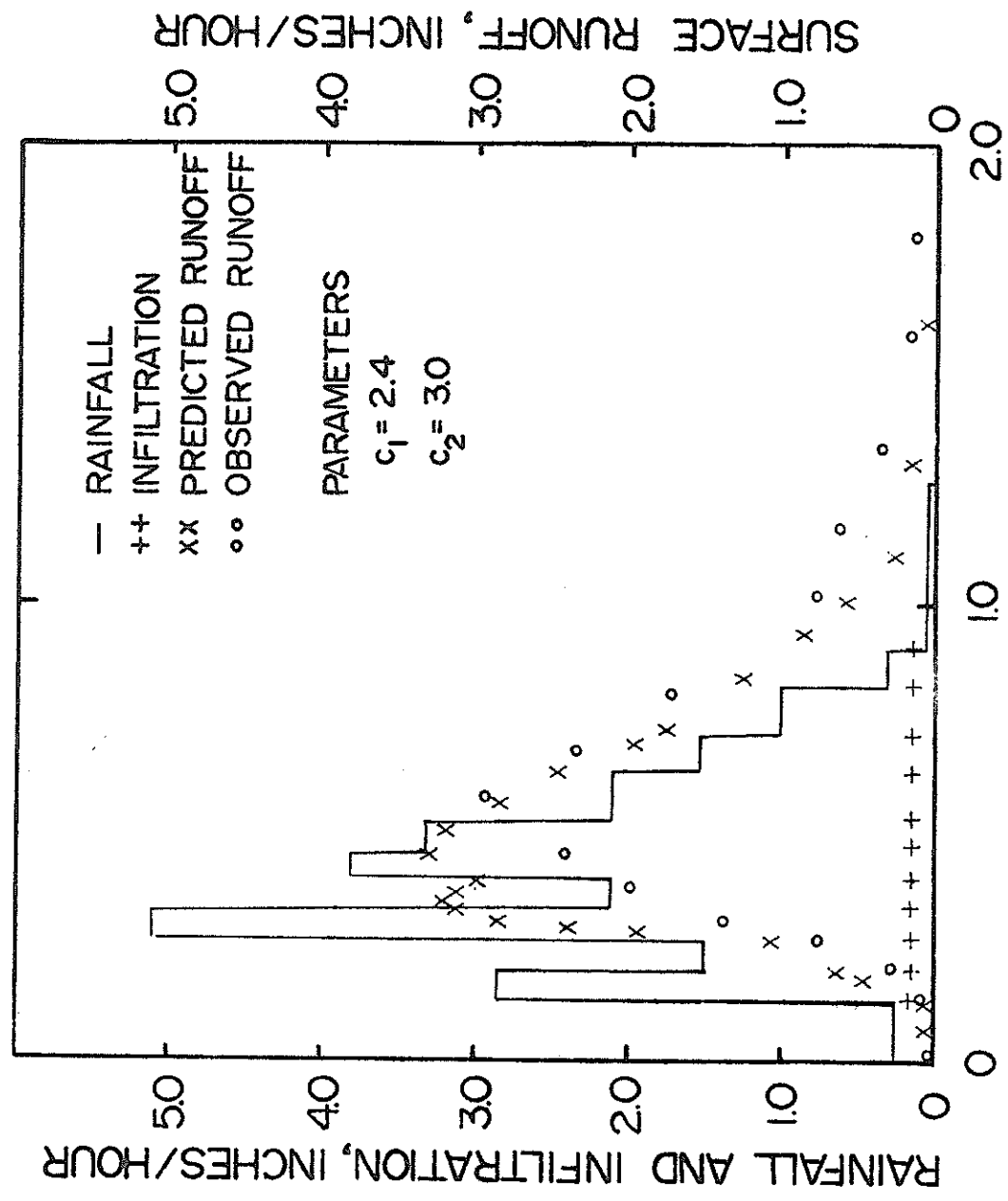

Fig. 7-5. Hydrograph prediction by distributed kinematic wave model for rainfall event of 4-24-1957 on watershed SW-17, Riesel (Waco), Texas.

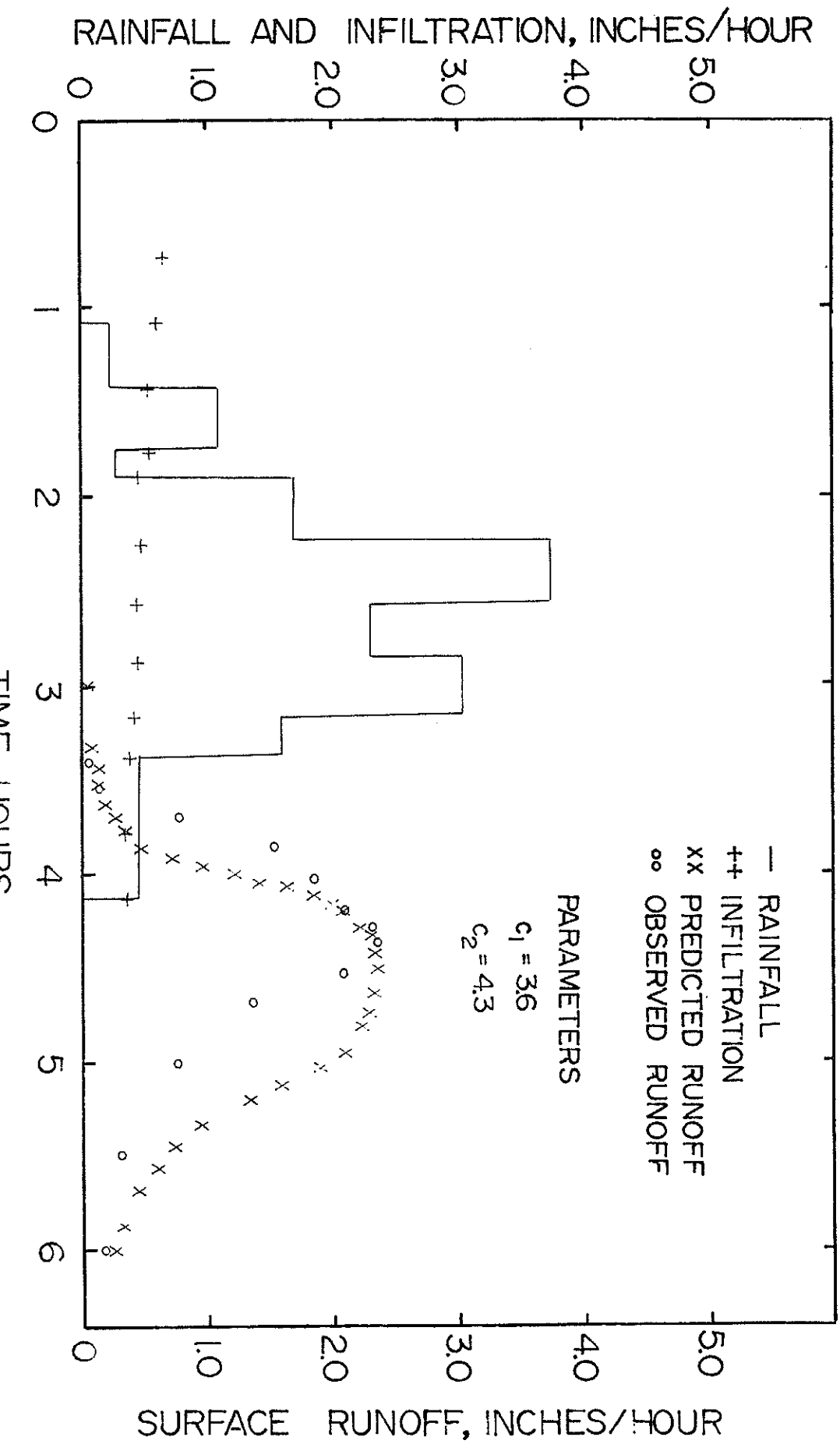

Fig. 7-6. Hydrograph prediction by distributed kinematic wave model for rainfall event of 3-29-1965 on watershed Y-2, Riesel (Waco), Texas.

Table 7-1. Predictive performance of the distributed kinematic wave model on watershed Y-2, Riesel (Waco), Texas.

Constants: $C_1 = 3.6$, $C_2 = 4.3$

Serial number	Date of rainfall	Rainfall volume	Runoff volume	Observed hydrograph peak	Parameters in Philip's equation of infiltration		Predicted hydrograph peak	Error in prediction	
								Absolute	Relative
		(Inches)	(Inches)	(Inches/hour)	a	b	(Inches/hour)	$Q_{p_o}(j)-Q_{p_e}(j)$	$(Q_{p_o}(j)-Q_{p_e}(j))/Q_{p_o}(j)$
1	4-24-1957	1.84	1.61	1.68	0.025	0.0716	2.02	-0.34	-0.20
2	5-13-1957	1.56	1.38	1.24	0.025	0.0865	1.43	-0.19	-0.15
3	6-4--1957	2.00	1.26	1.79	0.025	1.0145	1.60	+0.13	+0.10
4	3-29-1965	5.51	3.34	2.35	0.025	1.6092	2.35	+0.00	+0.00

Table 7-2. Predictive performance of the distributed kinematic wave model on watershed SW-12, Riesel (Waco), Texas.

Constants: $C_1 = 2.3$, $C_2 = 2.9$

Serial number	Date of rainfall event	Rainfall volume	Runoff volume	Observed hydrograph peak	Parameters in Philip's equation of infiltration		Predicted hydrograph peak	Error in prediction	
								Absolute	Relative
		(Inches)	(Inches)	(Inches/hour)	a	b	(Inches/hour	$Q_{p_o}(j)-Q_{p_e}(j)$	$(Q_{p_o}(j)-Q_{p_e}(j))/Q_{p_o}(j)$
1	3-12-1953	0.93	0.76	2.17	0.05	0.1473	2.41	-0.24	-0.11
2	3-29-1965	5.56	4.58	4.00	0.05	0.4321	4.02	-0.02	-0.01

Table 7-3. Predictive performance of the distributed kinematic wave model on watershed SW-17, Riesel (Waco), Texas.

Constants: $C_1 = 2.4$, $C_2 = 3.00$

Serial number	Date of rainfall	Rainfall volume	Runoff volume	Hydrograph peak observed	Parameters in Philip's infiltration equation		Predicted hydrograph peak	Error in prediction	
								Absolute $Q_{p_o}(j)-Q_{p_e}(j)$	Relative $\frac{Q_{p_o}(j)-Q_{p_e}(j)}{Q_{p_o}(j)}$
		(Inches)	(Inches)	(Inches/hour)	a	b	(Inches/hour)		
1	4-24-1957	1.75	1.73	2.90	0.01	0.0062	3.32	-0.42	-0.14
2	5-13-1957	1.62	1.36	1.74	0.01	0.1700	2.56	-0.82	-0.47
3	6--9-1962	2.08	1.67	3.79	0.01	0.5218	3.95	-0.16	-0.04
4	3-29-1965	4.99	3.50	2.43	0.01	1.3470	3.57	-1.13	-0.46

only. There was no consideration given to the runoff timing, yet the hydrograph shape and time characteristics are well predicted.

(3) For its simplicity the distributed approach appears to be promising. The need is for an exhaustive testing of the proposed approach on a number of natural watersheds in a variety of physiographic and climatic settings. Another aspect would be to investigate into the problem of determining the constants C_1 and C_2 from physically measurable watershed quantities. If the problem of a priori determination of the constants C_1 and C_2 can be tackled the utility of this approach will be greatly enhanced.

7.3 CONCLUSIONS

Based on the limited testing it can be safely said that the proposed distributed model is promising and deserves more exhaustive investigation. Its simplicity, coupled with physical realism and mathematical rigor, is sufficient to justify the above statement. On the whole the model is capable of predicting hydrograph peak, time and shape characteristics well, especially for its simplicity. There is, however, a need to correlate the constants C_1 and C_2 with physically measurable watershed characteristics. It will also be useful to study the variability of these constants from one watershed to another.

LITERATURE CITED

Amorocho, J. and G. T. Orlob: Nonlinear analysis of hydrologic systems. Water Resources Center, Contribution No. 40, 174 p., University of California, Berkeley, California, 1961.

Amorocho, J.: Measures of the linearity of the hydrologic systems. J. Geophys. Res., Vol. 6, pp. 2237-2249, 1963.

Amorocho, J. and W. E. Hart: A critique of current methods in hydrologic systems investigation. Trans. AGU, Vol. 45, No 2, pp. 307-321, 1964.

Amorocho, J. and W. E. Hart: The use of laboratory catchments in the study of hydrologic systems. J. Hydrology, Vol. 3, pp. 106-123, 1965.

Brakensiek, D. L.: Hydrodynamics of overland flow and nonprismatic channels. Trans. ASAE, Vol. 9, No. 1, pp. 113-122, 1966.

Brakensiek, D. L.: A simulated watershed flow system for hydrograph prediction: a kinematic application. Proc. Int'l Hydro. Symposium, pp. 18-24, Fort Collins, Colorado, 1967a.

Brakensiek, D. L.: Kinematic flood routing. Trans. ASAE, Vol. 10, No. 3, pp. 340-343, 197b.

Chery, D. L.: Design and tests of a physical watershed model. J. Hydrology, Vol. 4, pp. 224-235, 1966.

Chow, V. T.: Laboratory study of watershed hydrology. Proc. Int'l Hydro. Symposium, pp. 194-202, Fort Collins, Colorado, 1967.

Chow, V. T., and T. E. Harbaugh: Raindrop production for laboratory watershed experimentation. J. Geophys. Res., Vol. 70, pp. 6111-6119, 1965.

Conte, S. D.: Elementary numerical analysis; an algorithm approach. 278 p., McGraw-Hill Book Company, 1965.

Dass, K. C. and L. F. Huggins: Laboratory modeling and overland flow analysis. Water Resources Research Center, Purdue University Lafayette, Indiana, 1970.

Dodge, J. C. I.: A general theory of the unit hydrograph. J. Geophys. Res., Vol. 64, No. 2, pp. 241-256, February 1959.

Eagleson, P. S.: A distributed linear model for peak catchment discharge. Proc. Int'l Hydro. Symposium, p. 1-8, Ft. Collins , Colorado, 1967.

Eagleson, P. S.: Modeling surface runoff in urban hydrology. ASCE Report, Urban Water Resources Research, Chapt. 4:A-32-A-78, 1968.

Eagleson, P. S.: Dynamic hydrology. 462 p., McGraw-Hill Book Company, 1970.

Eagleson, P. S.: The stochastic kinematic wave. Systems Approach to Hydrology, edited by V. Yevjevich, Water Resources Publications, Ft. Collins, Colorado, 1971.

Eagleson, P. S.: Dynamics of flood frequency. Water Resources Res., Vol. 8, No. 4, pp. 878-894, 1972.

Foster, G. B., L. F. Huggins, and L. D. Meyer: Simulation of overland flow on short field plots. Water Resources Res., Vol. 4, No. 6, pp. 1179-1188, 1968.

Golany, P., and C. L. Larson: Effects of channel characteristics on time parameters for small watershed runoff hydrographs. Univ. of Minnesota Water Resources Res. Center Bull., No. 31, pp. 1-130, 1971.

Grace, R. A. and P. S. Eagleson: Similarity criteria in surface runoff process. Hydrodynamics Lab Rep. No. 77, 6-23 p., MIT, Cambridge, Massachusetts, July 1965.

Grace, R. A. and P. S. Eagleson: Scale model of urban runoff from storm rainfall. J. Hydrau. Div., Proc. ASCE, Vol. 93, No. HY3, pp. 161-176, May 1967.

Hanks, R. J. and S. A. Bowers: Numberical solution of the moisture flow equation for infiltration into layered soil. Soil Sci. Soc. Amer. Proc., Vol. 26, No. 6, pp. 530-534, 1962.

Harbaugh, T.E.: Time distribution of runoff from watersheds. Ph.D. dissertation, University of Illinois, Urbana, Illinois, 1966.

Harbaugh, T. E. and V. T. Chow: A study of the roughness of conceptual river systems or watershed. IAHR Congress 12, ft. Collins, Colorado, 1967.

Harley, B. M., et al: A modular distributed model of catchment dynamics. R. M. Parsons Laboratory for Water Resources and Hydrodynamics, Report No. 133, 537 p., MIT, Cambridge, Massachusetts, December 1970.

Henderson, F. M.: Open channel flow. 522 p., The Macmillan Company 1966.

Henderson, F. M. and R. A. Wooding: Overland flow and groundwater flow from a steady rainfall of finite duration. J. Geophys. Res., Vol. 69, No. 8, pp. 1531-1540, 1964.

Himmelbau, D. M.: Applied nonlinear programming. pp. 158-167, McGraw-Hill Book Company.

Houghton, D. D. and A Kasahara: Nonlinear shallow fluid flow over an isolated ridge. Communications in Pure and Applied Mathematics, Vol. XXI, pp. 1-28, 1968.

Ishihara, Y.: Hydraulic mechanism of runoff. Proc. Conference on Hydraulics and Fluid Mechanics, University of Western Australia, 1964.

Iwagaki, Y.: The theory of flow on road surfaces. Memoirs of the Faculty of Engrg., Vol. 13, pp. 139-147, Kyoto Univ., Japan, 1951.

Iwagaki, Y.: Fundamental studies on the runoff analysis by characteristics. Kyoto Univ. Disaster Prevention Res. Inst., Bull. No. 10, pp. 1-25, Japan, 1955.

Izzard, C. F. and M. T. Augustine: Preliminary report on analysis of runoff resulting from simulated rainfall on a paved plot. Trans. AGU, Part 2, pp. 500-509, January 1943.

Issard, C. F.: Hydraulics of runoff from developed surfaces. Proc. Highway Res. Board, pp. 129-146, 1946.

Keulegan, G. H.: Spatially variable discharge over a sloping plane. Trans. AGU, pp. 956, 1944.

Kibler, D. B., and D. A. Woolhiser: The kinematic cascade as a hydrologic model. Colorado State Univ., Hydrology Paper No. 39, pp. 1-27, Fort Collins, Colorado, 1970.

Kibler, D. F. and D. A. Woolhiser: Mathematical properties of the kinematic cascade. J. Hydrology, Vol. 15, pp. 131-147, 1972.

Kundu, P. A.: Mechanics of flow over very rough surfaces. Ph. D. dissertation, 254 p., Purdue University, Lafayette, Indiana, August, 1971.

Lane, L. J.: Influence of simplifications of watershed geometry in simulation of surface runoff. Ph. D. dissertation, 198 p., Colorado State University, Fort Collins, Colorado, April 1975.

Langford, K. J. and A. K. Turner: An experimental study of the application of kinematic wave theory to overland flow. J. Hydrology, Vol. 18, pp. 125-145, 1973.

Li, R. M.: Mathematical modeling of response from small watersheds. Ph.D. dissertation, 212 p., Colorado State University, Fort Collins, Colorado, August 1974.

Li, R. M., D. B. Simons and M. A. Stevens: Nonlinear kinematic wave approximation for water routing. Water Resources Res., Vol. 11, No. 2, pp. 245-252, 1975.

Lighthill, M. J., and G. B. Whitham: On kinematic waves: flood movement in long rivers. Proc. Royal Society (London), Series A, Vol. 229, pp. 281-316, 1955.

Mahmood, K. and V. Yevjevich (eds.): Unsteady flow in open channels. Vol. 1, 484 p., Water Resources Publications, Fort Collins, Colorado, 1975.

Morgali, J. R.: Laminar and turbulent overland flow hydrographs. J. Hydrau. Div., Proc. ASCE, Vol. 96, No HY2, pp. 441-461, 1970.

Morgali, J. R., and R. K. Linsley: Computer analysis of overland flow. J. Hydrau. Div., Proc. ASCE, Vol. 91, No. HY3, pp. 81-100, 1965.

Mulvany, T. J.: On the use of self registering rain and flood gauges. Proc. Institution of Civil Engineers (Ireland), Vol. 4, No. 2, pp. 1-8, 1850.

Muzik, I.: State variable model of surface runoff from a laboratory catchment. Ph.D. dissertation, University of Alberta, Edmonton, Alberta, Canada, 1973.

Muzik, I.: Laboratory experiments with surface runoff. J. Hydrau. Div., Proc. ASCE, Vol. 100, No. HY4, pp. 501-516, April 1974a.

Muzik, I.: State variable model of overland flow. J. Hydrology, Vol. 22, pp. 347-364, 1974b.

Nash, J. E.: The form of the instantaneous unit hydrograph. IASH Publication, Vol. 3, No. 45, pp. 1114-1121, 1957.

Overton, D. E.: Estimation of surface water lag time from the kinematic wave equations. Water Resources Bull., Vol. 7, No. 3, pp. 428-440, 1971.

Overton, D. E.: Kinematic flow on long impermeable planes. Water Resources Bull., Vol. 8, No. 6, pp. 1198-1204, 1972.

Overton, D. E., and D. L. Brakensiek: A kinematic model of surface runoff response. IASH-UNESCO Symposium on the Results of Research on Representative and Experimental Basins, Wellington, N. Z., 1970.

Philip, J. R.: The theory of infiltration: 1. the infiltration equation and its solution. Soil Science, Vol. 83, No. 5, pp. 105-116, 1957a.

Philip, J. R.: The theory of infiltration: 4. sorptivity and algebraic equations. Soil Science, Vol. 84, No. 3, pp. 257-264, 1957b.

Ragan, R. M. and J. O. Duru: Kinematic wave nomograph for times of concentration. J. Hydrau. Div., Proc. ASCE, Vol. 98, No. HY10, pp. 1765-1771, 1972.

Rastagi, R. A. and B. A. Jones: Simulation and hydrologic response of a drainage net of a small agricultural drainage basin. Trans. ASAE, Vol. 12, pp. 899-908, 1969.

Rastagi, R. A. and B. A. Jones: Nonlinear response of a small drainage basin model. J. Hydrology, Vol. 14, pp. 29-42, 1972.

Robertson, A. F., et al.: Runoff from impervious surfaces under conditions of simulated rainfall. Trans. ASAE, Vol. 9, No. 3, pp. 343-346, 1966.

Rosenblueth, A. and N. Wiener: The role of models in science. Philosophy of Science, Vol. XII, No. 4, pp. 316-321, 1945.

Rosenbrock, H. H.: An automatic method for finding the greatertest least value of a function. Computer Journal, Vol. 4, pp. 175-184, 1960.

Rovey, E. W.: A kinematic model of upland watersheds. M. S. thesis, 113 p., Colorado State University, Fort Collins, Colorado, September 1974.

Rubin, J.: Theory of rainfall uptake by solids initially drier than their field capacity and its application. Water Resources Res., Vol. 2, No. 4, pp. 739-749, 1966.

Sherman, L. K.: Streamflow from rainfall by the unit graph method. Engineering News Record, Vol. 108, pp. 501-505, 1932.

Singh, V. P.: University of Cincinnati urban runoff model. Discussion, J. Hydraulics Div., Proc. ASCE, Vol. 99, No. HY7, pp, 1194-1196, July 1973.

Singh, V. P.: A nonlinear kinematic wave model of surface runoff Ph.D. dissertation, 282 p., Colorado State University, Fort Collins, Colorado, May 1974.

Singh, V. P.: A laboratory investigation of surface runoff. J. Hydrology, Vol. 25, No 2, pp. 187-200, 1975a.

Singh, V. P.: Laboratory experiments with surface runoff. Discussion, J. Hydraulics Div., Proc. ASCE, Vol. 101, No. HY3, pp. 555-557, March, 1975b.

Singh, V. P.: Derivation of time of concentration. J. Hydrology, 1975c.

Singh, V. P.: Derivation of surface water lag time for coverging overland flow. Water Resources Bull., Vol. 113, No. 3, pp. 505-513, 1975d.

Singh, V. P.: Hybrid formulation of kinematic wave models of watershed runoff. J. Hydrology, Vol. 27, pp. 33-40, 1975e.

Singh, V. P.: Kinematic wave modeling of watershed surface runoff: a hybrid approach. International Symposium on the Hydrological Characteristics of River Basins and the Effect of these Characteristics of Better Water Management, December 1975f, Tokyo, Japan.

Singh, V. P.: Estimation and optimization of kinematic wave parameters. Water Resources Bull., Vol. 11, No 6, pp. 1091-1102, 1975g.

Singh, V. P.: A distributed approach to kinematic wave modeling of watershed runoff. Proc. National Symposium on Urban Hydrology and Sediment Control, University of Kentucky, Lexington, July, 1975h.

Smith, R. E.: Mathematical simulation of infiltreating watersheds. Ph.D. Dissertation, Colorado State University, Fort Collins, Colorado, June 1970.

Smith, R. E., and D. A. Woolhiser: Mathematical Simulation of infiltrating watersheds. Colorado State University Hydrology Paper No. 47, pp. 1-44, Fort Collins, Colorado, 1971a.

Smith, R. E. and D. A. Woolhiser: Overland flow on an infiltrating surface. Water Resources Res., Vol. 7, No. 4, pp. 899-913, 1971b.

Wei, T., and C. L. Larson: Effects of areal and time distribution of rainfall on small watershed runoff hydrographs. Univ. of Minnesota Water Resources Res. Center Bull., No. 30, pp. 1-118, 1971.

Whisler, F. D. and A. Klute: The numerical analysis of infiltration, considering hysteresis, into vertical soil column of equilibrium under gravity. Soil Sci. Soc. Amer. Proc., Vol. 29, No. 5, pp. 489-494, 1965.

Woo, D. C., and E. F. Brater: Spatially varied flow from controlled rainfall. J. Hydraulics Div., Proc. ASCE, Vol. 88, No. HY6, pp. 31-56, 1962.

Wooding, R. A.: A hydraulic model for the catchment-stream problem: 1. kinematic wave theory. J. Hydrology, Vol. 3, No. 3, pp. 254-267, 1965a.

Wooding, R. A.: A hydraulic model for the catchment-stream problem; 2. numerical solutions. J. Hydrology, Vol. 3, No. 3, pp. 268-282, 1965b.

Wooding, R. A.: A hydraulic model for the catchment-stream problem: 3. comparison with runoff observations. J. Hydrology, Vol. 4, pp. 21-37.

Woolhiser, D. A., and J. A. Liggett: Unsteady, one-dimensional flow over a plane--the rising hydrograph. Water Resources Res., Vol. 3, No. 3, pp. 753-771, 1967.

Woolhiser, D. A.: Overland flow on a converging surface. Trans. ASAE, Vol. 12, No. 4, pp. 460-462, 1969.

Woolhiser, D. A., C. L. Hanson, and A. R. Kuhlman: Overland flow on rangeland watersheds. J. Hydrology (N.Z.), Vol. 9, No. 2, pp. 336-356, 1970.

Woolhiser, D. A., et al: Experimental investigation of converging overland flow. Trans. ASAE, Vol. 14, No. 4, pp. 684-687, 1971.

Woolhiser, D. A., and E. F. Schulz: Large material models in watershed hydrology research. Int'l Symposium on River Mechanics, IAHR, Bangkok, Thailand, 1973.

Yen, B. C., and V. T. Chow: A laboratory study of surface runoff due to moving rainstorms. Water Resources Res., Vol. 5, No. 5, pp. 989-1006, 1969.

Yevdjevich, V. M.: Analytical intergration of the differential equation for water storage. J. Res., National Bureau of Standards, Vol. 63B, No. 1, pp. 43-52, July-September 1959.

Yu, Y.S., and J. S. McNown: Runoff from impervious surface. J. Hydraulic Res., Vol. No. 1, pp. 3-24, 1964.

APPENDIX A

We will show that the curves $t = t(x,t_o)$, $o \leq t_o \leq T$, fill out all of S above $t = t(x,o)$. For this purpose it is sufficient to prove that, for fixed $x>o$, $t(x,t_o) \to \infty$ as $t_o \to T$. Together with our assumption that the curves $t = t(x,t_o)$ do not intersect in S for distinct values of t_o , this implies that $h(x,t)$ is defined throughout S .

We assume that $n > 1$; $\alpha_1 \leq \alpha(x) \leq \alpha_2$; $o \leq q(x,t) \leq q$ if $t \leq T$, $q(x,t) = o$ if $t > T$. From Eq. (4-12) we obtain:

$$o < h(x,t_o) < \left\{\frac{1}{\alpha_1}\int_o^x q\, d\xi\right\}^{\frac{1}{n}} = \left\{\frac{qx}{\alpha_1}\right\}^{\frac{1}{n}} \tag{A-1}$$

From Eq. (4-13) we see:

$$\frac{dt}{dx} > \frac{1}{n\alpha_2}\left\{\frac{qx}{\alpha_1}\right\}^{\frac{1-n}{n}} = \frac{C_1}{n}\, x^{\frac{1-n}{n}} \tag{A-2}$$

where $C_1 = \left(\frac{q}{\alpha_1}\right)^{\frac{1-n}{n}} \frac{1}{\alpha_2}$

Integrating Eq. (A-2) between o and x,

$$t(x,t_o) > t_o + C_1\, x^{\frac{1}{n}} \tag{A-3}$$

Let $x^*(t_o)$ be the solution of $T = t(x^*,t_o)$. Then, from Eq. (A-3) we obtain:

$$x^*(t_o) < \left[\frac{T - t_o}{C_1}\right]^n$$

We have, referring to Eq. (4-13)

$$\int_o^{\eta} q(\xi,t(\xi,t_o))\, d\xi < \int_o^{x^*(t_o)} q\, d\xi = qx^*(t_o) < q\left\{\frac{T - t_o}{C_1}\right\}^n$$

Thus we can write

$$t(x,t_o) > t_o + \int_o^x \left(\frac{1}{\alpha_2}\right) \left\{ \left(\frac{T - t_o}{C_1}\right)^n \right\}^{\frac{1-n}{n}} d\eta = t_o + \frac{C_2 x}{(T - t_o)^{n-1}} \qquad (A-4)$$

where $C_2 = \dfrac{C_1^{n-1}}{\alpha_2 n}$

It follows from Eq. (A-4) that $t(x,t_o) \to \infty$ as $t_o \to T$ for fixed $x > o$. It follows from Eq. (A-1) that

$$o < h(x,t) < \left(\frac{qx}{\alpha_1}\right)^{\frac{1}{n}} \qquad (A-5)$$

Equation (A-5) implies that $h(o,t) = o$ for $t > T$.

APPENDIX B

When $q(x,t) = q$ the curves $t = t(x,t_o)$ do not, for distinct values of t_o, intersect in S. This follows from Eqs. (4-15) and (4-94); the curves of Eq. (4-94) are the prolongation beyond $t = T$ of the curves of Eq. (4-15). Equation (4-15) implies that $t(x,t_o)$ is, for fixed x, an increasing function of t_o, and Eq. (4-94) implies that $t(x,x_o^*)$ is, for fixed x, a decreasing function of x_o^*.

To prove that the curves $t = t(x,t_o)$ do not intersect in domain D_3 we impose the condition that $\alpha(x) = \alpha$, a constant; We also retain the condition $q(x,t) = q$. Under these conditions we show that Eq. (4-37) is, for fixed x, a decreasing function of x_o. Similarly, it is clear from Eq. (4-21) for domain D_2 that $t(x,t_o)$ is an increasing function of t_o. In domain D_1 it is clear from Eq. (4-61) that $t(x,x_o^*)$ is a decreasing function of x_o^*.

To conclude the discussion we need to prove that the curves $t = t(x; x_o, x_o^*)$ do not intersect in domain D_{12}. This indeed is true from Eq. (4-103) since $t(x; x_o, x_o^*)$ is a decreasing function of x_o.

This discussion can be extended, without complication, to the case when $\alpha(x)$ is not a constant. It would simply require to impose the condition that $\alpha(x)$ is an increasing function of x.

APPENDIX C

COMPUTATION OF RUNOFF HYDROGRAPHS

C-1 EQUILIBRIUM HYDROGRAPH

Given the following information: L_o = 10,000 cm, α = 10 , q = 10cm/hr, T = 1,000 sec, n = 2 ., and width = 1 cm. We show the computations in steps.

Step 1. Compute the time of equilibrium, t_e., to determine whether, in fact, we are in equilibrium situation. From Eq. (4-80) we obtain:

$$te = \left(\frac{10}{3600}\right)^{-\frac{1}{2}} \left(\frac{10,000}{10}\right)^{\frac{1}{2}} = 600 \text{ secs}$$

The duration of effective rainfall is 1000 seconds. This implies that we are in equilibrium situation.

Step 2. We obtain the solution in domain D_3. We have from Eqs. (4-36) and (4-37):

$$t(x,x_o) = \left(\frac{10}{3600}\right)^{-\frac{1}{2}} \left\{\frac{x - x_o}{10}\right\}^{\frac{1}{2}} = 6(x - x_o)^{\frac{1}{2}} = (10,000 - x_o)^{\frac{1}{2}}\ 6$$

$$h(x,x_o) = \left(\frac{10}{3600}\right)^{\frac{1}{2}} \left\{\frac{x - x_o}{10}\right\}^{\frac{1}{2}} = \left(\frac{1}{60}\right) (x - x_o)^{\frac{1}{2}} = \frac{1}{60} (10,000 - x_o)^{\frac{1}{2}}$$

Remember here x = 10,000 centimeters, $o \leq x_o \leq 10,000$. Let x_o vary between o and 10,000 at the interval of 1000. We have.

x_o (cm)	t (sec)	h (cm)	Q (cm/hour)
0	600.0	1.67	10
1,000	586.2	1.58	9
2,000	536.7	1.43	8
3,000	502.0	1.39	7
4,000	464.8	1.29	6
5,000	424.3	1.18	5
6,000	379.5	1.05	4
7,000	328.6	0.91	3
8,000	268.3	0.75	2
9,000	189.7	0.53	1
10,000	0.0	0.00	0

Step 3. We obtain solution for domain D_2. For this example the function h will depend only on x. We have from Eqs. (4-20) and (4-21)

$$t(x,x_o) = t_o + \left(\frac{10}{3600}\right)^{-\frac{1}{2}} \left(\frac{10,000}{10}\right)^{\frac{1}{2}} = t_o + 600$$

$$h(x,x_o) = \left\{\frac{10}{3600} \cdot \frac{10,000}{10}\right\}^{\frac{1}{2}} = 1.67$$

Remember here t_o assumes values on $o \leq t \leq T$. We thus have:

t_o (sec)	t (sec)	h (cm)	Q (cm/hr)
0	600	1.67	10
100	700	1.67	10
200	800	1.67	10
300	900	1.67	10
400	1,000	1.67	10

Step 4. We obtain solution for domain D_1. From Eqs. (4-59)-(4-61) we have:

$$h_o = \left\{\frac{10}{3600} \cdot \frac{x_o}{10}\right\}^{\frac{1}{2}} = \frac{x_o^{\frac{1}{2}}}{60}$$

$$h(x,x_o) = h_o$$

$$t(x,x_o) = 1000 + \left[\frac{10}{10} \cdot \frac{3600}{x_o}\right] \frac{(10,000 - x_o)}{10 \times 2} = \frac{3}{x_o^{\frac{1}{2}}} (10,000 - x_o)$$

Remember here x_o varies between o and 10,000 cm. Thus we obtain:

x_o (cm)	h (sec)	h (cm)	Q (cm/hr)
1,000	1,853.8	0.53	1
2,000	1,536.7	0.75	2
3,000	1,383.4	0.91	3
4,000	1,284.6	1.05	4
5,000	1,212.1	1.18	5
6,000	1,154.9	1.29	6
7,000	1,107.5	1.39	7
8,000	1,067.1	1.49	8
9,000	1,031.6	1.58	9
10,000	1,000.0	1.67	10

This example is graphically illustrated in Fig. C-1.

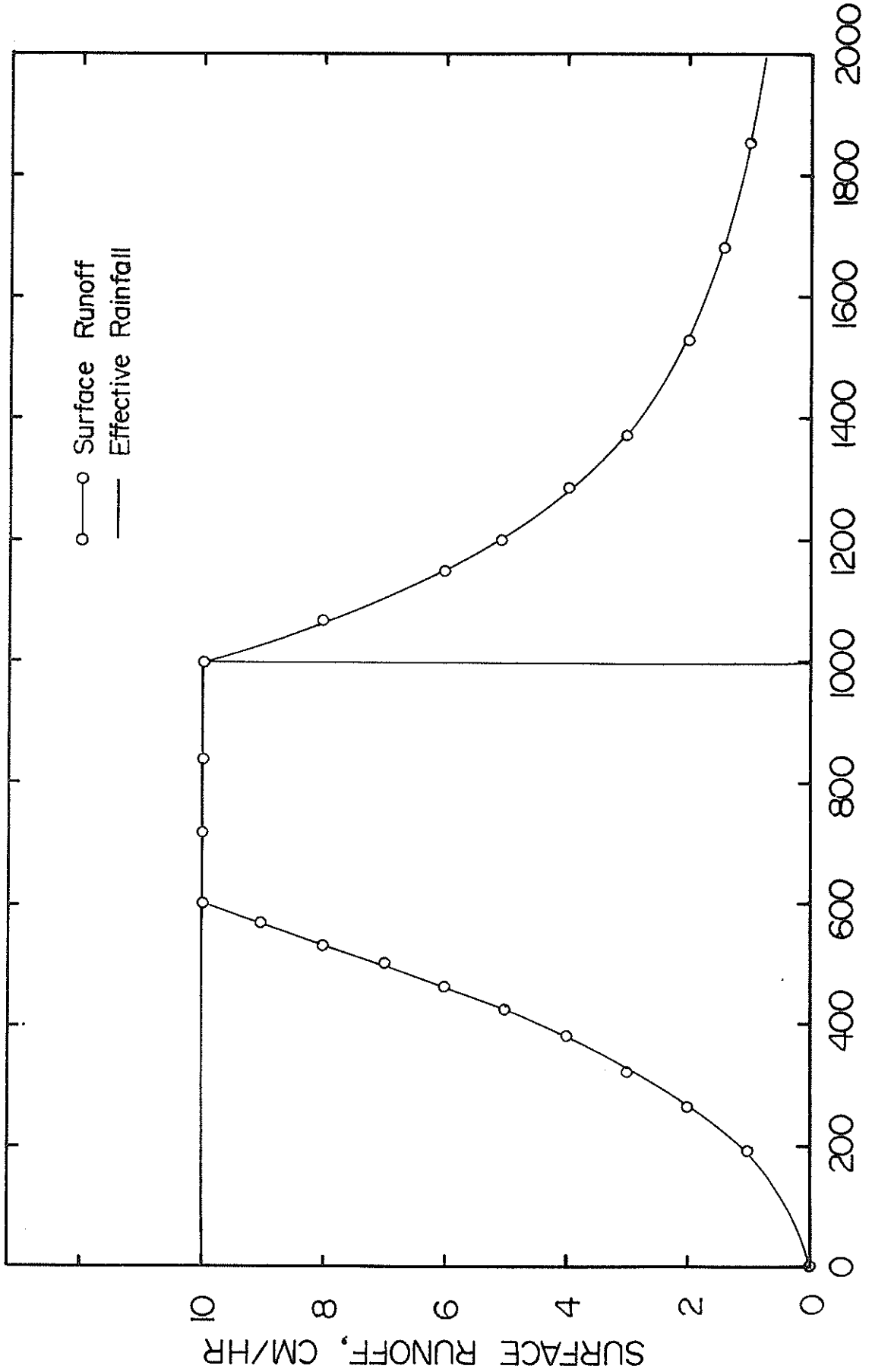

Fig. C-1. A typical runoff hydrograph for equilibrium case.

C-2. PARTIAL EQUILIBRIUM HYDROGRAPH

Let $n = 1.5$ and $T = 20$ hr; we retain the remainder of information utilized in the equilibrium hydrograph. Again, we perform computation in steps.

Step 1. The characteristic curve originating from the origin is $t = t(x,o)$, and is obtained by putting $x_o = o$ in Eq. (4-37). From Eq. (4-133) we obtain:

$$T = q^{\frac{1-n}{n}} \left(\frac{x}{\alpha}\right)^{\frac{1}{n}}$$

We can also write:

$$x = \alpha\, T^n\, q^{n-1} = x^*$$

This gives the point x^* where the limiting characteristic hits the line $t = T$. If $x^* \geq L_o$, we are in equilibrium situation, and if $x^* < L_o$, we are in partial equilibrium situation. Let us now determine if we are in partial equilibrium situation.

$$x^* = 10\ (20)^{1.5}\ (10)^{0.5} = 2{,}828.43 \text{ cm}$$

This indicates that we are, indeed, in partial equilibrium situation.

Step 2. We now obtain solution in domain D_3. We have from Eqs. (4-36) and (4-37)

$$t(x,x_o) = \left\{\frac{10}{3600}\right\}^{-\frac{1}{3}} \left\{\frac{10{,}000 - x_o}{10}\right\}^{\frac{2}{3}}$$

$$h(x,x_o) = \left\{\frac{10}{3600} \cdot \frac{10{,}000 - x_o}{10}\right\}^{\frac{2}{3}}$$

Remember that $o \leq x_o \leq 10{,}000$, $o \leq t \leq T$. Then we have:

x_o (cm)	t (hr)	h (cm)	Q (cm/hr)
10,000.00	0.00	0.00	0.00
9,500.00	6.30	63.00	0.50
9,000.00	10.00	100.00	1.00
8,500.00	13.10	131.04	1.50
8,000.00	15.87	158.74	2.00
7,171.57	20.00	200.00	2.83

Step 3. We now obtain solution in domain D_{11} . We have from Eqs. (4-60) and (4-61):

$$h(x,x_o^*) = \left\{\frac{10}{3600} \cdot \frac{x_o^*}{10}\right\}^{\frac{2}{3}}$$

$$t(x,x_o^*) = 20 + \left\{\frac{10}{\frac{10}{3600} \cdot x_o^*}\right\}^{\frac{1}{3}} \left[\frac{10{,}000 - x_o^*}{10 \times 1.5}\right]$$

Remember here that $o \leq x_o^* \leq x^*$. Then we have:

x_o^* (cm)	t (hr)	h (cm)	Q (cm/hr)
0.00	∞	0.00	0.00
500.00	99.80	63.00	0.50
1,000.00	80.00	100.00	1.00
1,500.00	69.50	131.04	1.50
2,000.00	62.33	158.74	2.00
2,500.00	56.84	184.20	2.50
2,828.43	53.81	200.00	2.83

Step 4. We now obtain the solution in domain D_{12} . We have from Eqs. (4-101) - (4-103). We obtain:

x_o^* (cm)	t (hr)	h (cm)	Q (cm/hr)
2,828.43	53.81	200	2.83
10,000.00	20.00	200	2.83

Remember here that $x^* \leq x_o^* \leq L_o$; x_o and x_o^* are bound by Eqs. (4-91).

We now illustrate this example graphically in Fig. C-2.

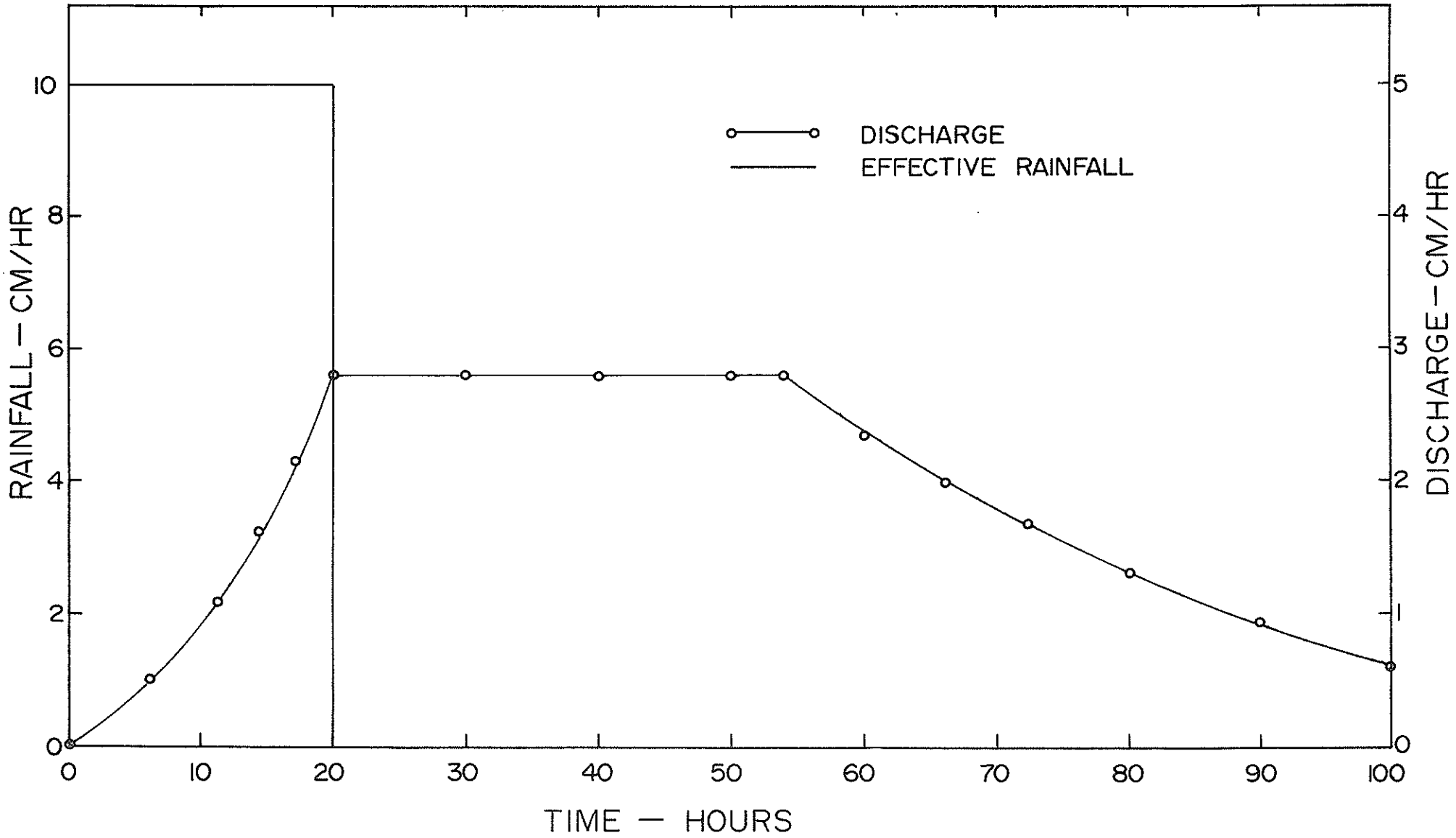

Fig. C-2. A typical runoff hydrograph for partial equilibrium case.

APPENDIX D

It follows from appendix B that the curves $t = t(x,t_o)$ do not intersect in domain D_2, and, on the assumption that $\alpha(x)$ is an increasing function of x, the curves $t = t(x,x_o)$ do not intersect in domain D_3. It follows from Eq. (5-19) that $t_{x_o^*}(x,x_o^*) < o$, so the curves $t = t(x,x_o^*)$ do not intersect in domain D_1 (case A) or in domain D_{11} (cases B_1 and B_2). Now we prove that the curves $t = t(x;x_o,x_o^*)$ do not intersect in domain D_{12}. If we require $\alpha(x)$ to satisfy that some assumption, it is then obvious from Eq. (5-31) that $t_{x_o}(x;x_o^*(x_o),x_o) < o$.